On the Role of Red Blood Cells in Regulation of Vascular Tone

Inaugural-Dissertation

zur Erlangung des Doktorgrades
der Mathematisch-Naturwissenschaftlichen Fakultät
der Heinrich-Heine-Universität Düsseldorf

vorgelegt von

Lukas Dominik Vornholz geb. Diederich
aus Mainz

Düsseldorf, Oktober 2018

aus der Klinik für Kardiologie, Pneumologie und Angiologie des Universitätsklinikum Düsseldorf, Direktor: Univ.-Prof. Dr. Malte Kelm, der Heinrich-Heine-Universität Düsseldorf.

Gedruckt mit der Genehmigung der
Mathematisch-Naturwissenschaftlichen Fakultät der
Heinrich-Heine-Universität Düsseldorf

Berichterstatter:

Referent: Univ.-Prof. Dr. Dr. Miriam M. Cortese-Krott

Korreferent: Univ.-Prof. Dr. Holger Gohlke

Tag der mündlichen Prüfung: 10.12.2018

Ich versichere an Eides Statt, dass die Dissertation von mir selbständig und ohne unzulässige fremde Hilfe unter Beachtung der „Grundsätze zur Sicherung guter wissenschaftlicher Praxis an der Heinrich-Heine Universität Düsseldorf" erstellt worden ist.

Diese Dissertation wurde weder in gleicher noch in ähnlicher Form in einem anderen Prüfungsverfahren vorgelegt. Außerdem erkläre ich, dass ich bisher noch keine weiteren akademischen Grade erworben oder zu erwerben versucht habe.

Düsseldorf, den 02.01.2019

Lukas Dominik Vornholz (geb. Diederich)

Meiner Familie und meinen Freunden gewidmet

Parts of this dissertation were already published in peer-reviewed scientific journals and presented on scientific conferences.

Original publications:

Diederich, L., Suvorava, T., Sansone, R., Keller, T.C.S.T., Barbarino, F., Sutton, T.R., Kramer, C.M., Luckstadt, W., Isakson, B.E., Gohlke, H., Feelisch, M., Kelm, M., and Cortese-Krott, M.M. (2018). On the Effects of Reactive Oxygen Species and Nitric Oxide on Red Blood Cell Deformability. *Front Physiol* 9**,** 332.

Keller, A.S., **Diederich, L.,** Panknin, C., Delalio, L.J., Drake, J.C., Sherman, R., Jackson, E.K., Yan, Z., Kelm, M., Cortese-Krott, M.M., and Isakson, B.E. (2017). Possible roles for ATP release from RBCs exclude the cAMP-mediated Panx1 pathway. *Am J Physiol Cell Physiol* 313**,** C593-C603.

Reviews:

Erkens, R., Suvorava, T., Kramer, C.M., **Diederich, L.**, Kelm, M., and Cortese-Krott, M.M. (2017). Modulation of Local and Systemic Heterocellular Communication by Mechanical Forces: A Role of Endothelial Nitric Oxide Synthase. *Antioxid Redox Signal* 26**,** 917-935.

Kuhn, V., **Diederich, L.,** Keller, T.C.S.T., Kramer, C.M., Luckstadt, W., Panknin, C., Suvorava, T., Isakson, B.E., Kelm, M., and Cortese-Krott, M.M. (2017). Red Blood Cell Function and Dysfunction: Redox Regulation, Nitric Oxide Metabolism, Anemia. *Antioxid Redox Signal* 26**,** 718-742.

Brown, I., **Diederich, L.**, Good, M., DeLalio, L.J., Murphy, S., Cortese-Krott, M.M.,

Hall, J., Le, T., and Isakson, B.E. (2018)). Vascular Smooth Muscle Remodeling in Conductive and Resistance Arteries in Hypertension. *Arterioscler Thromb Vasc Biol.* 38, 1969-1985

Poster:

1. 26-28.09.2016 in Frankfurt am Main: **Joint International Meeting Perspectives in Vascular Biology**
(Poster presentation: 'S-Nitrosation of spectrin: a possible regulator of red blood cell deformability?'; **Lukas Diederich**, T.C. Keller IV, Markus Dick, Malte Kelm, Holger Gohlke, Miriam M. Cortese-Krott)

2. 16-19.11.2016 in San Francisco: **The Society for Redox Biology and Medicine's Annual Meeting**

(Poster presentation: 'The Role of Cytoskeletal S-Nitrosation in Red Blood Cell'; **Lukas Diederich**, T.C. Keller IV, Wiebke Lückstädt, Markus Dick, Malte Kelm, Holger Gohlke, Miriam M. Cortese-Krott)

Abstract

Red blood cells (RBCs) are the main cell type of whole blood and have the task to transport gases, nutrients and metabolites. For a long period of time, RBCs were seen as enucleated, dead cells without any further physiological function.

In contrast, multiple studies pointed to a role of RBCs for the regulation of vascular tone via release of vasoactive molecules – including adenosine triphosphate (ATP) and nitric oxide (NO) and that their function may be controlled by intracellular signals, but the mechanisms behind these findings are controversially discussed. In particular it was found that RBCs carry a functional endothelial nitric oxide synthase (eNOS) and soluble guanylate cyclase (sGC) pathway. Similar to endothelial cells, RBCs were found to be able to synthesize NO and stimulate the downstream sGC pathway. The physiological function of the discovered eNOS-sGC pathway is not completely understood yet.

The hypothesis of this work was that RBC derived NO and its metabolites may contribute to the regulation of intrinsic properties and vascular tone.

The aim of the study was to analyze the unknown role of NO derived from RBCs in modulation of intrinsic properties and vascular tone. Three aspects were investigated: 1) how NO modulates RBC deformability, 2) how NO dependent signaling regulates ATP release from RBCs and 3) the effects of lack of eNOS in RBCs on vascular endothelial function and hemodynamics.

The main findings were: 1) NO per-se did not affect RBC deformability, but protected from oxidative stress induced reduction of RBC deformability. 2) NO in RBCs activated the sGC pathway, however this did not lead to controlled release of ATP. Moreover, intracellular increase of cyclic adenosine monophosphate (cAMP) did not lead to controlled release of ATP. 3) Transgenic RBC eNOS knockout (KO) mice exhibit increased blood pressure and preserved vascular endothelial function ex-vivo.

Therefore, it can be concluded that NO plays a major role for the regulation of RBC mechanoproperties. Moreover, activation of the intracellular eNOS–sGC pathway does not mediate controlled release of ATP by RBCs. Finally, eNOS in RBCs plays a role in the regulation of systemic hemodynamics; however, the underlying molecular mechanisms need to be further investigated.

Zusammenfassung

Die mit Abstand zahlenmäßig am häufigsten vorkommenden Zellen im Vollblut sind rote Blutkörperchen (RBCs), die die Aufgabe haben Gase, Nährstoffe und Stoffwechselprodukte zu transportieren. Eine lange Zeit wurden RBCs als kernlose, tote Zellen angesehen, die keinen weiteren physiologischen Zweck erfüllen.

Basierend auf wissenschaftliche Untersuchungen konnte gezeigt werden, dass RBCs auf die Regulation des vaskulären Tonus Einfluss nehmen. Die Mechanismen dieser Regulation jedoch bleiben kontrovers diskutiert, oder sind bis heute unklar. Insbesondere war die Entdeckung der Expression einer endothelialen Stickstoffmonoxidsynthase (eNOS) und löslichen Guanylatcyclase (sGC) in RBCs interessant. Übereinstimmend mit Ergebnissen in Endothelzellen, sind auch RBCs in der Lage Stickstoffmonoxid (NO) zu synthetisieren und den sGC Signalweg zu aktivieren. Die Aufgabe des eNOS–sGC - Signalwegs in der Regulation intrinsischer RBC-Eigenschaften und der Regulation des vaskulären Tonus bleibt jedoch weiterhin ungeklärt.

Basierend auf den bisherigen Ergebnissen wurde die dieser Arbeit zu Grunde liegende Hypothese aufgestellt, dass von RBCs stammendes NO und dessen Metabolite an der Regulation intrinsischer RBC-Eigenschaften und des vaskulären Tonus beteiligt sind.

Das Ziel der Studie war also die Analyse der Rolle von NO in RBCs. Die drei untersuchten Aspekte sind: 1) die Regulation der Verformbarkeit von RBCs durch NO, 2) die Regulation der Adenosintriphosphat (ATP) – Freisetzung durch RBCs und 3) die möglichen Effekte eines eNOS-Mangels auf die vaskuläre endotheliale Funktion und Hämodynamik.

Zu den wichtigsten Ergebnissen zählen: 1) NO hat keinen Einfluss auf die Verformbarkeit von RBCs, ist jedoch in der Lage durch Oxidantien induzierte Reduktion der Verformbarkeit von RBCs zu vermindern. 2) es konnte gezeigt werden, dass NO in RBCs den sGC-Signalweg aktiviert, jedoch keine kontrollierte Freisetzung von ATP induziert. Darüber hinaus verursachten intrazellulär erhöhte Konzentrationen von cyclischem Adenosinmonophosphat keine Freisetzung von ATP. 3) in genetisch veränderten Mäusen

ohne eNOS in RBCs konnte ein erhöhter Blutdruck mit intakter vaskulärer endothelialer Funktion festgestellt werden.

Zusammengefasst spielt NO eine wichtige Rolle in der Regulation der mechanischen Eigenschaften von RBCs, wobei Aktivierung des intrazellulären sGC–eNOS Signalwegs nicht zur kontrollierten Freisetzung von ATP führte. Schlussendlich konnte gezeigt werden, dass eNOS in RBCs eine hohe Relevanz für die Regulation der systemischen Hämodynamik hat, die Mechanismen hierfür jedoch weiter untersucht werden müssen.

Index of contents

Index of figures

Abbreviations

AC	adenylate cyclase
ADP	adenosine 5'-diphosphate
AMP	adenosine 5'-monophosphate
ATP	adenosine 5'-triphosphate
BMI	body mass index
BPM	beats per minute
cAMP	cyclic adenosine monophosphate
cGMP	cyclic guanosine monophosphate
CLD	chemiluminescence detection
ctrl	control
CVD	cardiovascular disease
CysNO	S-nitrosated L-cysteine
DCF	2',7'-dichlorofluorescein
DEA/NO	diethylammonium (Z)-1-(N,N-diethylamino)diazen-1-ium-1,2-diolate
DMSO	dimethyl sulfoxide
DPBS	Dulbecco's phosphate buffered saline
EC	endothelial cell
EI	elongation index
EImax	maximal elongation index
eNOS	endothelial nitric oxide synthase
EPR	electron paramagnetic resonance
ERT2	estrogen receptor 2
FMD	flow mediated dilation
GFR	glomerular filtration rate
GSH	glutathione
GSSG	glutathione disulfide
Hb1Ac	glycated hemoglobin
HBSS	Hanks' balanced salt solution
IBMX	3-isobutyl-1-methylxanthin
iNOS	inflammatory nitric oxide synthase
KI	knock-in
KO	knockout
LC-MS/MS	liquid-chromatography tandem mass spectrometry
L-NAME	L-N^{G}-nitroarginine methyl ester
LORCA	laser optical rotational cell analyzer
MFI	mean fluorescence intensity
MPV	mean platelet volume
NADPH	nicotinamide adenine dinucleotide phosphate

NO	nitric oxide
NOS	nitric oxide synthase
Nrf2	nuclear factor (erythroid-derived 2)-like2
ODQ	1H-[1,2,4]oxadiazolo-[4-3-a]quinoxylin-1one
P2Y1	purinergic G protein-coupled receptor Y1
P2Y2	purinergic G protein-coupled receptor Y2
PKA	protein kinase A
RBC	red blood cell
RDW	red blood cell distribution width
ROS	reactive oxygen species
sGC	soluble guanylate cyclase
SNP	sodium nitroprusside
$SS_{1/2}$	half maximal shear stress
Tam	tamoxifen
t-BuOOH	$tert$-butyl hydroperoxide
WT	wildtype

1 Introduction

1.1 Cardiovascular disease

Cardiovascular disease (CVD) is the major cause of death worldwide and is responsible for 31 % of all deaths (WHO 2017). Even though treatment options have improved in the last decades, death to CVD is predicted to gain more importance, due to a growing world population and the increased life expectancy, as the occurrence of disease highly correlates with age (Roth, Forouzanfar et al. 2015). Economically, CVD is ranked under the group of diseases that burdens the health care system the most, causing 12 % of overall health care costs in the year 2006 in Europe (Tarride, Lim et al. 2009). High mortality rates and costs for the health care system clearly demonstrate the importance of research undertaken in this field.

Dysfunction or pathophysiological processes in the functionality of heart, vessels, or blood are combined under the general term CVD. The heart is the pump that moves blood through the tubing system of vessels. Speaking in general terms, blood can be seen as a complex transporting and distribution system that has the task to carry vital gases, nutrients, hormones and metabolites throughout the body to the organs. CVD can lead to undersupply to organs indispensable for life, and by this ultimately to failure of the whole system and death. Possible risk factors that can contribute to the development of CVD are sedentary lifestyle, hypertension, obesity, smoking, age, gender and a history of CVD in the family (Braunwald 1997).

1.2 Hypertension and endothelial dysfunction

Higher blood pressures are directly related to the existence of CVD (Lewington, Clarke et al. 2002). Blood pressure itself is controlled strictly and by many mechanisms. Maintenance of a minimal pressure is of vital importance to supply all tissues with nutrients and oxygen, whereas high blood pressure is shown to have detrimental effects on the cardiovascular system. The blood pressure regulating parameters, for example humoral mechanisms (renin-angiotensin-aldosterone system, antidiuretic hormone,

adrenaline etc.), neuronal mechanisms (sympathetic and parasympathetic nervous system signaling) and physical mechanisms (cardiac output, rheological properties of whole blood etc.), are in a steady interplay for short and long-term adaption.

Hereby the endothelium – the layer of cells in direct contact to the blood stream – holds a particular important role. Endothelial cells (EC) were identified to play a key role in the regulation of vascular tone, thrombocyte adhesion, and inflammatory processes of the vessel wall (Lekakis, Abraham et al. 2011). To regulate vascular tone there is a steady, fine-tuned interplay and communication between ECs and vascular smooth muscle cells (VSMCs). As a hallmark of hypertension, a dysregulation of this balance was found, referred to as endothelial dysfunction (Panza, Quyyumi et al. 1990). In a first study describing endothelial dysfunction, hypertensive patients demonstrate increased vascular resistance of brachial artery in response to acetylcholine compared to healthy controls, but reactivity to the nitric oxide (NO) donor sodium nitroprusside (SNP) was unchanged (Panza, Quyyumi et al. 1990). Many following studies could confirm these findings and demonstrated that the signaling of the endothelium derived, vasodilatory signaling molecule NO is impaired in hypertensive patients, but the general ability of the vessels to dilate is preserved (Panza, Quyyumi et al. 1990, Panza, Casino et al. 1993, Panza, Casino et al. 1993, Taddei, Virdis et al. 1997).

It is until today unclear if endothelial dysfunction is an underlying cause of hypertension or result of hypertension (Bernatova 2014). In transgenic mouse models of the main NO generating enzyme of ECs - endothelial nitric oxide synthase (eNOS) - global knockout (KO) of eNOS results in endothelial dysfunction and development of high blood pressure (Huang, Huang et al. 1995).

Methods to measure endothelial function in humans include invasive insertion of a plethysmograph into the brachial artery and application of pharmacological stimuli (Panza, Quyyumi et al. 1990) and as an advancement a non-invasive method using high-resolution ultrasound to monitor vessel diameter (Celermajer, Sorensen et al. 1992). In animal models, in addition to the non-invasive method of high-resolution ultrasound, isolation of vessel section and measurement of endothelial function in organ baths settings is undertaken. This method has the advantage of observing endothelial function under exclusion of humoral or neuronal influences.

1.3 NO as vasodilator and product of eNOS

The starting point of the discovery of NO being an important signaling molecule in the cardiovascular system was in 1980, when Furchgott et al. demonstrated the release of molecules that were able to dilate vessels after application of acetylcholine (Furchgott and Zawadzki 1980). Since the identity of the molecules was unknown, this molecule was named endothelium derived relaxing factor (EDRF) according to its function. It took eight more years of research to identify EDRF to be NO (Palmer, Ashton et al. 1988).

In ECs, the enzyme eNOS was identified to be the key source of NO in the cardiovascular system. It belongs to a family of NO synthases, which include neuronal nitric oxide synthase (nNOS) where the synthesized NO takes over the function of a neurotransmitter and inflammatory nitric oxide synthase (iNOS) that is important in host defense against pathogens.

In the functional state eNOS is found as a homodimer stabilized by 5,6,7,8-tetrahydrobiopterin and zinc (Chen, Tsai et al. 1994, Crane, Arvai et al. 1998) and each subunit consists of one oxygenase and reductase domain, connected by a calmodulin binding site. For the synthesis of NO, nicotinamide adenine dinucleotide phosphate (NADPH) is bound to the reductase domain of one eNOS protein in the homodimer and electrons are shuttled to the oxygenase domain of the second eNOS subunit in the homodimer, where the synthesis of NO from L-arginine and O_2 is catalyzed (**Equation 1**).

Equation 1 NO synthesis from L-arginine catalyzed by eNOS

$$2\,L-arginine + 4\,O_2 + 3\,NADPH \rightarrow 2\,L-citrulline + 2\,NO$$
$$+3\,NADP^+ + 2\,H_2O$$
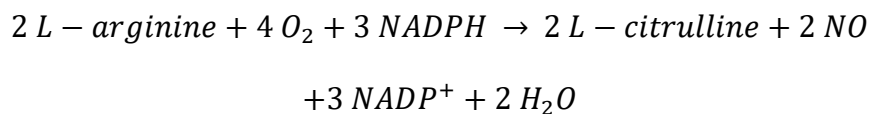
Activity of eNOS is hereby strictly regulated by intracellular levels of Ca^{2+} (Buckley, Mirza et al. 1995, Garcin, Bruns et al. 2004), phosphorylation either enhancing or inhibiting eNOS activity (Michell, Harris et al. 2002, Fulton, Church et al. 2005, Fisslthaler, Loot et al. 2008) and binding of regulatory proteins, as for example caveolin-1 that inhibits eNOS activity by its binding (Ju, Zou et al. 1997).

NO is a highly diffusible gas and radical that possesses hydrophobic properties and thus is capable to diffuse through cell membranes (Moller, Botti et al. 2005). NO signaling by eNOS in ECs is mediated by diffusion of NO to VSMCs and binding of NO to a heme group of the heterodimer soluble guanylate cyclase (sGC) that catalyzes the reaction of guanosine-5'-triphosphate (GTP) to cyclic guanosine monophosphate (cGMP) (Arnold, Mittal et al. 1977). Vasodilation thus occurs, when NO diffuses from ECs to VSMCs and binds to sGC. In the following protein kinase G (PKG) is activated by increased levels of cGMP, leading to decreased levels of intracellular Ca^{2+} and inhibition of myosin phosphorylation by myosin light chain kinase (**Figure 1**)(Zhao, Vanhoutte et al. 2015).
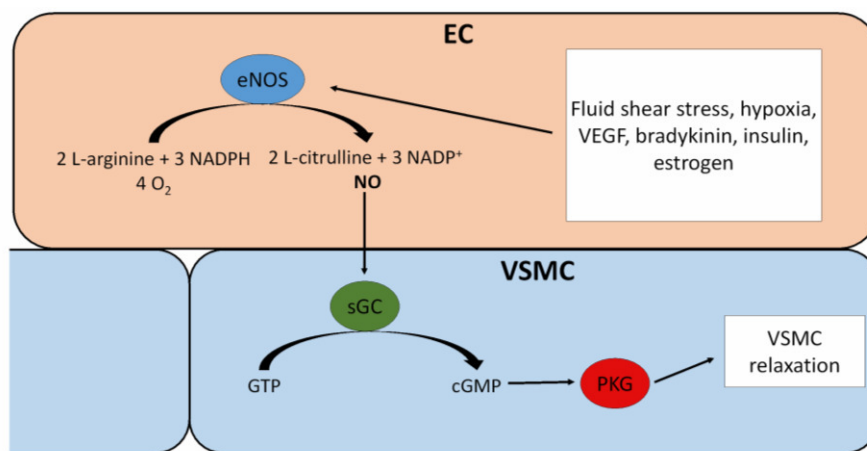
Figure 1 eNOS–sGC signaling in the cells of the vascular wall

Activated by stimuli, eNOS catalyzes the synthesis of NO in EC. NO diffuses to VSMC and activates the transformation of GTP to cGMP. cGMP binds to PKG and leads to relaxation of the VSMC (vascular endothelial growth factor (VEGF)).

Besides binding of sGC, NO has been shown to exert signal transmission by modification of accessible thiol groups and formation of *S*-nitrosated cysteine (Ignarro, Lippton et al. 1981). The formation of *S*-nitrosated cysteine has been shown to be a specific process (Xu, Eu et al. 1998) and mechanisms of enzymatic denitrosation have been proposed to terminate nitrosation mediated signaling (Mannick, Hausladen et al. 1999). A recent study by Wolhuter et al. hypothesized that NO binding to thiol groups itself is too instable to mediate signaling and is therefore an intermediate step to the formation of disulfides that could lead to downstream signaling by conformational changes of the targeted protein (Wolhuter, Whitwell et al. 2018).

As the nomenclature implies and persists until today, *endothelial* nitric oxide synthase was first identified in ECs (Forstermann, Pollock et al. 1991). However, expression of eNOS was until today confirmed in several blood stream cells, including platelet rich plasma (Radomski, Palmer et al. 1990, Sase and Michel 1995, Chen and Mehta 1996), leukocytes (Chen and Mehta 1996, de, Sanchez de Miguel et al. 2001, Muhl and Pfeilschifter 2003, Saluja, Jyoti et al. 2011) and red blood cells (RBCs) (Kleinbongard, Schulz et al. 2006, Cortese-Krott, Rodriguez-Mateos et al. 2012).

The magnitude of NO formation in the cells was hierarchically ranked with the highest amount of NO formed in leukocytes (monocytes, neutrophils, lymphocytes), followed by RBCs and with the lowest amount of NO formed by platelets (Cortese-Krott, Rodriguez-Mateos et al. 2012). The total abundance of RBCs in the blood stream thus makes the role of NO signaling of RBCs an interesting target of further research.

This work is focused on how the blood interacts with the cardiovascular system. In specific the investigations centered on the main cellular component of blood, RBCs and aspects of its role in the cardiovascular system.

1.4   The RBC

Depending on gender and age, whole blood is composed of approximately 42 – 47 % cellular components in healthy adults. RBCs make up approximately 99 % of the volume of the cellular portion of cells in whole blood and have the well-established task to transport gases and nutrients.

To fulfill their task, RBCs are highly specialized cells. They descend from hematopoietic stem cells in the bone marrow and precursor cells called reticulocytes are released into the blood stream that then mature in approximately one week to fully functional RBCs. Before the release in the blood stream, mammalian RBCs progenitor cells lose their nuclei, mitochondria and the endoplasmic reticulum disabling synthesis of proteins. The disability to synthesize new proteins probably determines their short life time of approximately 120 days in humans (Dzierzak and Philipsen 2013).

1.4.1   RBC membrane structure

RBCs are rather simple structured cells that contain no organelles and rely completely on the glycolytic pathway for production of energy. The RBC membrane – starting from the luminal side – is composed of a glycocalyx, phospholipid bilayer membrane and, beneath the membrane, the cytoskeleton. The cytoskeleton is essential for the maintenance of the typical "donut"-like, discoid shape and forms a two-dimensional layer under the cell membrane that is connected to the membrane by the two protein complexes centered around the proteins ankyrin or protein 4.1R. These complexes are interconnected by the tetrameric protein spectrin in a hexagonal fashion. Spectrin is a high molecular weight molecule that consists of two 280 kDa heavy α-subunits and two 246 kDa β-subunits and has a helical structure that enables it to be highly flexible and reversibly deformable.

1.4.2   RBC cytosolic proteins

In their cytosol, RBCs contain 10 mM concentrations of the protein hemoglobin (Helms and Kim-Shapiro 2013). Hemoglobin in adults is generally composed of two α and two β subunits that respectively contain a prosthetic heme group with a central iron(II) ion. This complex is able to reversibly bind oxygen in the lungs and release oxygen in tissues.

To uphold their life time, it is of critical importance for RBCs to effectively neutralize reactive oxygen species (ROS), since RBCs themselves and in particular hemoglobin are a steady sources of ROS (Rifkind, Zhang et al. 1991). This process is due to hemoglobin autoxidation and involves the oxidation of the central iron(II)-ion, of the main RBC protein hemoglobin, to iron(III) and the formation of superoxide anions (**Equation 2**). Under healthy conditions in average 3 % of hemoglobin can be found in the oxidized form named methemoglobin. To neutralize ROS, RBCs are equipped with an antioxidant system, composed of enzymatic defense mechanisms (superoxide dismutase, catalase, glutathione peroxidase, etc.) and antioxidant molecules (glutathione (GSH) / glutathione disulfide (GSSG), ascorbate / dehydroascorbate, etc.).

Equation 2 Hemoglobin autoxidation

$$Hb(II)O_2 \rightarrow Hb(III) + O_2^{\bullet-}$$
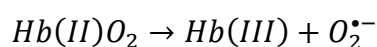
The existence of signaling proteins, as for example, eNOS and sGC, suggested functions of RBCs in the cardiovascular system beyond the transport of oxygen and nutrients

(Kleinbongard, Schulz et al. 2006, Cortese-Krott, Evathia et al. 2018). Many efforts have been undertaken to elucidate the role of eNOS and its product NO in RBCs and it was proposed that NO derived from RBCs could play a role in regulation of hemostasis (Chen and Mehta 1998, Srihirun, Sriwantana et al. 2012, Liu, Wajih et al. 2015), regulation of RBC deformability (Bor-Kucukatay, Wenby et al. 2003, Grau, Pauly et al. 2013) and regulation of vascular tone (Wood, Cortese-Krott et al. 2013, Richards, Bowles et al. 2015). Many of these functions however are under dispute and highly controversially discussed.

1.4.3   RBC deformability

One main feature, determined by the intrinsic properties of RBCs, is the RBC's ability to reversibly deform and extend up to 2.5-fold in its linear axis. Due to this ability, RBCs are able to squeeze through vessels smaller than their own diameter of 8 µm (Canham and Burton 1968). The smallest diameter they encounter is in the spleen, where they have to pass vessel with a diameter of 3 - 5 µM, which was shown to be a "sorting instrument" to remove old and in their functionality impaired RBCs (Deplaine, Safeukui et al. 2011).

RBC deformability is of high importance, in particular in microcirculation and may affect RBCs ability to efficiently deliver oxygen to tissues (Parthasarathi and Lipowsky 1999, Tomaiuolo 2014). Impaired RBC deformability moreover affects whole blood viscosity (Baskurt and Meiselman 1997) and as illustrated by Hagen-Poiseuille's law, higher whole blood viscosity has the consequence of longer traverse times and lower blood flow (Q: volumetric flow rate, Δp: pressure difference, r: radius, l: length, η: viscosity). Even though this equation is only applicable for Newtonian fluids under laminar flow, the equation can be used for approximation of whole blood flow.

Equation 3 Hagen-Poiseuille's law

$$Q = \frac{\Delta p \times \pi \times r^4}{8 \times l \times \eta}$$

The mechanical properties and RBCs ability to deform are determined by three main factors: cell geometry, membrane properties and intracellular viscosity (Mohandas and Gallagher 2008).

RBC cell geometry is unique and optimized for efficient gas exchange and massive deformation. In average, the RBC has approximately a volume of 90 fl and a surface area of 136 μm^2. The ratio of surface area to volume is an important factor for the mechanical properties and changes will impair RBCs in their ability to deform. The peculiar biconcave shape of RBCs is determined by the interaction of the cytoskeleton and the phospholipid bilayer and the stability of the spectrin tetramer and by its binding to the protein complexes connecting the cytoskeleton to the phospholipid bilayer (Liu and Palek 1980, Chasis and Mohandas 1986). Disruptions of the functionality, due to mutation of proteins important for these interactions, lead to a disease picture called hereditary spherocytosis (Agre, Casella et al. 1985, Eber, Gonzalez et al. 1996, Jarolim, Murray et al. 1996). RBCs in hereditary spherocytosis are characterized by shifts in the ratio of surface area to volume that can lead to severe anemic conditions due to increased uptake of less deformable BRCs by the spleen (Crosby 1972).

Membrane properties as well are heavily dependent on the underlying cytoskeleton. In particular spectrin has been attributed an important role due to its structure of connected helical repeats that could be thought of as mechanical springs (Lux 2016). Posttranslational modifications of spectrin have been proposed to have influence on spectrin properties (Vilsen and Nielsen 1984, Bor-Kucukatay, Wenby et al. 2003) and a recent study could demonstrate that under shear stress, spectrin-repeats unfold and key cysteine groups get exposed (Krieger, An et al. 2011). This leaves room to speculate that posttranslational modification of these groups might be key regulators of spectrin properties and thus membrane properties.

Intracellular viscosity is the last of the three important regulators of RBC deformability. It is mainly regulated by intracellular content of hemoglobin and the ion hemostasis that indirectly regulates RBC volume (Mohandas and Gallagher 2008). The intracellular hemoglobin content is strictly regulated and the mean corpuscular hemoglobin concentration in humans is 33 g/dl. Higher concentrations of hemoglobin cause abrupt increases of intracellular viscosity and changed RBC deformability (Cokelet and Meiselman 1968).

1.5   Role of RBCs in control of NO metabolism

For a long period of time, RBCs were seen as scavengers of NO, due to the reaction of the central iron in the prosthetic heme group of hemoglobin with NO. The formation of nitrosylated hemoglobin happens extremely fast with a rate of 10^7 $M^{-1}s^{-1}$ (Cassoly and Gibson 1975), whereas the dissociation to hemoglobin and NO is extremely slow (Cooper 1999) (**Equation 4**). Moreover, NO reacts with oxygenated hemoglobin to the metabolite nitrate and methemoglobin (**Equation 5**) (Liu, Miller et al. 1998). Nitrate itself was seen as the biological inert metabolite and blood as a regulating mechanism to scavenge NO and inhibit endothelium derived NO signaling (Butler, Megson et al. 1998). However as described in a comprehensive review by Lundberg et al., newly reported data relativizes this view and suggests that nitrate can be transformed to the bioactive metabolite nitrite, by being actively excreted through saliva glands, reduced to nitrite by bacteria in the buccal cavity, swallowed and taken in by the intestines (Lundberg, Gladwin et al. 2015).

Equation 4 Binding of NO to deoxyhemoglobin

$$Hb(II) + NO \rightleftharpoons HbNO$$

Equation 5 Oxidation of NO to nitrate by oxygenated hemoglobin

$$Hb(II)O_2 + NO \rightarrow Hb(III) + NO_3^-$$
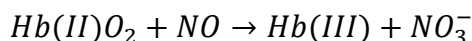
1.5.1.1 NO synthesis under normoxic conditions

Different mechanisms have been proposed that could mediate NO signaling, although the presence of high hemoglobin concentrations. One proposed mechanism is the compartmentalization of NO synthesis in RBCs. As demonstrated in a recent study, RBCs also possess a functional eNOS and sGC that – if localized in direct vicinity to eNOS - could mediate NO downstream signaling (Cortese-Krott, Mergia et al. 2018). Another theory is the synthesis of NO directly at the RBC membrane enabling the hydrophobic NO to diffuse though the membrane and escape dioxygenation via intracellular hemoglobin (Gladwin, Schechter et al. 2005).

1.5.1.2 NO synthesis under hypoxic conditions

Another possible mechanism to avoid hemoglobin inhibition of NO signaling could be the mediation of NO signaling by its metabolites. In particular, under hypoxic conditions, RBCs have been reported to cause vasodilation of vascular preparations and these findings were attributed to different NO metabolites (Cosby, Partovi et al. 2003, Crawford, Isbell et al. 2006, Webb, Milsom et al. 2008).

Different NO metabolites (Jia, Bonaventura et al. 1996, Cosby, Partovi et al. 2003, Herold 2004) and bio activation mechanisms have been proposed (Webb, Milsom et al. 2008, Aamand, Dalsgaard et al. 2009, Ghosh, Kapil et al. 2013). In the following the two most widely discussed mechanisms will be presented. As a first mechanism *S*-nitrosation of hemoglobin on cysteine-93 was proposed (Jia, Bonaventura et al. 1996). After nitrosylation of the central heme group, NO was proposed to be transferred to cysteine-93 of β hemoglobin. Release of NO then was regulated by conformational changes of hemoglobin (Jia, Bonaventura et al. 1996). However, multiple findings from several independent working groups heavily questioned this mechanism (Deem, Gladwin et al. 2001, Huang, Ucer et al. 2002, Joshi, Ferguson et al. 2002, Isbell, Sun et al. 2008).

The more accepted and established possible mechanism is the reduction of nitrite to NO by deoxygenated hemoglobin (**Equation 6**) (Cosby, Partovi et al. 2003). In support of this finding is that RBCs store high concentrations of nitrite (Dejam, Hunter et al. 2005), there is a gradient of nitrite from arterial to venous plasma, a finding in support of utilization of nitrite for hypoxic dilation (Gladwin, Shelhamer et al. 2000), and deoxygenated hemoglobin was shown to be essential for reduction of nitrite to NO under hypoxia (Liu, Wajih et al. 2015)

Equation 6 Reduction of nitrite to NO under hypoxic conditions

$$Hb(II) + NO_2^- + H^+ \rightarrow Hb(III) + NO + OH^-$$
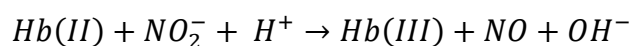
Thus, RBCs possess two sources of NO. First there is the enzyme eNOS, which would mainly take over NO production under normoxic conditions and second mechanisms taking over under hypoxic conditions, most likely regulated by the reduction of nitrite to NO by deoxygenated hemoglobin.

1.6   The intrinsic and paracrine roles of NO derived from RBCs

The effects of eNOS and NO in RBCs remain - until today – a matter of debate. Many efforts were put into the question of what effect NO has on intrinsic RBC properties and what effect NO has in paracrine signaling.

Regarding changes of intrinsic RBC properties, dependent on the eNOS–sGC pathway and NO, it was postulated that NO may be the main regulator of RBC deformability (Bor-Kucukatay, Wenby et al. 2003, Grau, Pauly et al. 2013), a finding that was questioned by findings of others that were unable to detect any changes of RBC deformability by application of NO or activation of the eNOS–sGC pathway (Barodka, Mohanty et al. 2014, Belanger, Keggi et al. 2015, Cortese-Krott, Mergia et al. 2018).

Furthermore, RBC-derived NO and RBC-eNOS were implicated with regulation of vascular tone and the questions remains, what role NO and RBC eNOS have in the controlled release of ATP by the pannexin-1 channel and in overall regulation of vascular tone.

1.6.1   eNOS–sGC pathway in RBCs and effects on RBC deformability

The role of NO and the eNOS–sGC pathway in the regulation of RBC deformability is under debate. The first study to propose an influence of NO on RBC deformability found that administration of a nitric oxide synthase (NOS) inhibitor significantly reduced deformability (Starzyk, Korbut et al. 1997). The following studies were able to demonstrate improvement of RBC deformability by the application of eNOS substrate, NO-donors and activators of the sGC, the receptor enzyme for NO (Mesquita, Picarra et al. 2002, Bor-Kucukatay, Wenby et al. 2003, Grau, Pauly et al. 2013). However, the mechanism of this effect remained unknown. It was proposed that the effects might be mediated in part by eNOS–sGC dependent signaling and *S*-nitrosation of spectrin (Bor-Kucukatay, Wenby et al. 2003, Grau, Pauly et al. 2013).

These findings were questioned by works of several independent groups that were unable to reproduce many of these data, starting a new discussion about the effects of NO on RBC deformability. In specific, the more recent studies were unable to reproduce NO dependent, effects of exogenously applied NO donors, eNOS substrate, eNOS inhibitors or sGC activators calling for a careful reassessment of the role of the eNOS–sGC pathway

and NO on RBC deformability (Barodka, Nagababu et al. 2014, Belanger, Keggi et al. 2015, Cortese-Krott, Mergia et al. 2018).

1.6.2 NO and its role in controlled release of ATP from RBCs

The release of adenosine 5'-triphosphate (ATP) into the blood stream and its property to induce vessel dilation were observed already 55 years ago (Berne 1963). In particular under conditions of hypoxia (Bergfeld and Forrester 1992, Bodin and Burnstock 1995) and under conditions of high shear stress (Bodin, Bailey et al. 1991, Bodin and Burnstock 1995) ATP was shown to be essential to ensure sufficient blood flow. Next to ATP, as a potent vasodilator, vasodilatory effects of AMP, ADP and UTP were found (Wolf and Berne 1956, Berne 1963).

The effects of purine based signaling and in specific of ATP are mediated by purinergic receptors on EC, namely $P2Y_1$ and $P2Y_2$ leading to vasodilation via activation of eNOS in ECs (Kennedy and Burnstock 1985, Buvinic, Briones et al. 2002)

As possible sources, the active release of ATP was found to be mediated by skeletal and heart muscle cells (Forrester and Lind 1969, Paddle and Burnstock 1974), endothelium (Pearson and Gordon 1979, Lollar and Owen 1981) and platelets (Born and Kratzer 1984). Already in 1989 it was assumed that RBCs may take part to the general pool of ATP in the blood stream by a steady release during deformation and by RBC hemolysis (Luthje 1989). This assumption was confirmed by the first work that was able to demonstrate release of ATP from RBCs and regulation of pulmonary vessel diameter (Sprague, Ellsworth et al. 1996). Several works investigated the possible mechanisms leading to release of ATP and found hypoxic conditions, deformation and nitrite - by a NO dependent mechanism - to be inducers of RBC mediated ATP release (Wan, Ristenpart et al. 2008, Cao, Bell et al. 2009, Sridharan, Adderley et al. 2010, Forsyth, Wan et al. 2011, Goldman, Fraser et al. 2012, Cinar, Zhou et al. 2015).

As result of these multiple investigations a mechanism dependent on activation of adenylate cyclase (AC) by a $G\alpha_i$ coupled protein receptor, intracellular increases of cyclic adenosine monophosphate (cAMP), protein kinase A (PKA) activation and by an unknown, subsequent intermediate step pannexin-1 activation (Sprague, Ellsworth et al. 2001, Ellsworth and Sprague 2012, Goldman, Fraser et al. 2012) was postulated. This process was hypothesized to be modulated by cGMP that led to inhibition of

phosphodiesterase 3, an esterase responsible for degradation of cAMP (**Figure 2**) (Richards, Bowles et al. 2015). However, the role of NO in controlled release of ATP from RBCs is unknown.
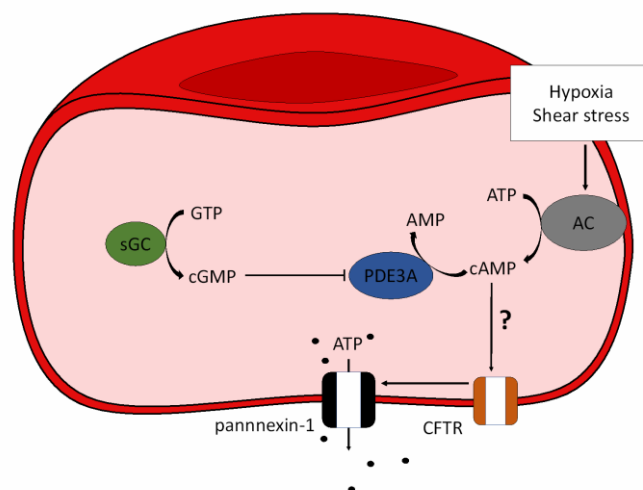
Figure 2 Proposed mechanism of ATP release from RBCs

It was proposed that intracellular increases of cAMP due to activation of AC by hypoxia or shear stress lead to pannexin-1 mediated release of ATP. As an unknown intermediate step involvement of cystic fibrosis transmembrane conductance regulator (CFTR) channel was proposed. sGC dependent synthesis of cGMP was suggested to influence intracellular signaling of this pathway by inhibition of phosphodiesterase 3A (PDE3A).

1.6.3 The role of RBC eNOS and NO for blood pressure regulation

The phenotypes in all mouse strains of eNOS genetic deficiency demonstrate high blood pressure and thus demonstrate the importance of eNOS for the cardiovascular system and blood pressure regulation. eNOS KO mice present with a phenotype of hypertension, reduced heart rate and increases of renin concentrations in plasma (Huang, Huang et al. 1995, Shesely, Maeda et al. 1996, Stauss, Godecke et al. 1999).

At that time, the phenotype of the eNOS KO mice was attributed to EC eNOS, however a reassessment of this findings after the discovery of a functional eNOS enzyme in blood cells was necessary (leukocytes (Chen and Mehta 1996, de, Sanchez de Miguel et al. 2001, Muhl and Pfeilschifter 2003, Saluja, Jyoti et al. 2011), platelets (Radomski, Palmer et al. 1990, Sase and Michel 1995) and RBCs (Kleinbongard, Schulz et al. 2006, Cortese-

Krott, Rodriguez-Mateos et al. 2012)). Although each RBC only produces 9.8 fmol/min of NO, their shear abundance in the blood stream might enable them to have physiological relevant effect on blood pressure regulation (Cortese-Krott, Rodriguez-Mateos et al. 2012).

In a work investigating the role of RBC eNOS in blood pressure regulation, the authors were able to demonstrate that lack of eNOS in blood cells causes increases of blood pressure (Wood, Cortese-Krott et al. 2013). Depletion of platelets or leukocytes did not impact the phenotype, leaving the deduction that RBCs were responsible for the hypertensive phenotype.

Using the eNOS chimeric mouse models, it was found that lack of eNOS resulted in a stepwise increase of blood pressure parameters dependent on the tissue eNOS was lacking (mean arterial pressure, systolic blood pressure and diastolic blood pressure). Starting with the chimeric mouse model exhibiting lowest blood pressure the following hierarchy was found: 1) mice expressing eNOS in endothelium and blood cells, 2) mice expressing eNOS in endothelium but deficient of eNOS in blood cells, 3) followed by mice expressing eNOS in blood cells and 4) deficient of eNOS in both compartments.

Furthermore, the study demonstrated that nitrite levels were significantly decreased in the absence of eNOS in blood cells and low levels of nitrite correlated with high values of mean arterial pressure. Decreases of nitrite levels might have detrimental effects on the cardiovascular system, since several works found important effects of nitrite on vascular relaxation in states of hypoxia (Cosby, Partovi et al. 2003, Maher, Milsom et al. 2008), platelet aggregation (Webb, Patel et al. 2008), hypoxic renal damage (Cantow, Flemming et al. 2017) and hypoxic damage of cardiomyocytes (Kamga Pride, Mo et al. 2014).

There is one major drawback to the study conducted in 2013 (Wood, Cortese-Krott et al. 2013). To achieve mouse models expressing eNOS in different tissue compartments wildtype (WT) and eNOS KO mice were irradiated and transplantation of bone marrow was undertaken. This procedure causes inflammatory reactions and up-regulation of iNOS (Schaue, Micewicz et al. 2015), another source of NO, which might contribute to the general pool of NO metabolites. In addition, the procedure was not specific for RBCs and remaining blood cells of the host could still be in circulation (Cortese-Krott and Kelm 2014). An approach without these disadvantages is the creation of genetically modified

mice, which would enable the identification of the mechanisms responsible for changes in blood pressure due to KO of eNOS from RBCs.

2   Aim of the Study
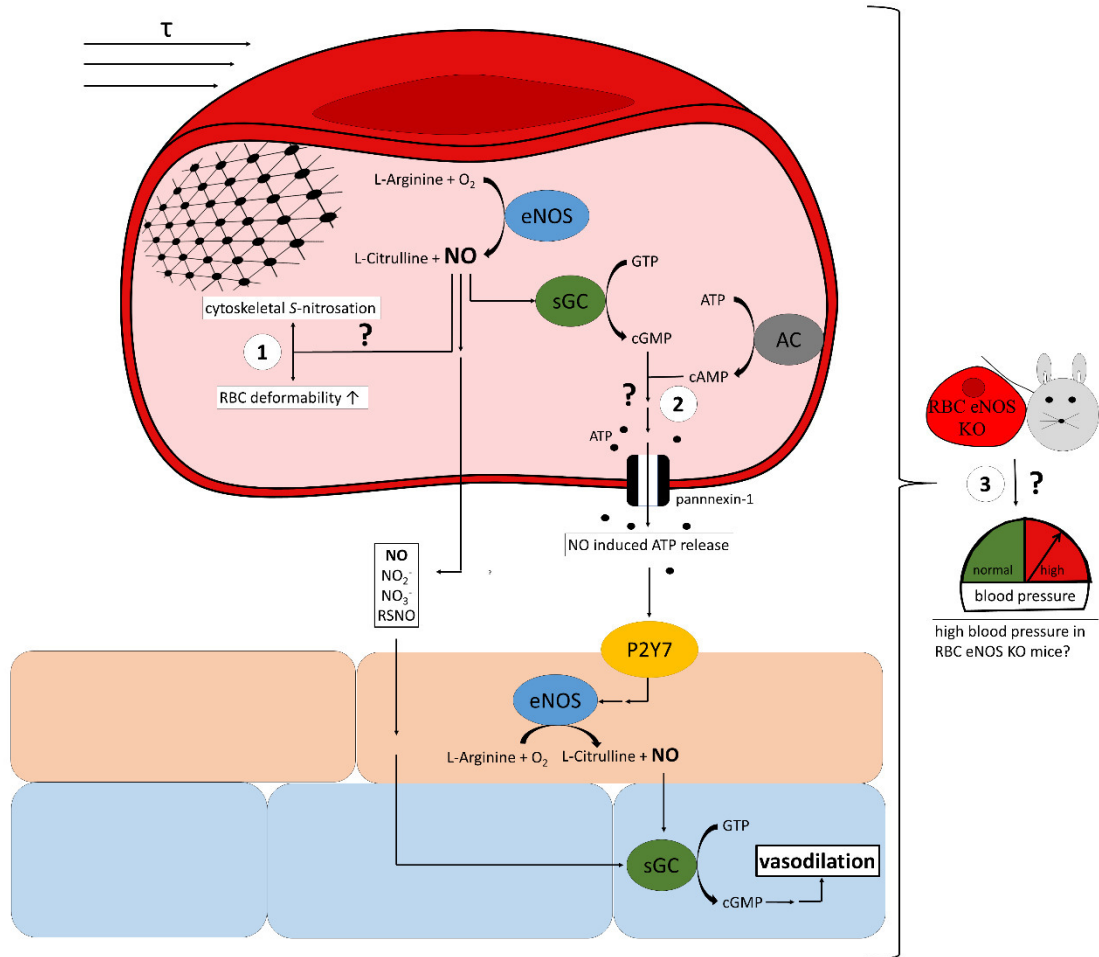
Figure 3 Graphical abstract

The working hypothesis of this work was that NO and its metabolites may contribute to the regulation of intrinsic properties of RBCs and vascular tone. The study can be separated in three parts: 1) The effects of NO on RBC deformability and on S-nitrosation of the cytoskeletal protein spectrin. 2) The effects of NO dependent signaling on the controlled release of ATP from RBCs. 3) The effects of lack of eNOS in RBCs on hemodynamics and vascular endothelial function.

Next to the classical role as transporters of gases, nutrients and metabolites, studies proposed that RBCs may possess more functions in the cardiovascular system. In particular the role of RBC-eNOS synthesized NO in regulation of intrinsic RBC properties including deformability and vascular tone are unknown or controversially discussed.

The hypothesis of this work was that NO and its metabolites derived from RBCs may contribute to the regulation of RBC functional properties including deformability and RBC mediated regulation of vascular tone.

In the following, three aspects of NO in RBCs will be analyzed:

1. The effect of NO on RBC deformability will be investigated. For that purpose, a study will be conducted investigating RBC properties in hypertensive patients. Moreover, isolated human RBCs will be incubated ex-vivo with the NO donors (DEA/NO, *S*-nitrosated L-cysteine) and ROS (*tert*-butyl hydroperoxide) and the effects on RBC deformability will be measured by ektacytometry. In addition, RBC deformability will be tested in transgenic mouse lines, i.e. eNOS KO and Nrf2 KO mice.

2. The effect of intracellular NO signaling on controlled ATP release by RBCs will be analyzed. In order to characterize this mechanism, stimulation of the guanylate and AC pathway of RBCs with ongoing measurements of extracellular ATP will be conducted.

3. Tissue specific RBC eNOS KO mice will be created and characterized. For that purpose, tissue specific eNOS KO and knock-in (KI) mouse models will be generated. Next to hemodynamic measurements, also vascular endothelial function will be assessed ex-vivo to exclude effects of the loxP-Cre system on vessel functionality.

3 Materials and Methods

3.1 Materials and stock solutions

If not stated otherwise, the chemicals used were purchased from Sigma Aldrich (St. Louis, USA) and of the highest purity available. All solutions and buffers - not purchased - were prepared using MilliQ water from an in-house station (Millipore, Darmstadt, Germany). The main purchased buffers used were Dulbecco's phosphate buffered saline (DPBS, Sigma Aldrich, St. Louis, USA, 136.9 mM NaCl, 8.1 mM Na_2HPO_4, 2.7 mM KCl, 1.5 mM KH_2PO_4, 0.9 mM $CaCl_2$ x H_2O, 0.5 mM $MgCl_2$ x 6 H_2O, pH = 7.4) and Hanks' balanced salt solution (HBSS, Thermo Fisher Scientific, Waltham, USA, 137.9 NaCl, 5.6 mM glucose, 5.3 mM KCl, 4.2 mM $NaHCO_3$, 1.3 mM $CaCl_2$, 0.5 mM $MgCl_2$ x 6 H_2O, 0.4 mM KH_2PO_4, 0.4 mM $MgSO_4$ x 7 H_2O, 0.3 mM Na_2HPO_4, pH = 7.0 – 7.4).

3.2 Studies of volunteers and hypertensive patients

For all human ex-vivo studies, whole blood was drawn from healthy volunteers in the age of 20 - 40 years, after being informed about the study and giving written consent before the enrollment (ClinicalTrials.gov: NCT02272530).

Hypertensive patients from the outpatient clinic of the department of cardiology, pneumonology and angiology of the university hospital Düsseldorf were recruited and enrolled after the regulations of the Declaration of Helsinki. The study was registered at the center for clinical trials of the University of Düsseldorf (KKS, registration ID 201307443).

3.3 Mouse studies

Mouse studies were conducted in agreement with the "Guide for the Care and Use of Laboratory Animals" and the German "Tierschutzgesetz", after being approved by the "Landesamt für Natur, Umwelt und Verbraucherschutz Nordrhein-Westfalen".

Exercise protocols on pannexin-1 KO mice and WT controls were conducted at the University of Virginia after approved animal protocols of the University of Virginia.

3.4   RBC isolation

Whole blood was isolated using a cannula (21 G, Becton Dickinson, Franklin Lakes, USA) by venipuncture of the antecubital vein into heparinized tubes (17 IU/mL, Becton Dickinson, Franklin Lakes, USA). The blood was transferred into a 20 mL syringe (B Braun Melsungen, Melsungen, Germany) with the plunger removed and the front tip closed by a lit. The syringe was inserted into a 50 mL Falcon tube (Greiner Bio-One, Kremsmünster, Austria) tip forward. After centrifugation (Rotina 38R, Andreas Hettich GmbH, Tuttlingen, Germany) for 10 minutes, at 4 °C and 800 g plasma and buffy coat were aspirated. The lower part of the RBC pellet was transferred into the Falcon tube by removal of the lit on the syringe's tip and washed using HBSS. Washing steps were repeated 3 times using HBSS and separated between each step by centrifugation for 10 minutes, at 4 °C and 300 g.

3.5   *S*-Nitrosated L-cysteine

A 100 mM stock solution was yielded by mixing four parts of a 250 mM $NaNO_2$ and four parts of 250 mM L-cysteine-HCl. This mixture was acidified with one part of 1 M HCl (Merck KGaA, Darmstadt, Germany), stored on ice and light protected. Immediately before use the mixture was neutralized with one part of self-prepared 1 M NaOH. pH indicator stripes were used to check for a pH value of 7.0.

3.6   RBC lysis

RBCs were lysed by dilution of RBC pellet one to five with a solution of 150 mM NH_4Cl, one tablet of cOmplete Ultra Tablets (Roche Diagnostics, Mannheim, Germany) and 2 mM DTT in H_2O_{dd}. To completely lyse RBCs, this solution was sonicated for 30 seconds (Sonorex, Bandelin electronic GmbH & Co. KG, Berlin, Germany) and frozen in liquid nitrogen. For further processing lysed RBCs were left on ice until completely thawed and centrifuged (MIKRO 200R, Andreas Hettich GmbH, Tuttlingen, Germany) for 15 minutes, at 4 °C and 20,000 g. The debris was disregarded and the clear, red supernatant used for further analysis,

3.7 Protein determination

Protein concentrations were determined using a kit based on the method of Lowry (Lowry, Rosebrough et al. 1951), which was modified according to the manufacturer's protocol (DC Protein Assay, Bio-Rad Laboratories Inc., Hercules, USA).

For every protein analysis standards were freshly prepared using bovine serum albumin (Carl Roth GmbH + Co. KG, Karlsruhe, Germany) in the range of 0.2 – 2 mg/ml protein concentration. 5 µL of samples or standards were incubated on 96-well plates (Greiner Bio-One, Kremsmünster, Austria) with 25 µL of solution A and 200 µL of solution B. After 15 minutes of incubation protected from light exposure, the samples were immediately analyzed at 740 nm wavelength using a microplate reader (FLUOstar Omega, BMG Labtech GmbH & Co. KG, Ortenberg, Germany).

3.8 Flow Cytometry

To measure intracellular levels of ROS blood was drawn as described in § 3.4 and the protocol conducted as previously described (Cortese-Krott, Rodriguez-Mateos et al. 2012). Until further processing within 2 hours blood was kept on ice. To reach a concentration of approximately $4 \cdot 10^5$ cells/µl, blood was diluted 1:500. Aliquots of blood were treated using 4-amino-5-methylamino-2',7'-dichlorofluoresceine diacetate (DAF-FM; Thermo Fisher Scientific, Waltham, USA), red mitochondrial superoxide indicator (MitoSOX; Thermo Fisher Scientific, Waltham, USA) and thiol tracker (Thermo Fisher Scientific, Waltham, USA) and analyzed in a FACSCantoII flow cytometer (Becton Dickinson, Franklin Lakes, USA).

3.9 RBC deformability measurements

Shear stress dependent changes in RBC shape were measured by ektacytometry. Samples were measured by addition of 25 µl of sample to 5 ml of a pre-warmed (37 °C), highly viscous PVP (RR Mechatronics, Zwaag, the Netherlands) solution in a laser optical rotational red cell analyzer (Lorrca®, RR Mechatronics, Zwaag, the Netherlands).

3.10 Whole blood viscosity measurements

Whole blood was measured using the LS300 system (proRheo, Althengstett, Germany). This measuring system is based on the Couette principle, which works with a cup rotating around a static bob that is constantly measuring the torque during the exposure of whole blood to different shear rates. The measuring cup was pre-heated to 37 °C and samples inserted until the turning bob was completely covered. Measurements were recorded using the manufactures software Low Shear LS 300.

3.11 RBC ghost preparation

RBCs were isolated as described in § 3.4. Except for the only difference of using an isotonic KCl solution (148 mM) for the washing steps. After the last washing step, the RBC pellet was diluted to a 50 % hematocrit using the isotonic KCl solution. All cells and solutions were kept at 0 °C during all steps.

The cells were lysed by addition of one part of RBC pellet to 10 parts of lysis buffer (4 mM $MgSO_4$, 3.8 mM CH_3COOH, pH = 7.0) in a 50 mL Falcon tube, incubated for 1 minute and centrifuged for 15 minutes, at 4 °C and 15,000 g. A hypertonic 200 mM KCl solution was added to the residual membranes of the RBCs and the solution thoroughly mixed, to efficiently remove cytoplasmic proteins from RBCs. After 2 minutes of incubation, the solution was washed by the addition of washing medium (4 mM $MgSO_4$, 1.2 mM $NaCH_3COO$, 2 mM NaH_2PO_4, pH = 7.0) and again thoroughly mixed. Centrifugation for 15 minutes, at 4 °C, 15,000 g and addition of washing medium was repeated for at least two times until ghosts had a greyish / white color. RBC ghosts were resealed by the addition of a solution of 180 mM KCl and 2.25 Tris / HCl first at 0 °C for 10 minutes, followed by 45 minutes at 38 °C. RBCs were washed afterwards in the buffer needed for further experiments (Bjerrum 1979).

3.12 Biotin switch assay

The biotin switch assay was conducted according to the manufactures protocol of the *S*-nitrosylated protein detection kit (Cayman Chemical, Ann Arbor, USA). For the assay, samples were diluted to a protein concentration of 0.8 mg/ml.

In short, to each RBC pellet five volumes of Buffer A containing Blocking Reagent were added to alkylate free, accessible thiol groups. After an incubation time of 30 minutes at 4 °C, samples were transferred into a 15 ml Falcon tube and proteins precipitated by the addition of four volumes of ice-cold acetone and incubation for 1 hour at -20 °C. Subsequently samples were centrifuged for 10 minutes, at 4 °C at 3,000 g. The supernatant was disregarded and the yielded pellet was dissolved in Buffer B containing Reducing and Labeling Reagent and incubation for 1 hour at ambient temperature. With this mixture S-nitrosated groups in proteins were reduced to thiols and directly labeled with a biotin tag. The treatment was then removed as previously described by addition of ice-cold acetone, incubation for 1 hour and centrifugation. The yielded pellet was dissolved in Wash buffer and protein concentrations determined. Samples then were further processed according to § 3.13 SDS-page (Western Blotting).

3.13 SDS- page (Western Blotting)

Dependent on tissue and cell type the in the figure legend indicated amounts of protein were loaded on the SDS gel. For the experiments 7 % and 3 – 8 % Tris-acetate Novex precast gels (Thermo Fisher Scientific, Waltham, USA) were used after manufactures instructions. Samples were mixed before application to the gel with NuPAGE sample reducing agents (Thermo Fisher Scientific, Waltham, USA) and NuPAGE LDS sample buffer (Thermo Fisher Scientific, Waltham, USA) and denatured at 70 °C for 10 minutes (Thermoshaker TS-100, bioSan, Riga, Latcia). SDS-page was run after the manufactures protocol at 150 V for 60 minutes.

After the SDS-page, run proteins were transferred to a nitrocellulose membrane (Amersham Protran 0.2, GE Healthcare Life Sciences, Chicago, USA) for 1 hour at 30 V in a transfer buffer (10 % methanol, 5 % NuPage transfer buffer, 1% antioxidant and H_2O_{dd}). After the transfer of proteins to the nitrocellulose membrane, the membranes were blocked for 1 hour at room temperature using ECL blocking reagent (GE Healthcare Life Sciences, Chicago, USA). Dependent on the protein of interest different first antibodies (**Table 1**) were used as indicated dilution overnight at 4 °C. Antibody was removed by four consecutive washing steps using tris-buffered saline (Bio-Rad Laboratories Inc., Hercules, USA). Secondary antibody (**Table 1**) was chosen dependent on the host the first antibody was produced in. After incubation for 1 hour at room temperature,

secondary antibody was washed from the membrane by four consecutive washing steps. Western blots were analyzed using the ImageQuant LAS 4000 (GE Healthcare Life Sciences, Chicago, USA) and Amersham ECL Select Western Blotting Detection Reagent (GE Healthcare Life Sciences, Chicago, USA). Evaluation of the bands by densitometry was conducted using the ImageStudio Lite software (LI-COR Biosciences, Bad-Homburg, Germany).

Table 1 Antibodies used for Western blotting

Antibody	Vendor	Ordering number
Anti-eNOS	Becton Dickinson, Franklin Lakes, USA	610297
Anti-spectrin	Sigma Aldrich, St. Louis, USA	S3396
Anti-mouse – horseradish conjugate	Bio-Rad Laboratories Inc., Hercules, USA	170-6516
Anti-mouse – Cy 3 conjugate	Thermo Fisher Scientific, Waltham, USA	A10521
Streptavidin – Cy 5 conjugate	Thermo Fisher Scientific, Waltham, USA	438316

3.14 Chemiluminescence detection

To analyze nitrosated bindings to proteins the chemiluminescence detector (CLD) 88 e (ECO PHYSICS GmbH, Munich, Germany) connected to a PowerChrom 280 (eDAQ Pty Ltd, Denistone East, Australia) was used. To release NO from proteins with *S*-nitroso bindings, the samples were injected into a reaction chamber heated to 60 °C containing a triiodide solution (45 mM potassium iodid, 10 mM iodine in 7 % Millipore-water in acetic acid). In the reaction chamber *S*-nitroso bindings are reduced and NO is released. NO is carried to the detector by a constant stream of helium through the reaction chamber. In the detector, NO reacts with in excess available ozone to nitrogen dioxide with an excited electron. With the transfer of the electron a photon is released, which is measured by a photomultiplier.

All incubations and solution described in the following were stored on ice and protected from light exposure. To measure nitrosated modifications, the samples were incubated with a solution of 5 % sulfanilamide in an aqueous 3.25 % HCl to remove impurities of nitrite. In order to be able to distinguish between *S*-nitrosocysteine and *N*-nitrosamines,

S-nitroso bindings were removed by the reaction with a solution of 0.2 % $HgCl_2$ in 0.9 % NaCl. In the following the samples were treated with the 5 % sulfanilamide in 3.25 % HCl solution to remove residual nitrite impurities. The amount of S-nitroso bindings was then calculated by subtraction of values for N-nitrosoamines from values for all nitroso modifications.

For quantification S-nitrosated cysteine (CysNO) was used as a standard.

3.15   Electron paramagnetic spin measurement

Electron paramagnetic spin (EPR) measurements were conducted at the Max-Planck-Institut in Mülheim, Germany by Anton Savitsky, PhD using a Bruker ELEXSYS E-500 CW X-band spectrometer (Bruker Corporation, Billerica, USA). The machine ran in the perpendicular mode of the ER 4116DM dual mode cavity. To set the sample temperature to 15 K an ESR900 cryostat (Oxford Instruments, Abingdon, the UK) was used.

3.16   Incubation of RBCs under hypoxic conditions

RBCs were isolated as described in § 3.4. To deoxygenize RBCs, a stream of argon was led through the RBC pellet for 15 minutes. Then the RBCs were transferred into a glovebox (Coy Laboratory Products Inc, Grass Lake, USA) with an atmosphere of 98 % of nitrogen and 2 % of hydrogen and incubated with $1 - 1000\,\mu M$ $NaNO_2$. Samples were removed after 1, 5, 15 and 30 minutes for EPR measurements and Biotin switch assay.

3.17   GSH and GSSG measurements using LC-MS / MS

RBC pellet was treated in a ratio of ten to one with a solution of 100 mM N-ethylmaleimide and 20 mM ethylene diamine tetra acetic acid in phosphate buffered solution. After centrifugation at 4 °C, for 10 minutes and 800 g and removal of the supernatant the pellet was washed three times by the addition of 0.5 % bovine serum albumin in HBSS and centrifugation at 4 °C, for 10 minutes and 300 g. Cells were lysed and precipitated by the addition of 5 % sulfosalicylic acid and 10 mM N-ethylmaleimde in H_2O. To this solution an internal standard was added (glutathione ethyl ester) to a final concentration of 50 µM. This solution was put into the ultrasonic bath for 20 seconds and centrifuged for 10 minutes, at 4 °C and 10,000 g. The supernatant was separated and the

cell debris washed. After another centrifugation for 10 minutes, at 4 °C and 10,000 g the supernatant was merged with the previously collected supernatant. This was transferred for measurement to an Agilent Technologies 1290 Infinity coupled to an Agilent Technologies 6550 I Funnel Q-TOF LC/MS (Agilent Technologies Inc, Santa Clara, USA). For separation of the analytes a Zorbax Eclipse Plus C18 RRHD 2.1x50 mm 1.8 µm column (Agilent Technologies Inc, Santa Clara, USA) was used. The ionization source was set to a gas temperature of 220 °C, drying gas flow of 12 l/min, nebulizer pressure of 35 psig, sheath gas temperature 330 °C, sheath gas flow of 11 l/min, VCapillary voltage 2500 V, nozzle voltage 1000 V, fragmentor voltage 30 V and Oct1 RF Vpp 750 V. For data analysis, the MassHunter Workstation software version B07.00/Build7.0.457.0 was used.

3.18   Measurement of intracellular purines using LC-MS / MS

Isolated RBCs were diluted to a hematocrit of 20 % in a solution of 0.5 % HBSS and incubated with pharmacological activators (10 µM isoproterenol, 200 µM DEA/NO, 10 µM Bay41 , 50 µM forskolin) and inhibitors (10 µM IBMX, 100 µM sildenafil-citrate) at 37 °C for 20 minutes (first 10 minutes inhibitor then second 10 minutes activator). After 20 minutes incubation samples were centrifuged for 10 minutes, at 300 g at room temperature. The supernatant was removed and ATP levels in the supernatant measured (method § 3.19). RBCs were lysed by addition of an ice-cold mixture of 20 % acetonitrile, 40 % methanol and 40 % water and cells additionally lysed by sonication for 20 seconds. Samples were heated to 60 °C for 10 minutes to complete enzyme denaturation. Subsequently samples were cooled on ice and a solid pellet of cell debris was formed by centrifugation for 90 minutes, at 4 °C and 3000 g. The supernatant was put aside and cell debris were washed again using the same mixture as before and merged after both extracts after centrifugation. The supernatant was taken to dryness in a Speedvac centrifuge (Thermo Fisher Scientific, Waltham, USA) and further processed by Dr. Jackson using a reversed-phase liquid chromatography for separation (UPLC BEG C18 column, 1.7 µm beads, 2.1 x 150 mm, Waters Corporation, Milford, USA) and analyzed by using a triple quadrupole (TSQ Quantum Ultra, Thermo Fisher Scientific, Waltham, USA) as published (Jackson, Ren et al. 2009).

3.19 ATP measurement using a luciferin / luciferase based assay

Concentrations of ATP were determined using a commercially available ATP determination kit (Thermo Fisher Scientific, Waltham, USA). This assay is based on the chemiluminescent reaction of luciferase utilizing ATP and luciferin. In short, standard curve was prepared in the range of 1 nM to 1 µM and to each part sample / standard 100 parts of standard reaction solution (1.25 µg recombinant firefly luciferase, 0.5 mM D-luciferin, 1 mM dithionite, 0.1 mM sodium azide, 0.1 mM ethylenediaminetetraacetic acid, 5 mM $MgSO_4$, 25 mM Tricine buffer pH = 7.8) was added and chemiluminescence immediately measured using the FLUOstar Omega plate reader.

3.20 Exercise protocol

Forced exercise protocols were conducted after an established protocol (Laker, Drake et al. 2017). To acclimatize mice to the training they were subjected to 10 minutes of treadmill training with an incline of 0 % and a speed of 13 m/minute on three consecutive days.

Maximal exercise capacity was tested on day 4 with the treadmill set to an incline of 5 %. The speed of the treadmill was set to a speed of 13 m/minute and was increased by 2.7 m/minute every 30 minutes. The maximum speed was set to 27 m/minute. Mice ran until total exhaustion which was determined by refusal to run for 20 seconds. To assure that the same exhaustion levels were reached blood lactate levels were determined before and after the test for maximal exercise capacity.

3.21 Crossing scheme of tissue specific eNOS KO and KI mice

In order to be able to dissect the influence of the eNOS enzyme in different tissues, Cortese-Krott et al. created transgenic mice using the Cre-loxP system found in the bacteriophage coliphage P1 (Sternberg and Hamilton 1981). This system works by Cre recombinase excising or inverting targeted gene sequences. Gene sequences are targeted by recognition regions named loxP-sequences, which flank the gene sequence of interest (Sauer and Henderson 1989). The gene of interest in this case was eNOS and exon two was targeted as sequence of interest. If both loxP sequences have the same orientation, the sequence of interest in the presence of Cre-recombinase is excised. These mice were

labeled eNOS^{fl/fl} in this work. If both loxP sequences show in the opposite direction the sequence of interest is inverted. With loxP sequences facing themselves, mice were created with a construct of inverted exon two before a functional exon two both framed in loxP sequences of eNOS. These mice will be labeled eNOS[inv/inv].

To induce tissue specific transgenic mice, Cre-recombinase can be expressed under the control of promoters that are active only in specific cell lines. To induce RBC specific KO, Cre-recombinase expression was encoded by the hemoglobin β gene promoter (Hbb-Cre) (Peterson, Fedosyuk et al. 2004). In order to achieve vascular endothelium specific KO an inducible Cre-ERT2 system was chosen. In this system a fusion protein of Cre-recombinase and estrogen receptor 2 (ERT2) is expressed under the control of the promoter for VE-cadherin (Metzger and Chambon 2001, Wang, Nakayama et al. 2010). The Cre-ERT2 fusion protein under baseline conditions is located to the cytoplasm and is translocated into the nucleus by injection of tamoxifen.
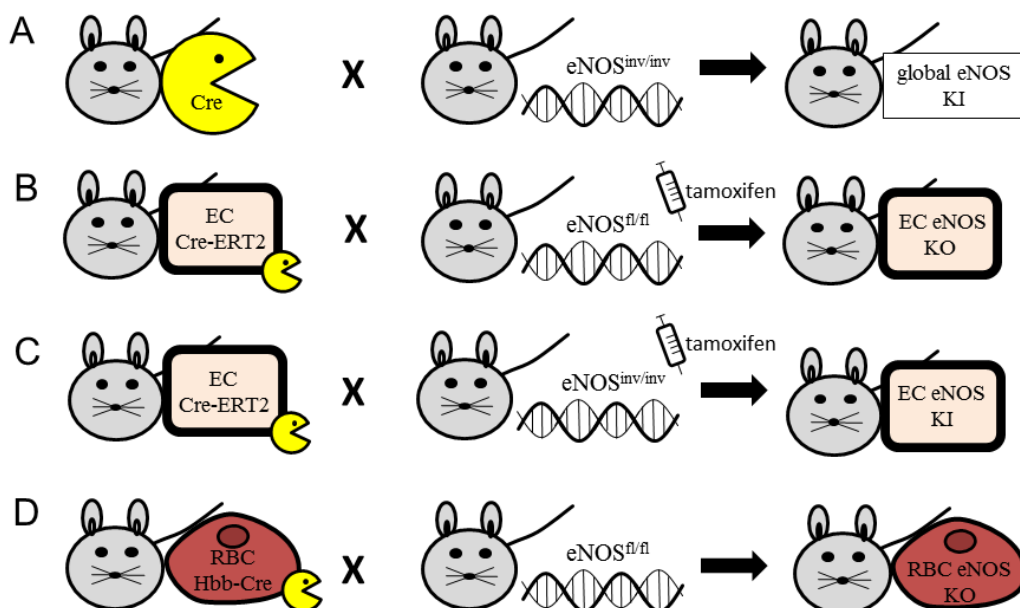
Figure 4 Crossing scheme of eNOS KO and KI mice

A) Global eNOS KI mice were created by crossing of mice globally expressing Cre protein and eNOS$^{inv/inv}$. B) Endothelial cell (EC) specific KO of eNOS was induced by injection of tamoxifen after crossing EC Cre-ERT2 mice with eNOS$^{fl/fl}$ mice. C) To induce EC eNOS KI tamoxifen was injected after crossing of EC Cre-ERT2 mice with eNOS$^{inv/inv}$. D) RBC eNOS KO was created by crossing of a mouse line expressing Cre under control of the promoter for the hemoglobin beta (Hbb) protein with an eNOS$^{fl/fl}$ mouse (RBC eNOS KO).

3.22 Blood pressure measurements

To measure diastolic and systolic blood pressure, mice were initially anesthetized using isoflurane (2 % vol., Piramal Healthcare Ltd, Mumbai, India) and anesthesia was continued using a facial mask flushed with isoflurane (1-2 % vol.). Mice were fixed on a 37 °C pre-heated surgery table. For pain-medication, a dose of 0.1 mg/kg buprenorphine (Indivior PLC, Richmond, USA) was administrated intra-peritoneal. After exclusion of

pain reflexes the arteria carotid communis was carefully dissected, without damage of the vagus nerve or other blood vessels nearby. After incision in the carotid communis a pressure measuring catheter (SPR-829, Millar Inc, Houston, USA) was inserted into the arteria carotid communis and pressure changes measured for 5 minutes. Data was analyzed using the LabChart 7 (ADInstruments, Sydney, Australia) software.

3.23 Pressure myography

Mesenteric arteries were isolated from mice killed using CO_2. In all further steps organs were kept in a Krebs-Hepes buffer (118.4 mM NaCl, 10 mM Hepes, 6 mM glucose, 4.7 mM KCl, 4 mM $NaHCO_3$, 1.2 mM $MgSO_4$, 1.2 mM $CaCl_2$, 1.2 mM KH_2PO_4) on ice. Intestines were dissected and transferred into a silicon coated petri dish. 3rd order mesenteric arteries were carefully cleaned from fat and transferred into an organ bath (Danish MyoTechnology A/S, Aarhus, Denmark). Here the mesenteric arteries were cannulated on glass pipets and fixed with sutures. Mesenteric arteries were pressurized to 80 mmHg and equilibrated for 20 minutes at 37 °C. For test of vascular endothelial function cumulative doses of acetylcholine (10^{-9} M – 10^{-3} M) were added into the circulating Krebs-Hepes buffer after an initial dose of 10^{-5} M phenylephrine. To check for maximal diameter of the vessel, at the end of the experiment the organ bath was flushed using Krebs-Hepes buffer excluding calcium. Changes in vessel diameter were constantly recorded by the MyoVIEW software.

3.24 Organ bath with aortic rings

Mice were anesthetized using a combination of ketamine (100 mg/kg, Pfizer Inc., New York City, USA) and xylazine (10 mg/kg, Bayer AG, Leverkusen, Germany). After lack of pain reflexes in the hind paws, organs were dissected and thoracic aorta was carefully freed from fat, isolated and transferred into HEPES buffer (98.9 mM NaCl, 4.7 mM KCl, 1.9 mM $CaCl_2$ x 2 H_2O, 1.2 mM $MgSO_4$ x 7 H_2O, 25 mM $NaHCO_3$, 1 mM KH_2PO_4, 20 mM Na-Hepes, 11.1 mM D-glucose). The artery was carefully flushed to remove residual blood and cut into 2 mm aortic rings.

For each mouse two until three aortic rings were transferred to the organ baths (Harvard Apparatus, Cambridge, USA), which were heated to 37 °C, containing Krebs-Hensleit

buffer (118 mM NaCl, 25 mM NaHCO$_3$, 10 mM glucose, 4.4 mM KH$_2$PO$_4$, 5 mM KCl, 1.2 mM MgSO$_4$, 1.6 mM CaCl$_2$ x H$_2$O) and were constantly gassed with carbogen (5 % v/v carbon dioxide and 95 % v/v oxygen). To equilibrate aortic rings, organ bath buffer was exchanged by fresh buffer every 15 minutes for 1 hour until the vessels tension was stable at 1 g.

For receptor-independent constriction 80 nM KCl was added and after 20 minutes constriction, noted as a measure for maximal constriction. The treatment was removed by changing buffer in the organ bath for 15 minutes until tension reached baseline values. To test for endothelium-dependent relaxation, vessels were pre-constricted by an initial dose of 0.4 μM phenylephrine. This dose was followed by cumulative doses of acetylcholine starting from 0.1 nM to 10 μM. After the last dose, treatment was again removed by changing organ bath buffer for 5 minutes. By administration of cumulative doses of phenylephrine, resulting in concentrations of 0.1 - 10 μM in the organ bath, normal functionality of smooth muscle cells was tested. This treatment was followed by SNP in concentrations from 0.01 nM – 10 μM.

If indicated in the figure legends the NOS inhibitor L-N^G-nitroarginine methyl ester (L-NAME) was added to organ baths to a final concentration of 0.1 mM and aortic rings were incubated with L-NAME for 20 minutes.

3.25   Induction of KO in endothelium specific KO / KI models

Mice were injected with a dose of 0.75 mg tamoxifen. A tamoxifen stock solution of 5 mg/ml was prepared by solving 50 mg of tamoxifen (Sigma-Aldrich) in ethanol, which was added to peanut oil (Sigma-Aldrich). This drug-solution was stored light protected at -20 °C. Before injection of 150 μl, solution was thawed and warmed to 37 °C. Injections followed for five consecutive days at the same time of day. For aortic ring experiments mice were housed for further 21 days to warrant maximal KO / KI efficiency and tamoxifen washout.

3.26   Body weight changes during tamoxifen treatment

Body weight was monitored on a Sartorius portable scale at the day of the last injection of tamoxifen day 0, day 1 and day 21.

3.27 Blood cell counts

Blood cell counts were measured using a scil Vet abc Plus+ (scil animal care company GmbH, Viernheim, Germany) at the ZETT of the Heinrich-Heine-University of Düsseldorf.

4 Results

4.1 The effects of NO on RBC deformability

The general working hypothesis of the chapter was that the eNOS–sGC pathway and NO are key regulators of RBC deformability.

4.1.1 RBCs of hypertensive patients demonstrated decreases in RBC deformability and increased levels of ROS

The aim of the observational study was to investigate, if the well documented decreases in RBC deformability (Sandhagen, Frithz et al. 1990, Vaya, Martinez et al. 1992, Cicco and Pirrelli 1999, Cicco, Carbonara et al. 2001) in hypertensive patients are due to lack of NO bioavailability in RBCs.

To address this open question, a study was designed with a group of hypertensive patients and an age-matched group of normotensive patients (for patient characteristics see **Table 2**). The parameters significantly different between the hypertensive group and the normotensive control group were body mass index (BMI) [healthy volunteers: 26.9 ± 4.2 kg/m^2 vs. hypertensive patients: 29.6 ± 2.4 kg/m^2] and flow mediated dilation (FMD) [healthy volunteers: 6.84 ± 0.66 % vs. hypertensive patients: 5.12 ± 0.48 %]. Previous studies demonstrated that occurrence of hypertension correlates with obesity (Chiang, Perlman et al. 1969). The finding of higher BMI values in the hypertensive group is in concert with these findings. In addition to that the presence of endothelium dysfunction and impairment of FMD was demonstrated in hypertensive patients (Panza, Quyyumi et al. 1990).

Measurement of RBC deformability carried out using a laser optical rotational cell analyzer (LORCA) resulted in the observation of decreased RBC deformability in the group of hypertensive patients (**Figure 5 A**). This decrease of RBC deformability was only detectable for low shear stresses. At a shear stress of 10 Pa, RBC deformability of hypertensive patients was not significantly different from normotensive volunteers

[hypertensive patients 0.5282 ± 0.0041 A.U. vs. healthy volunteers 0.5304 ± 0.0029 A.U.; Mann-Whitney-U test; $P = 0.7293$].

Table 2 Study characteristics

	Healthy subjects	**Hypertonic subjects**	**P-value**
n(M/F)	11/0	9/0	-
Age [years]	47.8 ± 5.5	50.6 ± 6.9	0.38
Systolic blood pressure [mmHg]	122.7 ± 6.7	144.7 ± 6.4	**<0.0001******
Diastolic blood pressure [mmHg]	76.7 ± 4.9	91.9 ± 6.0	**< 0.0001******
Mean arterial pressure [mmHg]	92.0 ± 4.9	109.5 ± 5.0	**< 0.0001******
Heart rate [1/min]	65.5 ± 8.6	64.0 ± 6.1	0.75
Ex Smoking individuals [%]	27.3	28.6	-
Smoking individuals [%]	9.1	14.3	-
Pack years	10.0 ± 18.3	12.2 ± 12.3	0.36
BMI [kg/m2]	26.9 ± 4.2	29.6 ± 2.4	**0.03***
GFR [ml/min]	91.2 ± 11.9	88.8 ± 17.4	0.70
Total Cholesterol [mg/dL]	210.5 ± 40.2	227.7 ± 38.7	0.70
HbA1c [%]	5.5 ± 0.5	5.4 ± 0.3	0.61
Plasma glucose [g/dl]	94.2 ± 5.9	92.8 ± 7.6	0.67
Hemoglobin [g/dl]	15.2 ± 0.8	15.0 ± 1.0	0.84
Brachial artery diameter			
baseline vessel size [mm]	5.01 ± 0.69	4.76 ± 0.49	
FMD [%]	6.84 ± 0.66	5.12 ± 0.48	**< 0.0001******
GTN induced dilatation [%]	11.3 ± 0.7	12.09 ± 1.32	0.15
relative RBC eNOS expression	1.00 ± 0.32	1.55 ± 1.20	0.35
DAF-FM ΔMFI	659.7 ± 216.5	697.1 ± 274.1	0.80
MitoSOX ΔMFI	4.00 ± 2.83	5.56 ± 7.25	0.53
Thiol Tracker ΔMFI	67790 ± 5744	71294 ± 18123	0.74
Nitrite [nM]	8.67 ± 1.39	12.71 ± 2.21	0.13

In this study, eleven age matched, male and healthy normotensive volunteers were recruited in addition to nine hypertensive patients. High systolic and diastolic blood pressures as well as mean arterial pressure were the inclusion parameters for the hypertensive group. (Statistics for all comparisons: Mann-Whitney-U test; body mass index (BMI), glycated hemoglobin (HbA1c), flow mediated dilation (FMD), glomerular filtration rate (GFR), glycerol trinitrate (GTN), 4-amino-5-methylamino-2',7'-

dichlorofluoresceine diacetate (DAF-FM), red mitochondrial superoxide indicator (MitoSOX), delta mean fluorescence intensity (ΔMFI)). Study recruitment by Roberto Sansone.

To test if the observed changes in RBC deformability could be due to a lack of NO, intracellular levels of NO were measured. However, no difference of intracellular NO bioavailability and levels of the NO metabolite nitrite were detectable in RBCs as assessed by flow cytometry and CLD (**Table 2**). Yet increased levels of intracellular ROS were evident in RBCs from hypertensive patients (**Figure 5 B**).
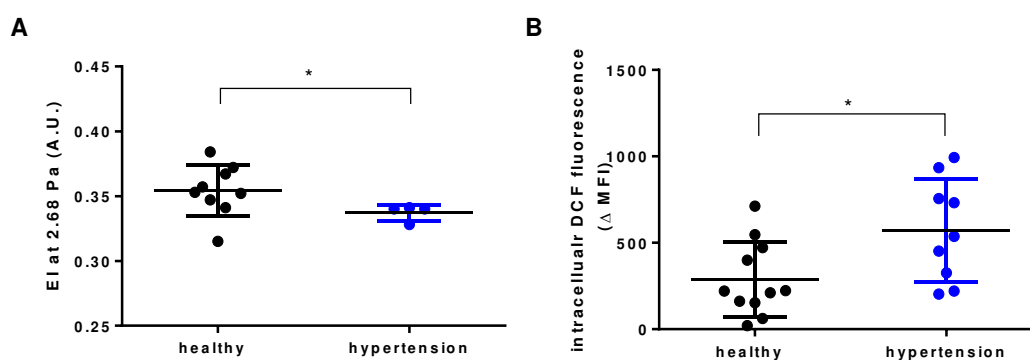
Figure 5 RBC characteristics in hypertensive patients

A) RBC deformability was measured in four hypertensive patients and compared to nine healthy volunteers. At a shear stress of 2.68 Pa RBCs from hypertensive patients demonstrated lower deformability vs. normotensive controls (Mann-Whitney-U test; P = 0.0378). B) Using flow cytometry intracellular ROS using the probe 2',7'-dichlorofluorescein (DCF) were measured in RBCs. ROS status in hypertensive patients in comparison to healthy volunteers was significantly increased (Mann-Whitney-U test; P < 0.05; median fluorescence intensity (MFI), ΔMFI = DCF loaded RBCs – DCF unloaded RBCs). Measurements conducted by Miriam M. Cortese-Krott.

These findings indicated that intracellular changes of redox status, and not the lack of NO corresponds to a decrease in RBC deformability, could be responsible for decreased RBC

deformability. To further clarify which posttranslational modifications impact RBC deformability, different methods to study intracellular oxidative stress were applied. The role of NO was tested in models of NO depletion and exogenous NO application.

4.1.2 Exhaustion of antioxidant capacity caused impairment of RBC deformability and increased whole blood viscosity

The aim of this section was to characterize the impact of oxidative stress on RBC deformability and whole blood viscosity. It was hypothesized that intracellular changes in redox state affect RBC physical properties.

To induce oxidative stress on human RBCs the organic peroxide *tert*-butyl hydroperoxide (*t*-BuOOH) was used. At first intracellular levels of GSH and its oxidized form GSSG were measured in a range of concentrations, starting from 10^{-9} to 10^{-1} M *t*-BuOOH. The ratio of GSH to GSSG can be seen as an indicator of intracellular redox status (Sies 1999, Griendling, Touyz et al. 2016). Markedly RBCs were capable to withstand high concentrations of pro-oxidant *t*-BuOOH. The ratio of GSH to GSSG dropped significantly starting at concentrations of 1 mM *t*-BuOOH (**Figure 6 A – B**).

In line with that, RBC deformability curves started to flatten from concentrations < 1 mM *t*-BuOOH, indicating decreased deformability (**Figure 6 C**). Whole blood viscosity, when treated with the same concentrations (3 – 5 mM) of *t*-BuOOH, presented increases in viscosity (**Figure 6 D**). Plotting elongation index (EI) and viscosity in one graph versus shear rates in the range of 10 – 177.67 $\frac{1}{s}$ clearly showed that a decrease of RBC deformability is accompanied by increased whole blood viscosity (**Figure 6 E**).
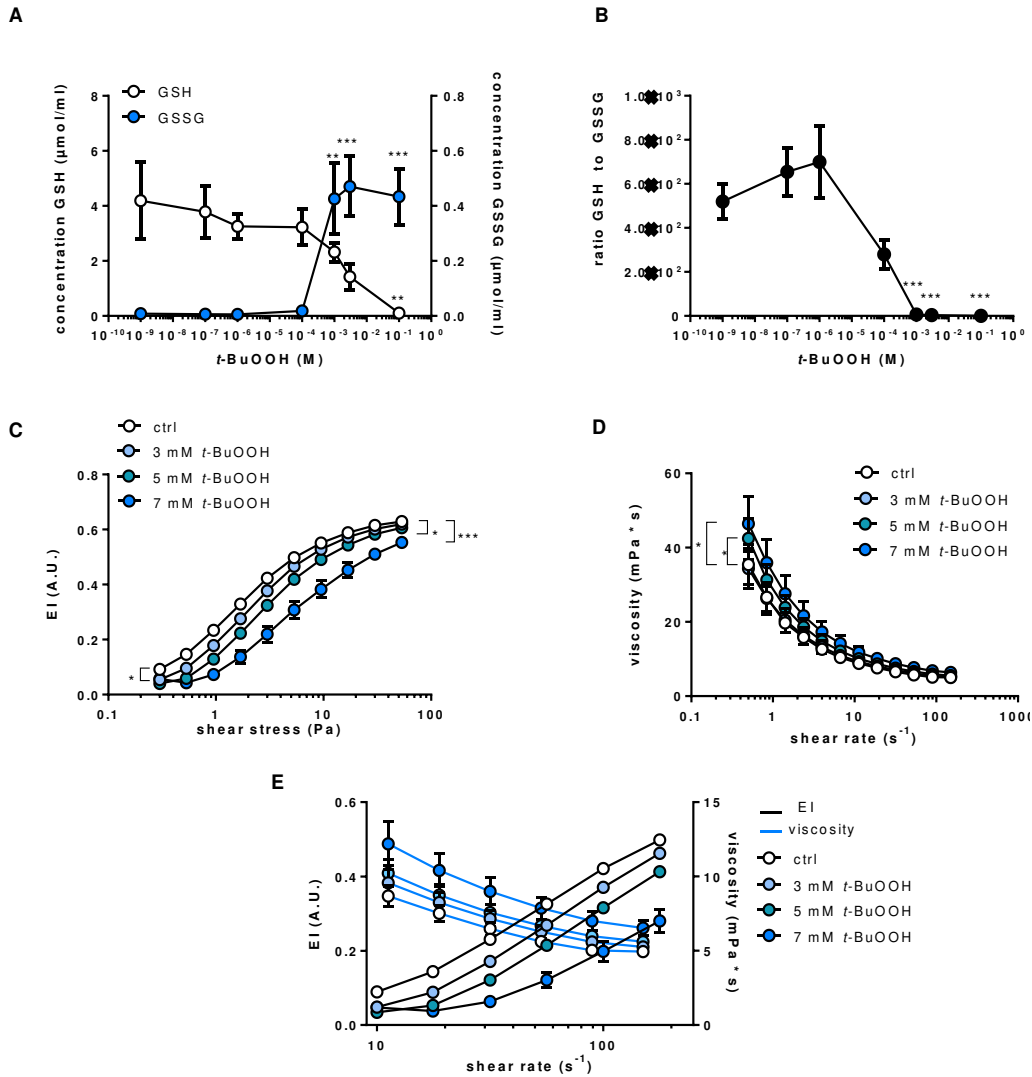
Figure 6 Effects of *t*-butyl hydroperoxide on intracellular redox state, RBC deformability and whole blood viscosity

*A) Intracellular GSH and GSSG levels were measured after treatment with $10^{-9} – 10^{-1}$ M t-BuOOH using LC-MS. GSH levels dropped significantly for values higher than 3 mM. Levels of GSSG abruptly increased starting at a concentration of 1 mM t-BuOOH (1-way RM ANOVA; GSH: P = 0.0218, GSSG: P < 0.0001; Dunnett's test vs. untreated ctrl, **: P < 0.01, ***: P < 0.0001 in five volunteers). B) Ratio of GSH and GSSG calculated from values in A). Relative excess of GSH to GSSG dropped significantly starting at 1 mM t-BuOOH (1-way RM ANOVA, P < 0.0001; Dunnett's test, ***: P < 0.001). C) EI of RBCs versus shear stress. With increasing concentrations of t-BuOOH deformability indices decreased in contrast to ctrl conditions (2-way RM ANOVA, P < 0.001; Dunnett's*

36

test vs untreated ctrl, *: P ≤ 0.05, ***: P < 0.001 (significant from 0.3 – 9.48 Pa for 3 mM and over the whole range of shear stresses for 5 and 7 mM) from six volunteers). D) Viscosity of whole blood versus shear rate. Viscosity increased with increasing concentrations of t-BuOOH (2-way RM ANOVA, P = 0.0004; Dunnett's test vs. untreated ctrl *: P ≤ 0.05 (significant for 5 mM at shear rates from 0.5 – 3.98 s^{-1} and for 7 mM at shear rates from 0.5 – 11.22 s^{-1}). E) EI and viscosity against shear rates in the range of 10 – 177.67 s^{-1} demonstrated an increase in whole blood viscosity with decreases in individual RBC deformability.

For evaluation of the theoretical value of maximal elongation (EImax) and half maximal shear stress ($SS_{1/2}$) values the Lineweaver-Burk transformation was used. The use of the Lineweaver-Burk transformation was suggested by Meiselman and co-workers as a general method to simplify RBC deformability data (Baskurt and Meiselman 2013). As shown in **Table 3** the coefficient of determination decreases steadily with increasing concentrations of *t*-BuOOH. This finding indicated that application of the Lineweaver-Burk transformation is not appropriate for these data sets and thus the theoretical values of EImax and $SS_{1/2}$ have to be interpreted with great care.

Table 3 Calculation of EImax and half-maximal $SS_{1/2}$ of RBCs with increasing concentrations of *t*-BuOOH.

concentration *t*-BuOOH	r^2 Lineweaver-Burk transformation	EI max	$SS_{1/2}$
0 mM	0.929	0.702±0.065	2.122±0.725
3 mM	0.876	1.126±0.600	6.927±5.822
5 mM	0.795	-0.271±1.722	-5.225±16.960
7 mM	0.612	0.527±0.541	4.223±5.356

Calculated values after application of the Lineweaver-Burk transformation for the coefficient of determination, maximal EI and $SS_{1/2}$ of RBCs after treatment using 3 – 7 mM t-BuOOH.

To confirm that treatment of RBCs with *t*-BuOOH did not cause hemolysis, RBCs were incubated with the similar concentrations of 3 – 7 mM *t*-BuOOH and hemoglobin was measured in the supernatants of these cells. Hemoglobin serves as a good marker for hemolysis since it accounts for 98 % of cytosolic proteins and is easily measurable due to its characteristic UV-Vis absorption spectra. No hemolysis was detectable in the tested concentrations of 3 – 7 mM *t*-BuOOH (**Figure 7**).
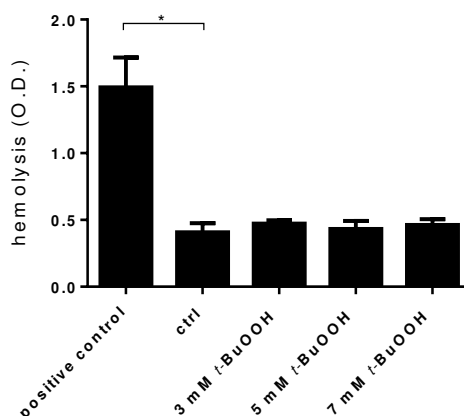
Figure 7 Hemolysis of RBCs due to *t*-BuOOH treatment

UV-Vis absorption at 570 nm and background absorption at 700 nm were measured in the supernatant of treated RBCs of five volunteers. Subtraction of the absorption at 570 nm from the absorption at 700 nm results in the Δabsorption-value. As positive control for hemolysis RBCs were treated with deionized water (RM 1-way ANOVA; P = 0.0041; Dunnett's multiple comparisons test; *: P < 0.05).

After characterization of *t*-BuOOH induced effects on RBC deformability from human volunteers in an ex-vivo model, an in-vivo mouse model of high susceptibility to oxidative stress was analyzed. For this purpose, the mouse strain chosen was the Nrf2 KO mice. Nrf2 is a transcription factor promoting antioxidant defense and a deficient in Nrf2, mice lack antioxidant enzymes essential for degradation of oxidants. Of note, at baseline conditions EI versus shear stress curves of WT and Nrf2 KO mice were comparable, but treatment with *t*-BuOOH concentrations, as low as 50 µM, already resulted in a first shift, manifesting in a statistically significant shift at a concentration of 100 µM (**Figure 8**).
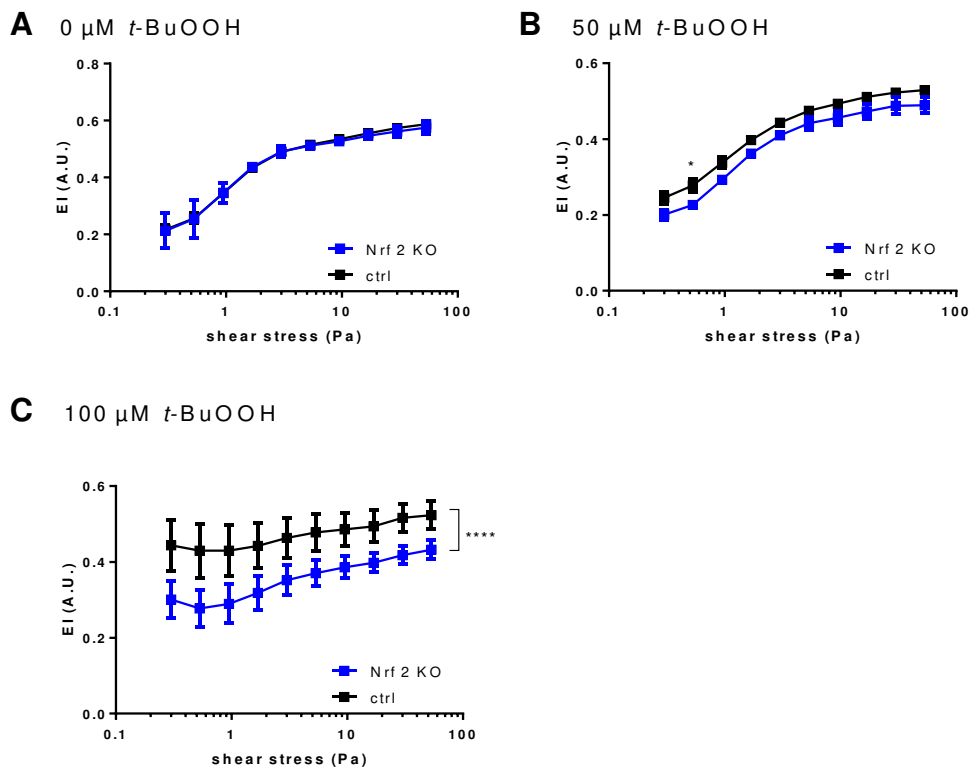
Figure 8 EI of Nrf2 KO mice with increasing concentrations of *t*-BuOOH

No changes in EI were detectable at baseline between Nrf2 KO and control. B) After incubation with 50 µM of t-butyl hydroperoxide (t-BuOOH) Nrf2 KO elongation curve started to flatten indicating decreased deformability of individual RBCs (2-way ANOVA, ctrl vs. Nrf2 KO, P = 0.0341, Sidak's multiple comparison test, *: P < 0.05). C) Incubation with a concentration of 100 µM t-BuOOH resulted in even more pronounced decreases of RBC deformability (2-way ANOVA, ctrl vs. Nrf2 KO, P =0.0095, Sidak's multiple comparison test, ****: P ≤ 0.0001). Experiments conducted by W. Lückstädt.

In summary, the results showed that as long as intracellular redox capacity is intact RBCs are able to compensate for increased oxidative burden. As shown in the ex-vivo model using human RBCs and the in-vivo mouse model of impaired antioxidant defense, as soon as the antioxidant capacity was exhausted RBC deformability was decreased and whole blood viscosity increased.

4.1.3 Endogenous and exogenous NO did not affect RBC deformability

The aim of this part of the project was to investigate the effects of NO on RBC deformability. In specific in models of NO deficiency and exogenously applied NO.

Effects of NO on RBC deformability are a highly debated topic and many different working groups published contradictive reports. Several groups demonstrated improvement of RBC deformability by exogenous applied NO and endogenously produced NO (Bor-Kucukatay, Wenby et al. 2003, Grau, Pauly et al. 2013). These findings were attributed to *S*-nitrosation of spectrin a cytoskeletal protein. Spectrin is a helical protein and a heterotetramer and is composed of two α-spectrin and two β-spectrin subunits. Upon deformation of RBCs, spectrin, as a highly flexible protein, is able to reversibly deform and plays a key role in shape regulation and membrane stability. However, these findings were not reproduced by others (Barodka, Mohanty et al. 2014, Belanger, Keggi et al. 2015)

4.1.3.1 Purified spectrin was a target of *S*-nitrosation

First, the aim was to investigate if *S*-nitrosation of spectrin takes place.

In order to answer this question first commercially available purified spectrin and *S*-nitrosation was tested using two different methods, such CLD and biotin switch assay. All samples were first treated under nitrosating conditions using CysNO, which was removed afterwards. As a first approach for this investigations CLD was used and *S*-nitrosation of spectrin could be confirmed (**Figure 9**).
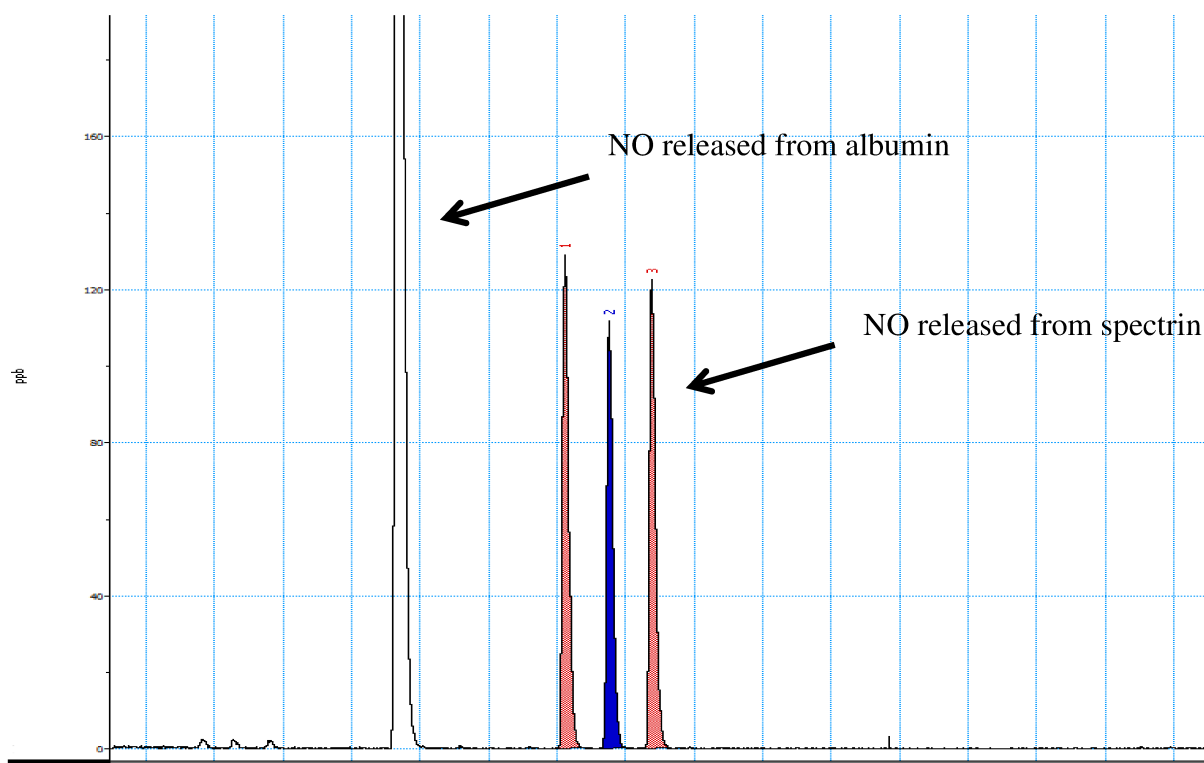
Figure 9 CLD for *S*-nitrosation of spectrin

Spectrin was S-nitrosated, after being treated under nitrosating conditions using CysNO, as indicated by the colored peaks. As a positive control for S-nitroso albumin under similar conditions was used.

In a next step the findings were confirmed in a biotin switch assay. In this assay *S*-NO binding sites were labeled by a biotin-tag which in the following were visualized using a fluorophore labeled streptavidin, as shown in **Figure 10 A**. In samples treated with CysNO higher signals for nitrosation of spectrin were detected than in the sample without nitrosating treatment (**Figure 10**).
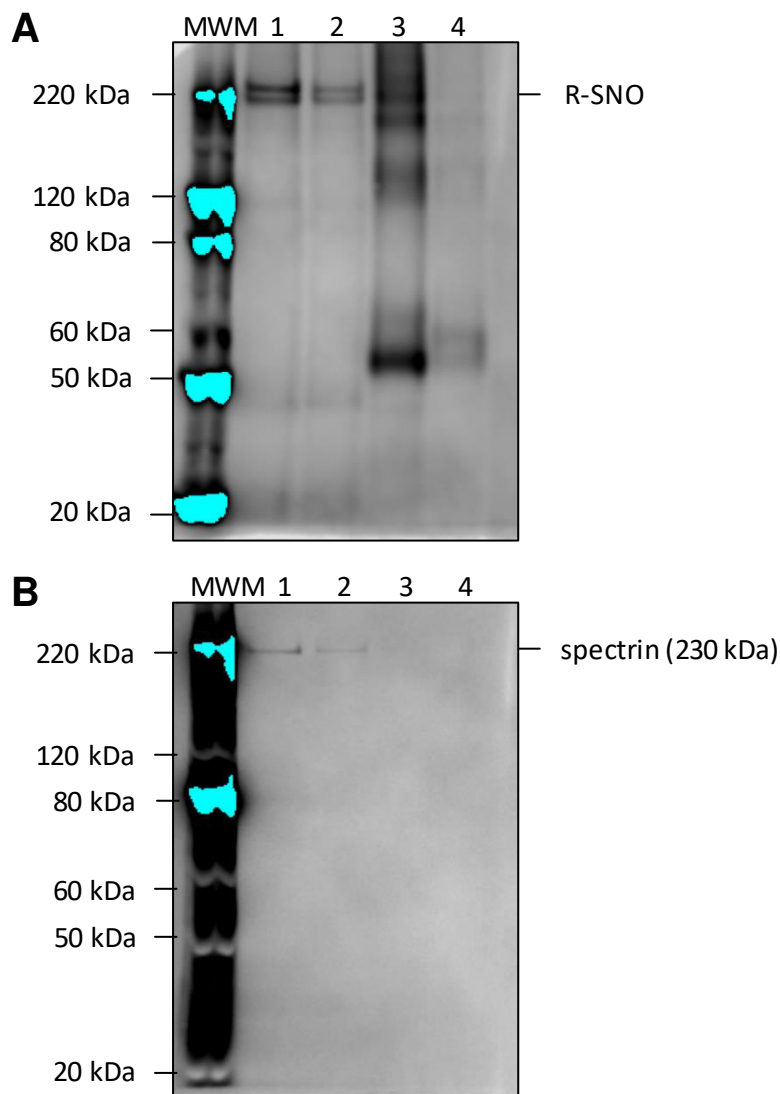
Figure 10 Biotin switch assay of purified spectrin and albumin after nitrosation

Albumin was used as a positive control (molecular weight marker (MWM), lane 1: spectrin + 50 mM CysNO, lane 2: spectrin + 0 mM CysNO, lane 3: albumin + 50 mM CysNO, lane 4: albumin + 0 mM CysNO). A) Upper membrane: Signal indicative of nitrosated sites. B) Lower membrane: The identical membrane incubated with antibody versus spectrin.

These results demonstrated that *S*-nitrosation of purified spectrin was possible.

4.1.3.2 Spectrin in RBCs and RBC ghosts was target for *S*-nitrosation

In a next step *S*-nitrosation of spectrin was investigated on a cellular level and the previous experiment were repeated to confirm nitrosation in RBC ghosts and RBCs.

Next the isolation of RBC ghosts was established. RBC ghosts are RBCs deprived of their intracellular proteins. For this purpose, RBCs were subjected to a hypotonic buffer leading to rupture and release of cytoplasmic proteins. After washing - until the remaining RBC membranes were greyish-white - the membranes were resealed and became RBC ghosts. To confirm complete removal of intracellular proteins UV-Vis spectra were recorded (**Figure 11**). Residual hemoglobin would have been indicated by a characteristic pattern of absorption. Since this was not the case the procedure to remove intracellular proteins was successful.
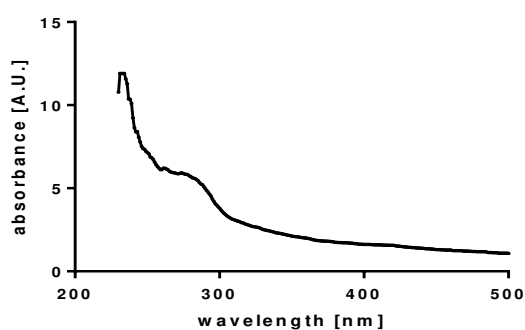
Figure 11 UV-absorption spectrum of RBC ghosts

Residual hemoglobin was measured by UV-Vis and an absorption spectrum was recorded in the range of 230 – 800 nm. No characteristic bands of hemoglobin were visible indicating complete loss of hemoglobin.

In the next experiment RBCs ghosts were tested for the removal of intracellular proteins. In a Western blot the presence of cytoskeletal proteins spectrin and actin was demonstrated (**Figure 12**).
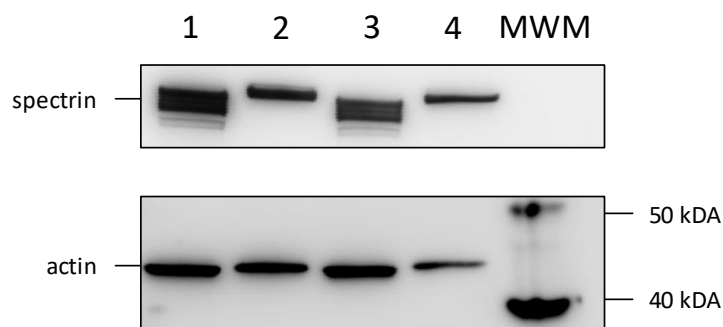
Figure 12 Cytoskeletal proteins of RBCs and RBC ghosts

After preparation of RBC ghosts the main cytoskeletal proteins were not removed. The existence of cytoskeletal proteins actin and spectrin was confirmed. Upper panel: spectrin; lower panel: actin (lane 1: RBC ghosts 10 μg, lane 2: RBCs 10 μg, lane 3: RBC ghosts 5 μg, lane 4: RBC ghosts 5μg, MWM: molecular weight marker).

RBC ghosts were able to completely reseal, shown by trapping of 5,6-carboxyfluorescein, a membrane impermeable fluorescence dye, that was trapped in the RBC ghosts during the resealing process and washed away later (**Figure 13**).
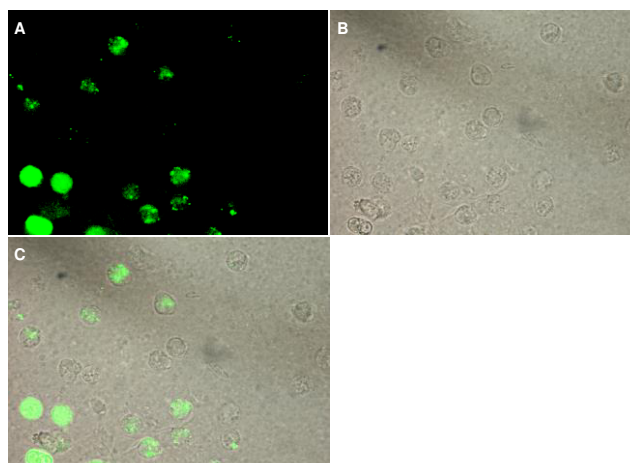
Figure 13 RBC ghosts re-sealed after removal of cytoskeletal proteins

RBC ghosts were able to reseal after removal of intracellular proteins. Before resealing RBC ghosts were co-incubated with the cell membrane impermeable fluorescent dye 5,6-carboxyfluorescein. The dye in the supernatant was removed by several washing steps

and ghosts imaged at 100x magnification. A) A representative image shows fluorescence signal with an excitation at 495 nm. B) A bright-field image was taken from the identical area. C) Merge of both images (A and B).

After the characterization of RBC ghosts, *S*-nitrosation in RBC ghosts and RBCs was investigated. Upon addition of increasing concentrations of CysNO to RBC ghosts also the signal for R-SNO increased steadily when 1 µg of sample was injected to the reaction chamber of the CLD (**Figure 14**).
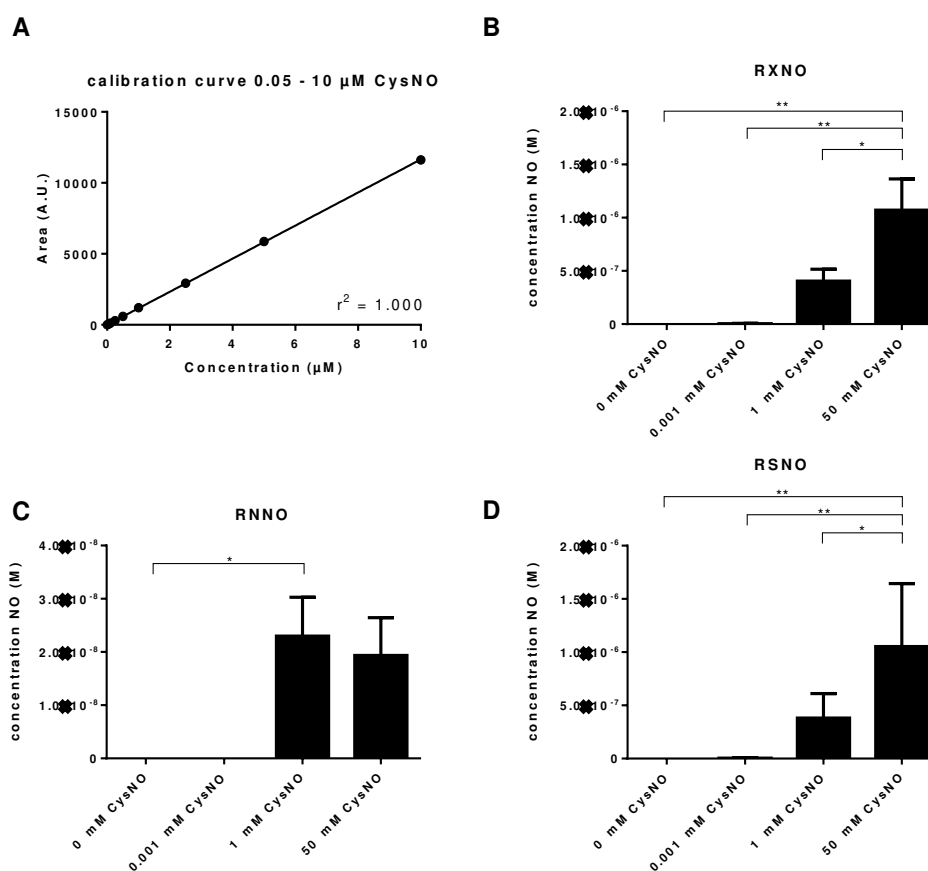
Figure 14 Nitrosation of RBC ghosts measured by CLD

RBC ghosts were prepared from four different volunteers, treated with the nitrosating agent CysNO and measured in triplicates. After removal of the treatments, NO was measured after injection of 1 µg of sample into an acidic triiodide solution. A) Linear regression curve of CysNO in a concentration range of 0.05 – 10 µM ($r^2 = 1.000$).

B) Determination of N-nitrosamine and S-nitrosothiol levels. C) Determination of N-nitrosamine. D) Calculation of S-nitrosothiol levels from values in A) and B). (Ordinary 1-way ANOVA, Tukey's multiple comparison test;*: P < 0.05, **: P < 0.01)

This finding though only confirmed *S*-nitrosation of cytoskeletal proteins. To specify if spectrin was the target of *S*-nitrosation, a biotin switch assay was conducted after lysis of RBC ghosts. Here as well *S*-nitrosation of spectrin could be detected (**Figure 15**). *S*-nitrosation of spectrin in RBCs after nitrosation was confirmed by a biotin switch assay (**Figure 16**).
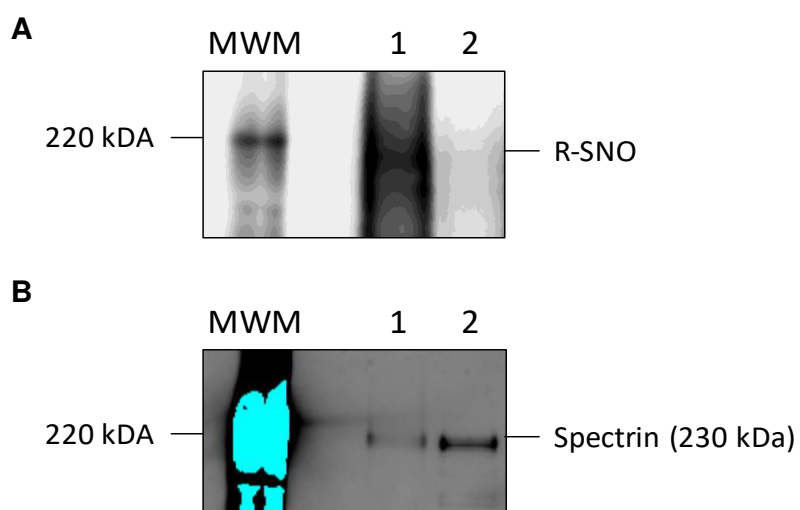
Figure 15 Biotin switch assay after nitrosation of RBC ghosts

S-Nitrosation of cytoskeletal spectrin in RBC ghosts the concentrations of 0 mM (lanes 2 and 8) and 50 mM (lane 1). A) Signal of spectrin B) R-SNO signal.
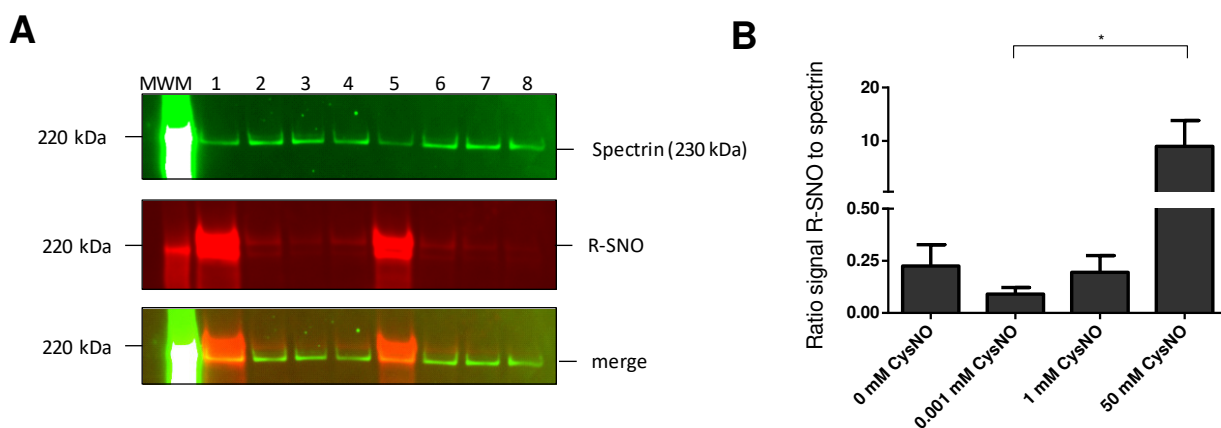
Figure 16 Biotin switch assay after nitrosation of several patients' RBCs

S-Nitrosation of cytoskeletal spectrin in RBCs of four volunteers for the concentrations of 0 mM (lanes 4 and 8), 0.001 mM (lanes 3 and 7), 1 mM (lanes 2 and 6) and 50 mM (lanes 1 and 5). A) Western blot of: upper panel: spectrin, middle panel: R-SNO, lower panel: merge of both channels. B) Ratio of biotinylation signal and spectrin signal for the different concentrations (Kruskal-Wallis test: P = 0.009, Dunn's multiple comparisons test: *: P ≤ 0.05).

Generation of NO in RBCs has been discussed as a possible source for nitrosation of cytoskeletal proteins. To test the hypothesis, RBCs were incubated under hypoxic conditions with increasing concentrations of nitrite. At time-points 0, 1, 5 and 15 minutes an aliquot was taken and measured by EPR. With increasing time the peak for iron(III) increased steadily and after 5 minutes an EPR-signal for nitrosated hemoglobin became visible (**Figure 17**) (Fago, Crumbliss et al. 2013). These two signals taken together indicate that under hypoxic conditions nitrite is reduced to NO (**Equation 6**).
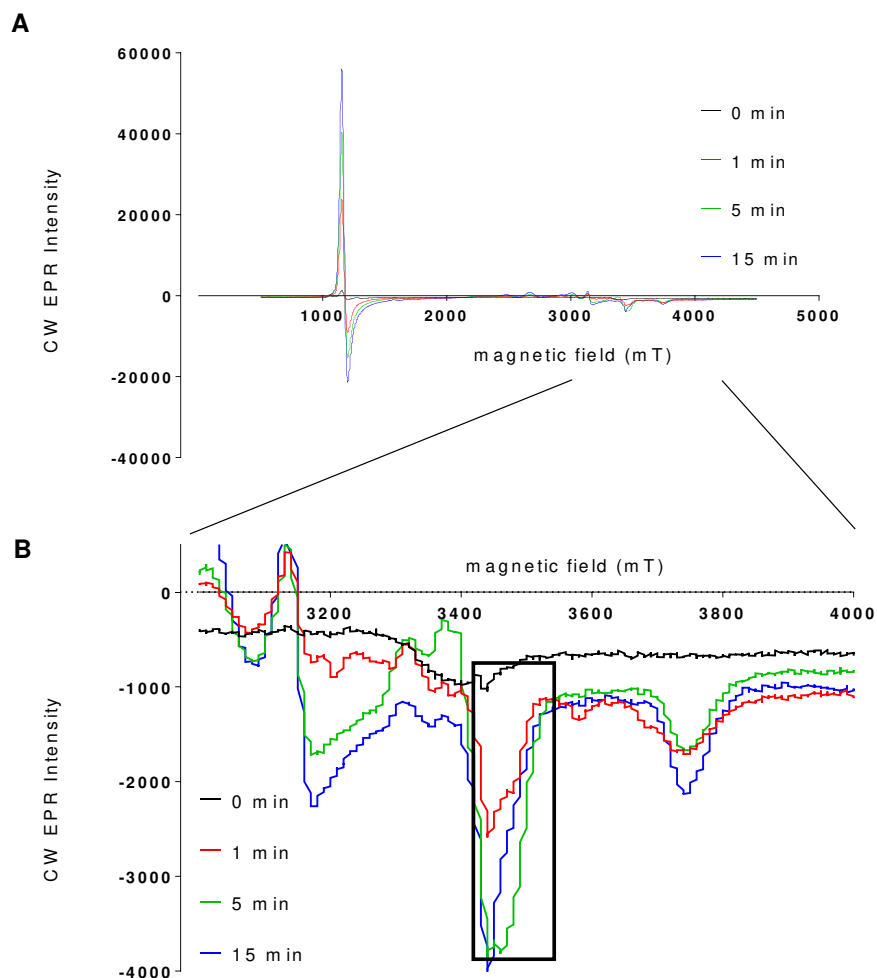
Figure 17 Detection of NO bound to hemoglobin using EPR

RBCs were incubated with 1 mM sodium nitrite under a nitrogen atmosphere. Using EPR, NO bound to hemoglobin after different time points was measured. Measurements were conducted at 15 K. A) Spectra over the whole range of the magnetic field. B) Spectra from 3000 – 4000 mT. NO bound to hemoglobin was found after 5 minutes demonstrated by the characteristic pattern marked by the black box. EPR measurements were conducted by A. Savitsky.

In parallel RBCs were incubated with increasing concentrations of nitrite. After 30 minutes the reaction was stopped and a biotin switch assay was conducted. With increasing concentrations of nitrite also the intensity of the R-SNO signal increased,

although not statistically significant the Western blots clearly demonstrate this trend (**Figure 18**).
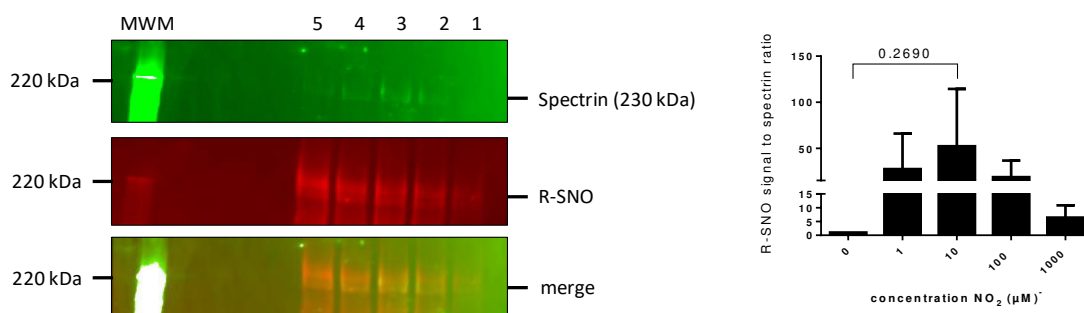
Figure 18 Biotin switch assay of RBCs after hypoxic conditions with addition of nitrite

S-Nitrosation of cytoskeletal spectrin in RBCs of two volunteers for the concentrations of 0 mM (lanes 1), 0.001 mM (lanes 2), 0.01 mM (lanes 3), 0.1 mM (lane 4) and 1 mM (lanes 5). A) upper panel: spectrin, middle panel: R-SNO, lower panel: merge of both channels. B) Ratio of biotinylation signal and spectrin signal normalized to the ratio of 0 mM for the different concentrations (Friedman test: P = 0.2583, Dunn's multiple comparisons test).

These results taken together indicated that spectrin of RBCs was a potential target for posttranslational modification by *S*-nitrosation and in addition to that there are thiol groups present that are accessible for posttranslational modifications. In particular interesting was that under hypoxic conditions in the presence of nitrite *S*-nitrosation was observable.

4.1.3.3 Nitrosation did not improve RBC deformability

The improvement of RBC deformability by NO is a widely and controversially discussed matter. The objective of this part was to shed light into the effect of NO on RBC deformability. In the following, two models were chosen to investigate possible improvement of RBC deformability by NO.

In the first model, human RBCs were treated ex-vivo using the NO donor DEA/NO and CysNO with different concentrations. No improvement of RBC deformability was

detectable for any condition (**Figure 19 A**) and only decreased deformability was evident for the highest concentration of 200 µM DEA/NO.

Since DEA/NO is a NO donor and per-se not capable to nitrosate thiol groups these experiments were repeated with CysNO, a donor of NO^+ which is capable to nitrosate thiol groups. Yet again no improvement of RBC deformability was detectable and the highest concentration of 50 mM CysNO decreased RBC deformability as seen before for the highest concentration of DEA/NO (**Figure 19 B**).

In a second model the effects of NO deprivation on deformability of RBCs in eNOS KO mice was compared to RBCs of control mice. Lack of NO by the global deletion of eNOS did not result in any impairment of RBC deformability as both curves were superimposable (**Figure 19 C**).
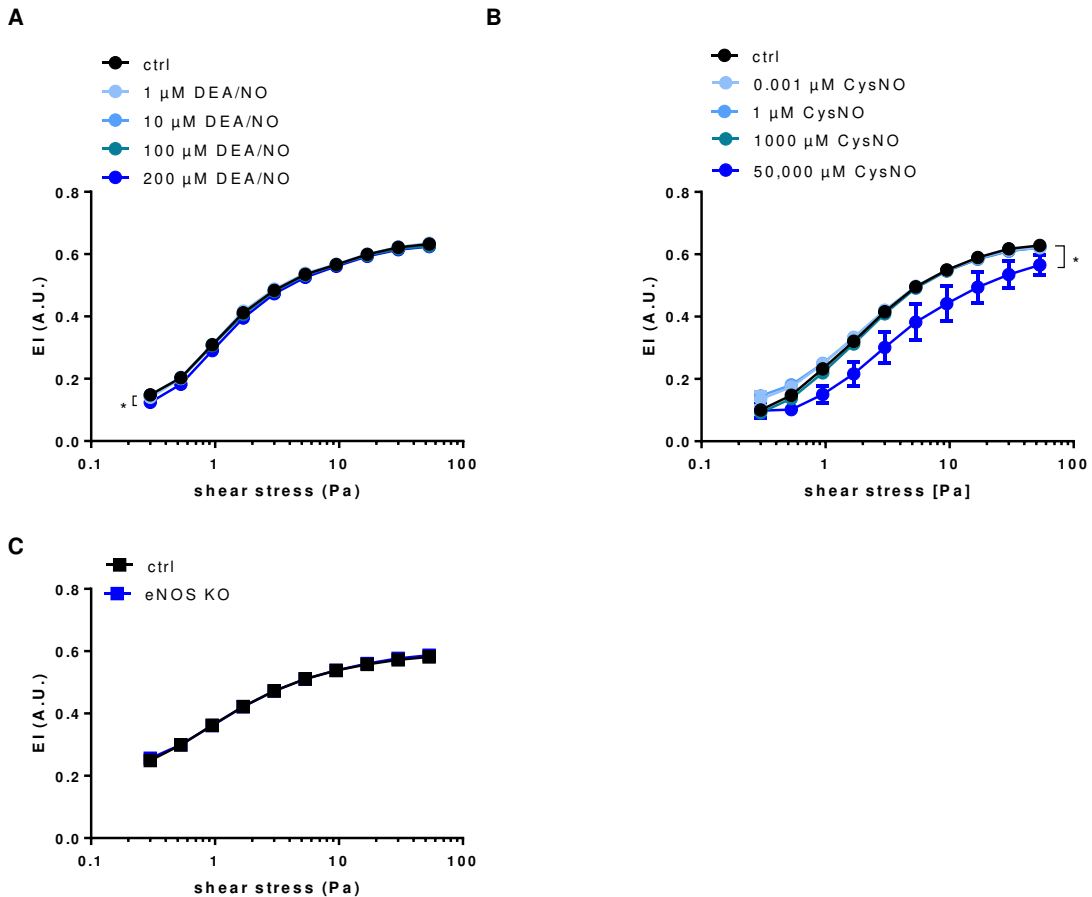
Figure 19 Effects of NO on RBC deformability

Using measurements of RBC deformability the effects of externally applied NO and internal lack of NO on RBCs were determined. A) No improvement of RBC deformability was found after application of different concentrations of the NO donor DEA/NO (2-way RM ANOVA; ctrl vs. treatments; P = 0.0001; Dunnett's test vs. ctrl; *: p < 0.05 (200 μM DEA/NO: significant at 0.3 - 5.3 Pa and 30 – 53.33 Pa)); RBCs from six donors in each group). B) No improvement of RBC deformability was found after application of the NO⁺ agent CysNO (2-way RM ANOVA; ctrl vs. treatments; P = 0.0059; Dunnett's test vs. ctrl; *: p < 0.05 (50,000 μM CysNO: significant at 0.53 - 53.33 Pa); RBCs from four donors in each group). C) RBC deformability of eNOS KO mice was not impaired (2-way RM ANOVA, eNOS KO vs. ctrl; P = 0.4725; RBCs from six mice in each group).

Summing up the addition of exogenous NO – ex-vivo - did not improve RBC deformability and the lack of endogenous NO – in-vivo - did not impair RBC deformability as well.

4.1.4 CysNO pre- or post-incubation attenuated oxidant induced decreases of RBC deformability

In the following section, the hypothesis that binding of NO could form short-term protection groups and by this could prevent oxidative modification of RBC proteins was investigated.

Therefore, human RBCs were incubated with different concentrations of CysNO before and after treatment of 3 mM oxidant t-BuOOH. Surprisingly pre- and post-treatment using concentrations ranging from 0.001 µM to 1000 µM CysNO resulted in concentration dependent protection against the decreased RBC deformability induced by addition of t-BuOOH (**Figure 20 A-B**).
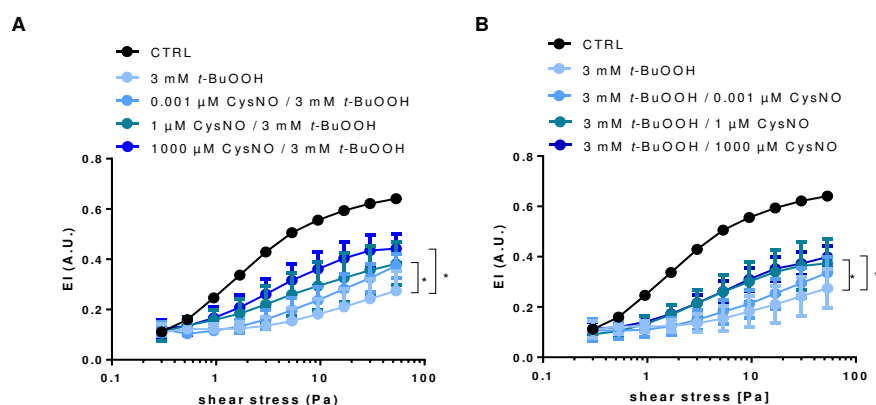
Figure 20 Effects of pre- and post-treatment with CysNO on oxidatively challenged RBCs

RBC deformability was measured with pre- and post-treatment of RBCs using a variation of CysNO concentrations (0.001 µM – 1000 µM) before or after treatment using 3 mM t-BuOOH. A) Incubation of RBCs with different concentrations of CysNO before addition of t-BuOOH was able to rescue RBC deformability in a concentration dependent manner (2-way RM ANOVA; ctrl vs. treatments; p = 0.0003; Tukey's test; ctrl. vs treatments; *:

P ≤ 0.05; significant for 1 µM CysNO in the range of 3 – 53.33 Pa; significant for 1000 µM CysNO in the range of 3 – 53.33 Pa). B) Incubation of RBCs with different concentrations of CysNO after addition of t-BuOOH was able to rescue RBC deformability in a concentration dependent manner (2-way RM ANOVA; ctrl vs. treatments; p = 0.0003; Tukey's test; ctrl. vs treatments; *: P ≤ 0.05; significant for 1 µM CysNO in the range of 5.33 – 53.33 Pa; significant for 1000 µM CysNO in the range of 0.3 – 53.33 Pa).

To exclude the simple chemical reaction of CysNO and *t*-BuOOH, both substances were co-incubated. To 0 mM or 50 mM *t*-BuOOH increasing concentrations of CysNO were added and UV-Vis absorption of CysNO was measured at 340 nm wavelength. There was no difference in absorption in samples with or without the presence of *t*-BuOOH suggesting that both substances did not chemically react (**Figure 21**).
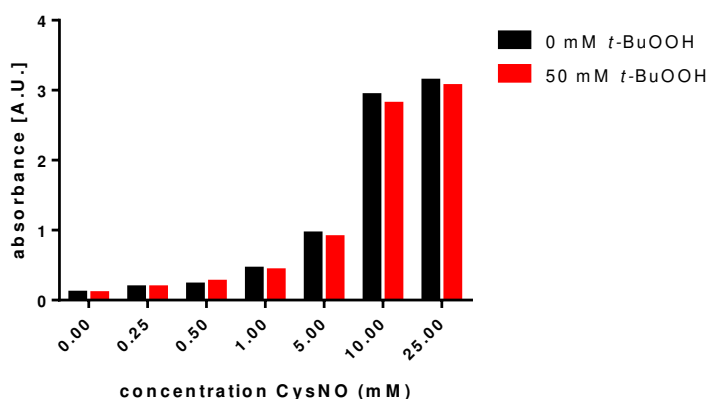
Figure 21 Measurement of CysNO absorption in the presence of *t*-BuOOH

Using UV-Vis, CysNO was measured in the presence of t-BuOOH. Both substances were incubated at the same time with a constant concentration of 50 mM t-BuOOH or 0 mM t-BuOOH and a range of concentrations of CysNO (0.25 mM – 50 mM).

This led to the conclusion that a treatment with nitrosating agent could be protective against oxidative induced changes of RBC deformability.

4.1.5 Summary

As a starting point of the studies, decreased RBC deformability was discovered in hypertensive patients concomitant with increased ROS levels. Surprisingly no change of intracellular NO bioavailability was detectable.

In further investigations it was found that with exhaustion of intracellular antioxidant defense also RBC deformability decreased and whole blood viscosity increased. NO at very high – not physiologically relevant concentrations – is capable to reduce RBC deformability and did not improve RBC deformability under any given shear stress or concentration of NO. Also lack of NO did not have any impact on RBC deformability.

However, NO was capable to dampen decreases of RBC deformability induced by an oxidant. Taken together, these data suggest that NO does not affect RBC deformability per se, but preserves RBC deformability in conditions of oxidative stress.

4.2   Role of NO in ATP release from RBCs

Deformation of RBCs and hypoxic conditions have been demonstrated to stimulate RBCs to release ATP and contribute to regulation of vascular tone (Ellsworth, Forrester et al. 1995, Wan, Ristenpart et al. 2008). That was surprising since for a long period of time RBCs were seen as enucleated cells with the only purpose of gas transport. Characterization of RBCs however demonstrated next to transport of gases more functions of RBCs. One of the functions attributed to RBCs is the release of ATP upon a variety of stimuli (e.g. hypoxia, shear stress). As a mechanism, activation of AC, followed by increases of cAMP, activation of PKA and release of ATP via pannexin-1 channel was proposed (Sprague and Ellsworth 2012). This pathway was proposed to be stimulated indirectly due to the activation of sGC and inhibition of phosphodiesterase 3 (Richards, Bowles et al. 2015).

In the following section it was hypothesized that intracellular increases of cAMP mediate ATP release via the pannexin-1 channel, a pathway that can be modulated by NO and the eNOS–sGC pathway.

4.2.1   cGMP and cAMP pathways were inducible in RBCs

The aim of this section was to characterize purine based intracellular signaling and in specific cAMP levels in response to different pharmacological stimuli in RBCs. The existence and activity of the enzymes necessary for cAMP and cGMP mediated signaling in RBCs remain poorly characterized. For this purpose, human RBCs were incubated ex-vivo with stimulators of intracellular purine based signaling. The activators used were 1) DEA/NO, a NO donor driving cGMP synthesis via sGC, 2) Bay 41, a sGC agonist, 3) forskolin, an AC activator, and 4) isoproterenol, a β-adrenergic receptor activator. To enhance the purine signals soluble phosphodiesterase inhibitors sildenafil (phosphodiesterase 5) and 3-isobutyl-1-methylxanthine (IBMX, an unspecific phosphodiesterase inhibitor) were added to treatments with pharmacological stimuli.

Of note the values for cAMP levels rose significantly to the magnitude of 3.4-fold in forskolin treated samples and 3.9-fold in forskolin and IBMX treated samples related to baseline levels (**Figure 22 A**). In isoproterenol treated samples relative cAMP levels rose to 1.9-fold compared to control for isoproterenol only and 2.6-fold levels for isoproterenol and IBMX treatment related to baseline, which did not reach statistical significance.

These findings suggested that AC initiated increase of cAMP occur in RBCs and that there was β-adrenergic receptor mediated activation of AC resulting in increased cAMP levels.

Measurements of cGMP levels demonstrated 2.5-fold increases after treatment with DEA/NO and Bay 41 [paired t-test, $P = 0.3084$, with RBCs from five volunteers in each group] and 6.6-fold after treatment with the combination of DEA/NO, Bay 41 and sildenafil [paired t-test, $P = 0.0374$, with RBCs from five volunteers in each group] (**Figure 22 G**). For a complete list of all measured purine based intracellular signaling molecules after the different stimulations please refer to **Table 4**.
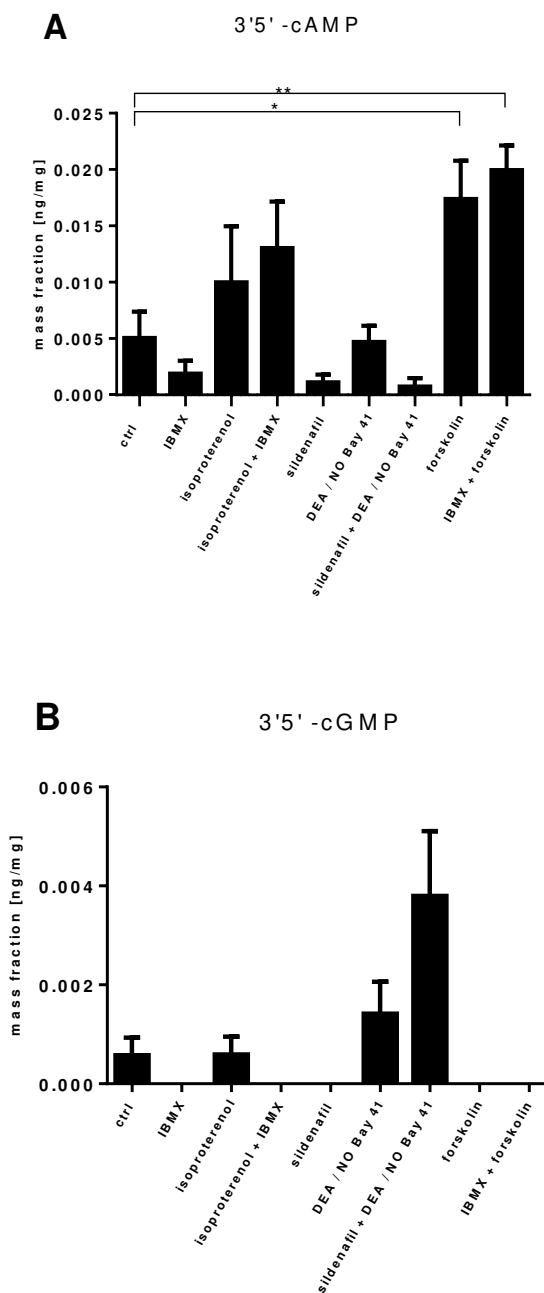
A 3'5'-cAMP

B 3'5'-cGMP

Figure 22 Changed RBC intracellular 3'5'-cAMP and 3'5'-cGMP levels after treatment with different pharmacological activators

Purine levels were measured by LC-MS/MS after being extracted from RBCs. A) Intracellular 3'5'-cAMP concentration (1-way RM ANOVA; P = 0.0098; Tukey's multiple comparison test;*: P < 0.05, **: P ≤ 0.01). B) Intracellular 3'5'-cGMP

concentration (1-way RM ANOVA; P = 0.0353). LC-MS/MS measurements were conducted in the lab of Dr. Jackson.

To sum up, the pharmacological stimuli applied here were capable to increase intracellular purine based signaling molecules and confirmed that the basis for the hypothesized pathway of cAMP and cGMP mediated ATP release exists in RBCs. In the next step it was tested if stimulation of cAMP or cGMP indeed results in increased extracellular ATP levels.

Table 4 Determination of intracellular purine levels after treatment using pharmacologic stimuli.

		treatment								
		control	IBMX	isoproterenol	IBMX + isoproterenol	sildenafil	DEA / NO Bay 41	sildenafil + DEA/NO BAY 41	forskolin	IBMX + forskolin
Intracellular purine [ng/mg]	cAMP	0.01	0.00	0.01	0.01	0.00	0.00	0.00	0.02	0.02
	AMP	65.21	63.35	55.58	53.36	49.95	49.86	48.46	51.63	51.51
	adenosine	0.15	0.14	0.14	0.13	0.13	0.14	0.14	0.14	0.14
	inosine	0.05	0.10	0.04	0.05	0.07	0.05	0.07	0.12	0.05
	hypoxanthine	2.78	2.75	2.14	2.12	2.05	2.76	2.51	2.80	2.45
	xanthine	0.03	0.05	0.03	0.04	0.04	0.04	0.05	0.05	0.03
	cGMP	0.00	0.00	0.00	0.00	0.00	0.00	0.00	0.00	0.00
	GMP	2.70	2.35	1.97	2.13	2.11	1.98	2.07	2.05	2.03
	guanosine	0.01	0.01	0.01	0.01	0.01	0.01	0.01	0.01	0.01
	guanine	0.12	0.13	0.12	0.16	0.10	0.13	0.10	0.12	0.14

Shown are mean values of intracellular purine levels after treatment with pharmacological stimuli. (Statistics 1-way RM ANOVA; 3'5'-cAMP: P = 0.0098, 5'-AMP: P = 0.1220, adenosine: P = 0.3968, inosine: P = 0.4341, hypoxanthine: P = 0.2297, xanthine P = 0.3819, 3'5'-cGMP: P = 0.0353, 5'-GMP P = 0.0646, guanosine: P = 0.3120, guanine: P = 0.2086)

4.2.2 Stimulation of neither cGMP, nor cAMP pathways increased levels of extracellular ATP

To evaluate if intracellular increases of cAMP or cGMP mediate extracellular ATP release, supernatants of stimulated RBCs were collected and ATP levels were measured with a chemiluminescence based assay (**Figure 23**).

No increased value of ATP was found for any of the conditions. Thus, conditions shown to increase intracellular cAMP production (forskolin, IBMX + forskolin) or cGMP production (DEA/NO, Bay 41 + sildenafil) did not stimulate the release of ATP. To exclude by hemolysis caused increases of extracellular ATP and wrong interpretation of the data hemoglobin was measured in the collected supernatants. Extracellular hemoglobin levels did not significantly differ within the treatment groups (**Figure 24**).
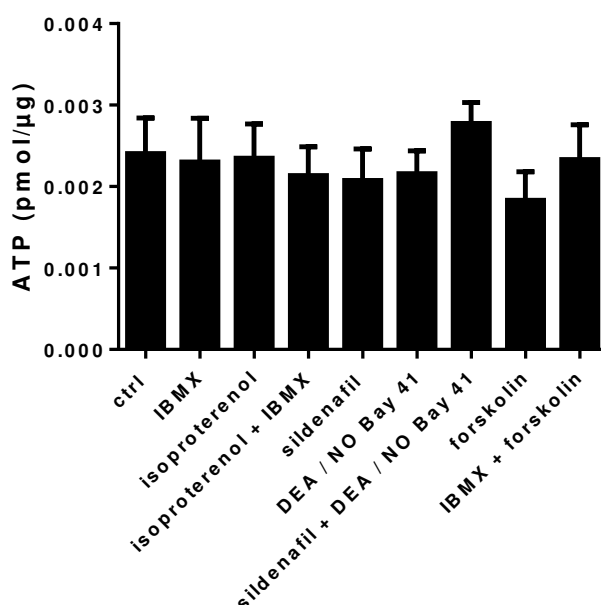
Figure 23 Extracellular ATP in the sample supernatant

Extracellular ATP was measured by a chemiluminescence based assay. No changes in release of ATP were detectable (1-way RM ANOVA, P = 0.2908, with RBCs from five volunteers in each treatment).
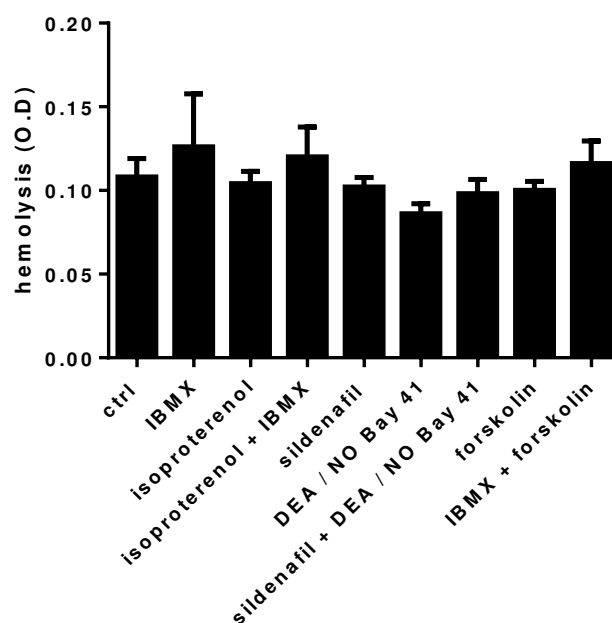
Figure 24 Extracellular hemoglobin after treatment of RBCs with different stimuli

Extracellular hemoglobin was measured by UV-Vis. No changes in release of hemoglobin were detectable (1-way RM ANOVA, P = 0.3938, with RBCs from five volunteers in each treatment).

However, in these measurements a moderate correlation of increased ATP levels and hemoglobin values was found [Pearson's correlation: $r^2 = 0.3295$, *P* = 0.0001]. This correlation was assumed not to confound the results since controlled release of ATP should exceed the levels measured by low levels of hemolysis. Interestingly, no increases of extracellular ATP were found in any treatment condition.
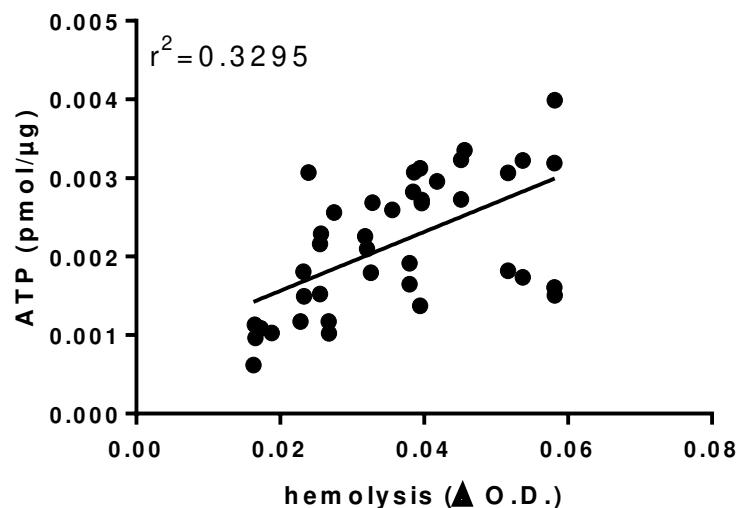
Figure 25 Correlation of ATP vs. extracellular hemoglobin

Extracellular hemoglobin (hemolysis) increases were measured via UV-Vis at 450 nm and subtracted by the baseline peak at 700 nm. Extracellular values for ATP concentrations were plotted against the values for hemolysis and a Pearson's correlation executed.

Bringing this finding in the context with the results of the previous section - where increases of second messengers and in particular cAMP and cGMP were found – the lack of increases in extracellular ATP suggested that the proposed mechanism of cAMP and cGMP mediated ATP release by pannexin-1 might not work as hypothesized. The experiments shown here were experiments ex-vivo and thus have their limitations. To finally clarify the role of the hypothesized pannexin-1 mediated pathway of ATP release by RBCs under physiological conditions, experiments with pannexin-1 KO mice were conducted in the next section.

4.2.3 Decreased exercise capacity of pannexin-1 KO mice

As an objective of these experiments the importance of pannexin-1 for adaption to exercise was investigated. If, after the hypothesis, pannexin-1 is the key enzyme releasing ATP from RBCs in conditions of high shear stress and hypoxia a forced exercise model should demonstrate impairment of maximal exercise capacity of pannexin-1 KO mice.

Long and intensive exercise training is known to cause a hypoxic condition and high blood flow in skeletal muscles.

Pannexin-1 KO mice were challenged with a forced exercise training protocol until total exhaustion and compared to WT control without pannexin-1 KO. Interestingly, no significant differences in exercise capacity were found comparing pannexin-1 KO mice to control WT (**Figure 26 A**) [distance covered: 1540 ± 135 m vs. 1761 ± 210 m; t-test, $P = 0.3777$]. No differences in body weight [control: 23.16 ± 0.89 g vs. pannexin-1 KO: 21.40 ± 0.97; t-test; $P = 0.19$] or exhaustion levels determined by lactate concentration in the blood [control: 4.33 ± 0.26 mM vs. pannexin-1: 4.19 ± 0.26 mM; t-test; $P = 0.72$] were evident (**Figure 26 B-C**).

Altogether pannexin-1 KO mice did not demonstrate reduced exercise capacity. This finding indicated that pannexin-1 does not play the important role for hypoxic adaptation as assumed.
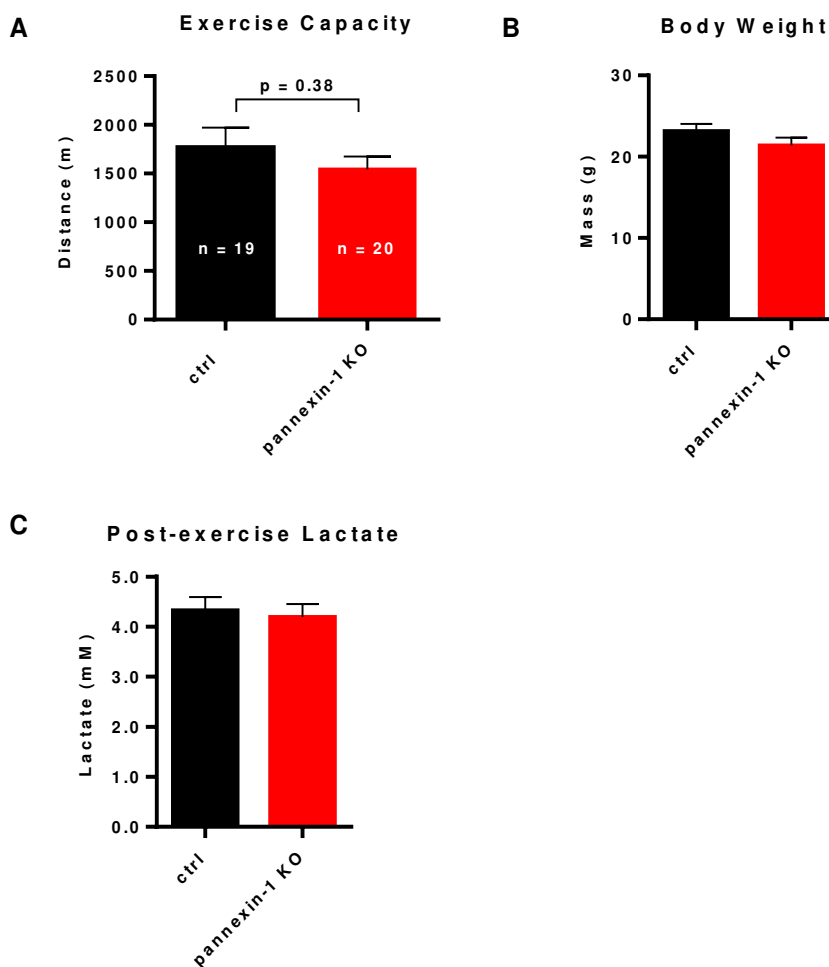
Figure 26 Exercise capacity of pannexin-1 KO mice

Exercise capacity of pannexin-1 KO mice vs. control mice was measured by a forced exercise protocol. Mice were run until total exhaustion on a treadmill. A) Average distance covered did not demonstrate any significant changes. B) No changes in body weights. C) Post-exercise lactate levels in plasma indicate no difference in anaerobic challenge. (Statistics A) - C) Unpaired t-test). Experiments conducted by A. Keller

4.2.4 Summary

In accordance with the hypothesis, cGMP and cAMP production could be stimulated by known activators of the sGC and AC pathways in RBCs. However, neither increases of cGMP nor cAMP led to controlled release of ATP in ex-vivo experiments. When pannexin-1 KO mice were subjected to a forced exercise protocol, no reduction of

maximal exercise capacity was evident, which led to the rejection of the hypothesis that regulated ATP release from RBCs is mediated by cAMP and cGMP signaling and pannexin-1 being the main channel releasing ATP.

4.3 Tissue specific transgenic eNOS KO and KI mice

The importance of eNOS expressed in the endothelium for the regulation of vasodilation decreases starting from large conductive arteries to small resistive vessel arteries and finally capillaries. Strikingly our lab could identify, in addition to expression of eNOS in vascular ECs, expression of eNOS in RBCs. To dissect the effects of the different NO generating tissues – RBC and vascular ECs - our lab created different models of tissue specific eNOS KO and KI mice using the Cre-loxP-system. With the help of the mouse models it will be possible to dissect the contribution of eNOS in the different tissue to blood pressure regulation. In order to do so full cardiovascular characterization of the mouse lines is necessary.

The aim of this section was the creation of tissue specific transgenic eNOS mice to investigate the role of eNOS in RBC in regulation of vascular tone and blood pressure.

4.3.1 Tamoxifen had no influence on vascular endothelial function

For EC specific models of KO and KI mouse a cadherin 5 promoter regulated Cre protein was used. The Cre protein is connected to an ERT2 domain which upon binding of tamoxifen is responsible for translocation of the fusion protein (Cre-ERT2) from the cytosol to the nucleus.

To exclude effects of tamoxifen on cardiovascular parameters - in this case in particular aortic endothelial function – WT mice were treated for five consecutive days with a dose of 0.75 mg of tamoxifen solved in peanut oil. After a waiting time of 21 days the highest efficacy of the tamoxifen treatment was expected and tamoxifen was washed out of the body.

As a measure for mouse health status during the washout period the gain of body weight was tracked. No differences in gain of body weight between control mice and tamoxifen injected mice were found [15.80 ± 1.79 % in six control mice vs. 14.59 ± 1.24 % in seven tamoxifen injected mice, $P = 0.35$] (**Figure 27 A – C**).
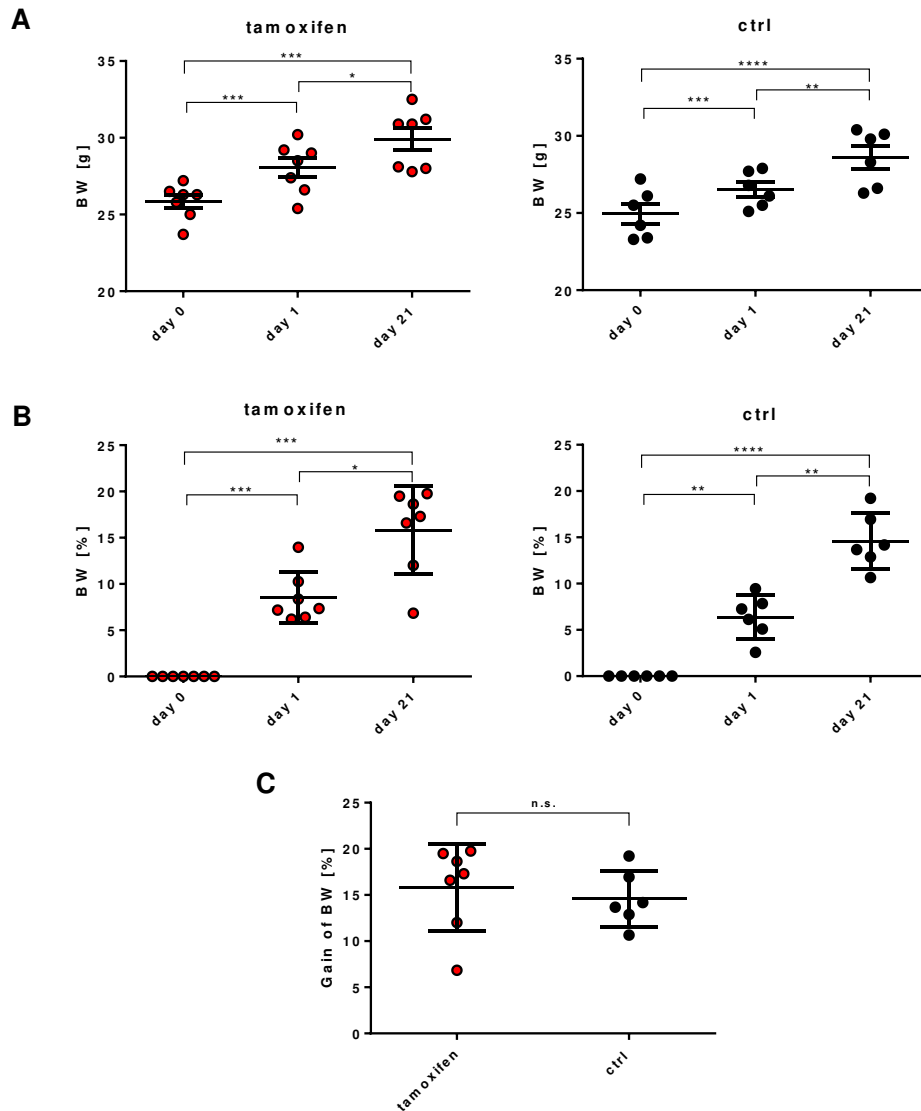
Figure 27 Gain of body weight during tamoxifen treatment

A) Absolute values of body weight before (day zero) and during tamoxifen treatment (day 1 and day 21) of seven tamoxifen treated mice (tamoxifen) vs. six vehicle treated mice (ctrl) (1-way ANOVA; tamoxifen: $P \leq 0.001$; ctrl: $P \leq 0.001$; Tukey's multiple comparisons test; *: $P < 0.05$, **: $P \leq 0.01$, ***: $p \leq 0.001$). In both groups a steady increase of body weight was observable. B) This observation was confirmed by the calculated per cent change of body weight after treatment of tamoxifen treated mice and vehicle treated mice (day 21) (1-way ANOVA; tamoxifen: $p < 0.001$; ctrl: $P < 0.001$; Tukey's multiple comparisons test; *: $P < 0.05$, ***: $P \leq 0.001$)). C) Comparison of per

cent body weight between tamoxifen and ctrl group after 21 days of treatment (t-test; P = 0.6017).

Blood parameters – measured at day 0 and day 21 after tamoxifen injection– were without significant changes except for an increase of RBC distribution width [14.07 ± 0.20 % control mice vs. 14.93 ± 0.10 % tamoxifen injected mice, *P* = 0.0376] and a decrease of the total amount of RBCs [11.11 ± 0.50 % in seven control mice vs. seven tamoxifen injected mice 10.04 ± 0.83 %, *P* = 0.0029]. A shift in RBC distribution width indicates a higher variability of the size of RBCs (**Table 5**).

Table 5 Blood cell counts of mice during tamoxifen treatment

			control			tamoxifen		
			baseline	day 21	*P*-value	baseline	day 21	*P*-value
blood paramters	white blood cells	10^3 / mm^3	6.78 ± 2.00	7.88 ± 3.81	*0.5353*	5.79 ± 1.96	9.14 ± 3.61	*0.0771*
	red blood cells	10^6 / mm^3	10.33 ± 1.40	9.77 ± 2.07	*0.6676*	11.11 ± 1.33	10.04 ± 0.83	***0.0376****
	lymphocytes	10^3 / mm^3	4.38 ± 1.32	4,87 ± 2.24	*0.7343*	4.13 ± 1.45	5.74 ± 1.76	*0.0629*
	monocytes	10^3 / mm^3	0.3 ± 0.25	0.4 ± 0.32	*0.4560*	0.2 ± 0.15	0.41 ± 0.36	*0.2079*
	granulocytes	10^3 / mm^3	1.36 ± 0.25	2.40 ± 1.37	*0.1448*	1.68 ± 1.25	2.20 ± 0.78	*0.3211*
	platelets	10^3 / mm^3	1179 ± 272	1346 ± 385	*0.4119*	1181 ± 322	1369 ± 247	*0.3346*
	hemoglobin	g/dl	16.02 ± 2.04	14.17 ± 2.50	*0.2057*	17.00 ± 1.79	15.59 ± 1.20	*0.0724*
	hematocrit	%	52.47 ± 7.23	45.57 ± 7.99	*0.1967*	55.40 ± 6.99	50.51 ± 3.71	*0.0721*
	mean corpuscular volume	µm^3	50.67 ± 1.03	50.33 ± 1.21	*0.3632*	49.83 ± 0.41	50.67 ± 0.82	*0.0925*
	mean corpuscular hemoglobin	%	15.63 ± 0.12	15.73 ± 0.22	*0.2292*	15.27 ± 0.31	15.56 ± 0.47	*0.1513*
	mean platelet volume	µm^3	5.10 ± 0.11	4.97 ± 0.12	*0.1576*	5.34 ± 0.53	5.13 ± 0.30	*0.1734*
	mean corpuscular hemoglobin concentration	g/dl	30.57 ± 0.81	31.25 ± 0.96	*0.1560*	30.80 ± 0.86	30.89 ± 1.40	*0.8826*
	red blood cell distribution width	%	14.57 ± 0.48	14.43 ± 0.23	*0.5632*	14.07 ± 0.35	14.93 ± 0.27	***0.0029*****

At baseline (day 0) and after treatment (day 21) blood counts were measured in tamoxifen treated mice (tamoxifen) and vehicle treated mice (ctrl). Only increases in RBC distribution width (RDW) were detected in the comparison of tamoxifen baseline to the

tamoxifen *group.*
Statistics: Paired t-test was applied to compare baseline values with values obtained 21 days after treatment (baseline ctrl vs. ctrl; baseline tamoxifen vs. tamoxifen).

The most important observation of this set of experiments was that vascular endothelium function did not change (**Figure 28 A – C**). The observation that tamoxifen itself had no effect on vascular endothelium function was essential for the interpretation of the following experiments in which tamoxifen was used to induce KO / KI.
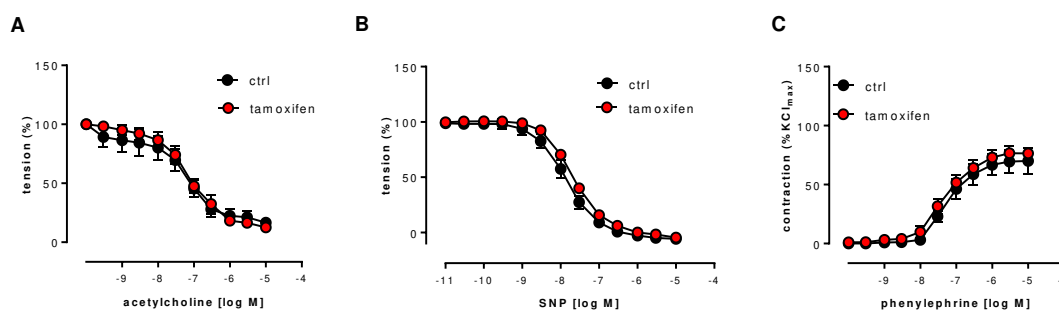
Figure 28 Effect of tamoxifen treatment on aortic endothelial function in WT mice

Aortic endothelial function (endothelium-dependent vasodilation, endothelium-independent vasodilation and vasoconstriction of aorta) in seven mice injected over five days with 0.75 mg tamoxifen (tamoxifen) and five control mice injected with the vehicle peanut oil only. A) Endothelium-dependent vasodilation tested with a cumulative dose of acetylcholine showed no difference between control and tamoxifen (2-way RM ANOVA; ctrl vs. tamoxifen; P = 0.6650). B) Endothelium-independent vasodilation tested with a cumulative dose of SNP did not show any difference between ctrl and tamoxifen (2-way RM ANOVA; ctrl vs. tamoxifen; P = 0.0759). C) Aortic constriction to cumulative doses of phenylephrine did not show any difference between ctrl and tamoxifen (2-way RM ANOVA; ctrl vs. tamoxifen; P = 0.4434).

4.3.2   Vascular endothelial function was impaired in global eNOS KO mice

To confirm that the construct was working measurement of vascular endothelium function in aortas of eNOS KO and WT mice was executed. eNOS KO mice should be

able to confirm findings of other eNOS KO lines strains (Shesely, Maeda et al. 1996, Godecke, Decking et al. 1998).

Mice with the genotype of homozygous inverted exon 2 of eNOS (eNOS[inv/inv]) were used for this investigation since they are expected to mimic the eNOS KO phenotype. A maximal cumulative dose of acetylcholine resulted in a maximal dilation of 108.72 ± 24.11 % in eNOS KO mice compared to 12.62 ± 2.13 % in WT mice (**Figure 29 A**). Endothelium-independent dilation was shifted towards lower concentrations in eNOS KO mice indicating higher sensitivity towards exogenously applied NO [EC_{50} 8.1•10^{-9} M in eNOS KO mice and 22.8•10^{-9} M in WT mice] (**Figure 29 B**). In addition to that eNOS KO mice responded to phenylephrine with a higher constriction of 126.33 ± 0.26 % compared to 76.42 ± 4.80 % in WT mice (**Figure 29 C**).

To sum up eNOS KO mice were characterized by blunted vascular endothelium-dependent vasodilation, higher sensitivity to exogenous NO and stronger response to vasoconstrictors.
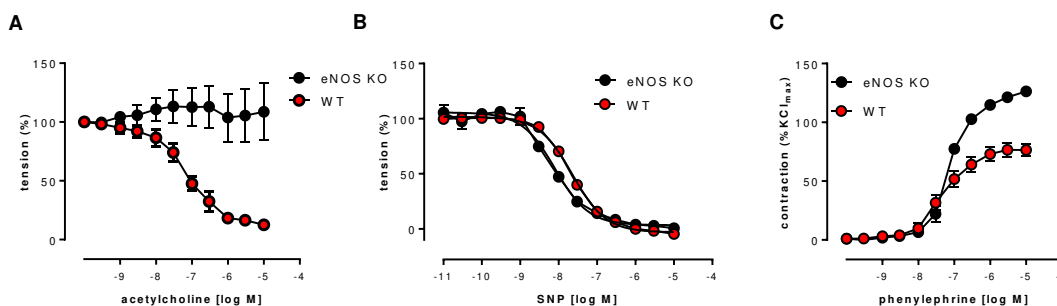
Figure 29 Aortic endothelial function in eNOS KO mice compared to WT

Organ bath experiments to investigate endothelium function in aorta of WT and global eNOS KO mice. A) Endothelium-dependent vasodilation was tested with a cumulative dose of acetylcholine showed significant difference between WT and eNOS KO (2-way RM ANOVA; WT vs. eNOS KO; P = 0.0015). B) Endothelium-independent vasodilation was tested with a cumulative dose of SNP did demonstrate a shift to lower concentrations indicating higher sensitivity of eNOS KO mice, yet not statistically significant (2-way RM ANOVA; WT vs .eNOS KO; P = 0.2819). C) Aortic constriction to cumulative doses of phenylephrine did demonstrate higher maximal constriction in eNOS KO mice vs. WT mice (2-way RM ANOVA; ctrl vs. tamoxifen; P = 0.0695).

4.3.3   Vascular endothelium function was reestablished in global eNOS KI mice

To test the functionality of eNOS KI construct, i.e. inversion of exon 2 catalyzed by Cre-recombinase, aortic endothelial function was investigated in global eNOS KI mice containing the inverted exon 2 sequence (eNOS KO).

At baseline, before crossing the two strains, the reactivity of mice aortas to acetylcholine was blunted and maximal constriction was increased in eNOS KO mice as demonstrated in the previous chapter 4.3.2 and **Figure 30 A**. After successful crossing of eNOS$^{inv/inv}$ mice with globally expressing Cre-mice the resulting global eNOS KI mice were expected to present with aortic endothelial function. Indeed, the resulting global eNOS KI mice matched WT mice in all tested characteristics. The aortic reactivity to acetylcholine matched to the aortic reactivity of WT mice (ctrl) (**Figure 30 B**). The typical shift of dose-response curves to SNP and stronger response to phenylephrine expected for mice lacking a functional eNOS as observed in the previous chapter was lost (**Figure 30 A**).

The loxP-Cre construct applied here was capable to re-establish vascular endothelium function in a mouse line characterized by a phenotype comparable to eNOS KO mice.
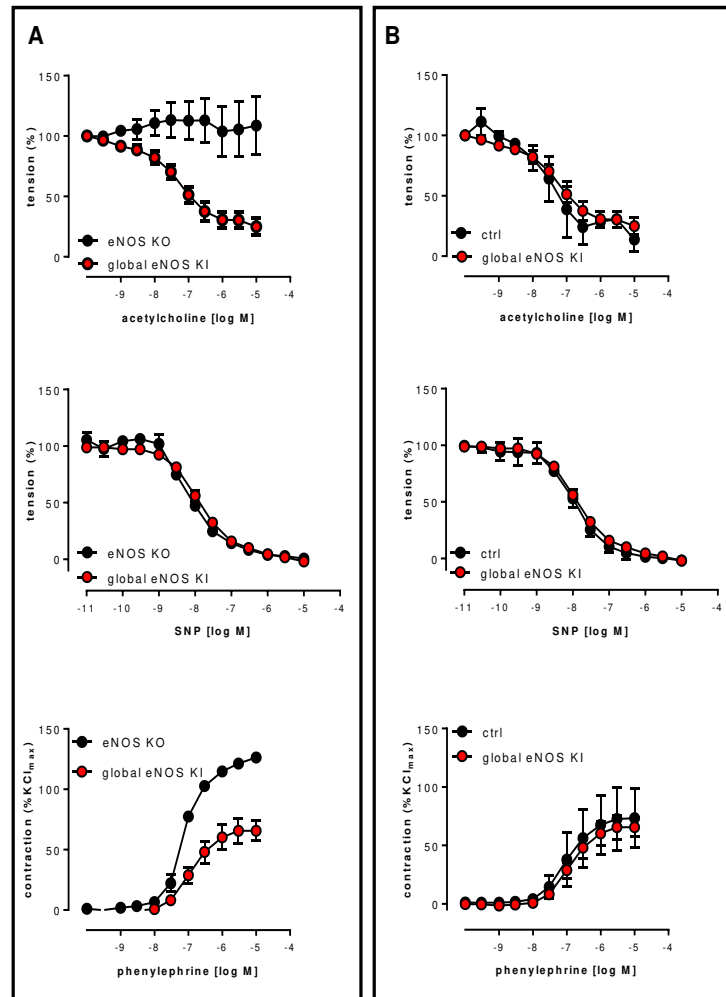
Figure 30 Aortic endothelial function of global eNOS KI mice

Aortic endothelial function from eight global eNOS KI mice, five eNOS KO mice and two WT mice (ctrl) were measured in an organ bath setting. A) Comparison of endothelium-dependent vasodilation of eNOS KO mice vs. global eNOS KI mice (2-way RM ANOVA; eNOS KO vs. eNOS global KI; P = 0.0034) Endothelium-independent vasodilation was tested with a cumulative dose of SNP (2-way RM ANOVA; eNOS KO vs. eNOS global KI; P = 0.8520). Aortic constriction to cumulative doses of phenylephrine (2-way RM ANOVA; ctrl vs. eNOS global KI; P = 0.0127). B) Endothelium-dependent vasodilation was tested with a cumulative dose of acetylcholine and showed re-established endothelium function (2-way RM ANOVA; ctrl vs. eNOS global KI; P = 0.8618). Endothelium-independent vasodilation was tested with a cumulative dose of SNP (2-way RM ANOVA; ctrl vs. eNOS global KI; P = 0.4173). Aortic constriction to cumulative

71

doses of phenylephrine was not statistically different (2-way RM ANOVA; ctrl vs. eNOS global KI; P = 0.6200).

4.3.4 Blood pressure was increased and vascular endothelium function impaired in EC eNOS KO mice

After the first confirmations of the constructs working, the effects of tamoxifen treatment on eNOS$^{fl/fl}$ mice crossed with a strain expressing Cre-ERT2 controlled by the cadherin 5 promoter were investigated.

Measurement of diastolic and systolic blood pressure using a pressure catheter demonstrated increased diastolic [55.83 ± 6.29 mmHg vs. 87.90 ± 3.86 mmHg; control vs. endothelial eNOS KO; $P < 0.0009$] and systolic blood pressures [87.17 ± 6.51 mmHg vs. 118.80 ± 4.22 mmHg; control vs. endothelial eNOS KO; $P < 0.0008$].
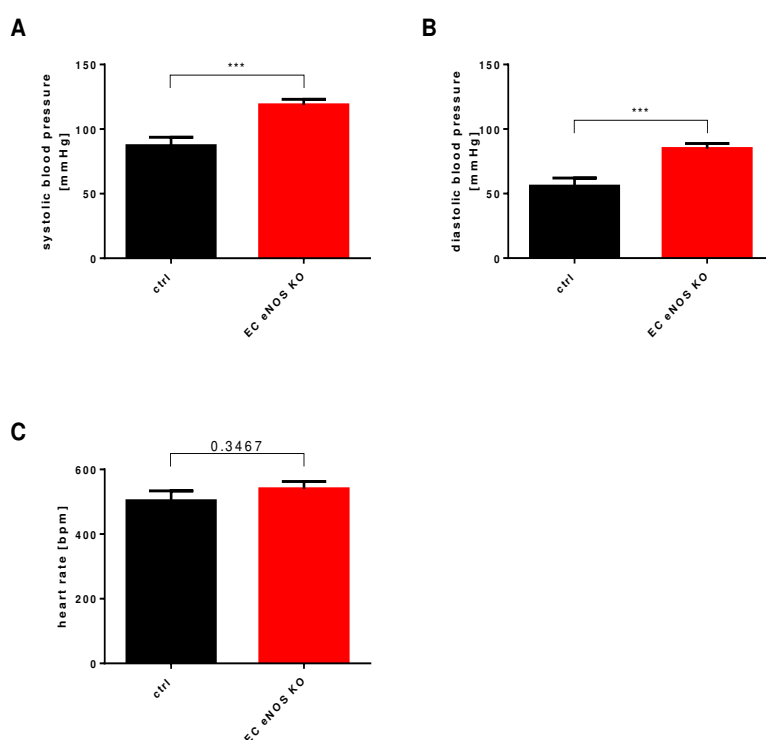
Figure 31 Systolic blood pressure, diastolic blood pressure and heart rate in EC eNOS KO mice

Using invasive pressure catheter measurements, blood pressure parameters were measured in ten endothelial eNOS KO mice vs. six controls. A) Systolic blood pressure

and B) diastolic blood pressure were significantly increased in RBC eNOS KO mice. C)
Heart rate was unchanged. (Unpaired t test; systolic blood pressure ***: P < 0.0008;
diastolic blood pressure P < 0.0009; beats per minute (bpm)). Measurements conducted
by S. Becher.

The functionality of eNOS was studied ex-vivo in the organ bath setting and eNOS
expression levels using Western blot. In the following the offspring of this breeding with
the genotype eNOS$^{fl/fl}$ and Cre-ERT2 expression will be labeled endothelial cell eNOS
knockout (EC eNOS KO). The conditional cadherin 5 promoter regulated Cre-ERT2 is
used for models of endothelium specific Cre protein expression. The activity of the Cre
is dependent on tamoxifen administration. In these experiments both groups, Cre-ERT2
positive and Cre-ERT2 negative mice (ctrl), were treated with tamoxifen.

On a functional level, EC eNOS KO mice had markedly blunted reactivity to control mice
(**Figure 32 A**) [maximal vasodilation: 95.00 ± 23.89 % vs. 25.83 ± 6.74 % in two EC
eNOS KO mice and three control mice]. Similar to the global eNOS KO mice a shift
towards higher sensitivity to exogenous NO was evident (**Figure 32 B**) [EC$_{50}$: 7.64•10^{-9}
M vs. 17.90•10^{-9} M, EC eNOS KO vs. control] and higher maximal constriction (**Figure
32 C**) [maximal constriction: 95.28 ± 20.56 % vs. 70.55 ± 8.85 %].
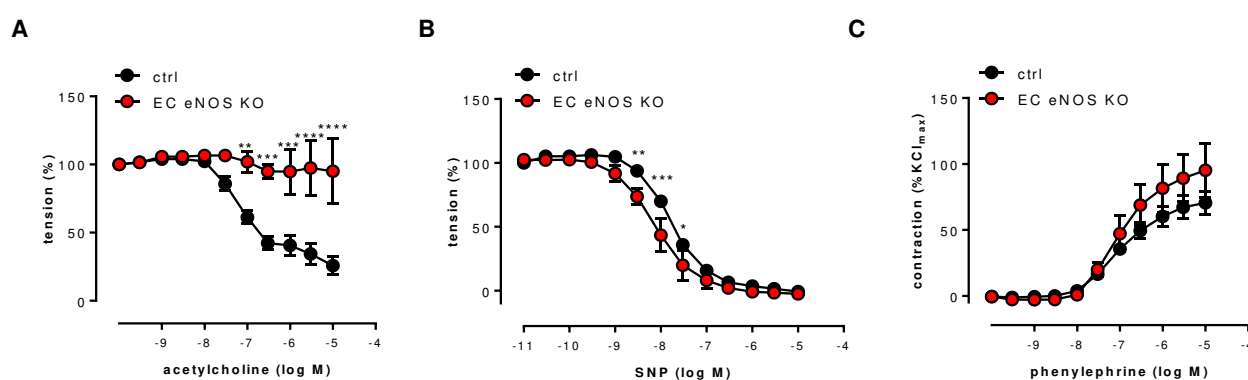
Figure 32 Aortic endothelial function of EC eNOS KO mice

Organ bath experiments were conducted in three control mice and two EC eNOS KO
mice. Both groups were injected with 0.75 mg tamoxifen for five consecutive days and
after a waiting period of 21 days analyzed. A) Endothelium-dependent vasodilation was

tested with a cumulative dose of acetylcholine. The response to acetylcholine was blunted in eNOS KO mice (2-way RM ANOVA; ctrl vs. EC eNOS KO; P = 0.0325; Sidak's multiple comparison test; **: P ≤ 0.01, ***: P ≤ 0.001, ****: P ≤ 0.0001). B) Endothelium-independent vasodilation was tested with a cumulative dose of SNP. EC eNOS KO mice were more responsive to endothelium-independent vasodilation (2-way RM ANOVA; ctrl vs. EC eNOS KO; p = 0.1035; Sidak's multiple comparison test; **: P ≤ 0.01, ***: P ≤ 0.001, ****: P ≤ 0.0001). C) Even though not statistically significant EC eNOS KO mice in tendency seem to constrict faster and stronger to the phenylephrine (2-way RM ANOVA; ctrl vs. EC eNOS KO; P = 0.3210; Sidak's multiple comparison test).

For Western blot analysis aortas, hearts and skeletal muscles were collected from control and EC eNOS KO mice. In aortas, KO efficacy of eNOS was 85.26 %, in skeletal muscle 97.66 % and cardiac tissue 98.57 % (**Figure 33** - **Figure 35**). On a functional level lower EC_{50} values in response to SNP application were found in EC eNOS KO mice vs. control [$7.64 \cdot 10^{-9}$ M vs. $17.90 \cdot 10^{-9}$ M] indicating higher sensitivity towards exogenously applied NO. One possible mechanism for that could have been a compensatory up-regulation of the NO receptor sGC (Hussain, Hobbs et al. 1999). However, no changes in expression levels were found for both sGC subunits (**Figure 33** - **Figure 35**).

To sum up, EC eNOS KO mice have impaired vascular endothelium function, caused by an efficient KO of the eNOS protein shown here on a protein level. The quicker response of the EC eNOS KO towards SNP was not explainable by an up-regulation of sGC.

A

B **C**
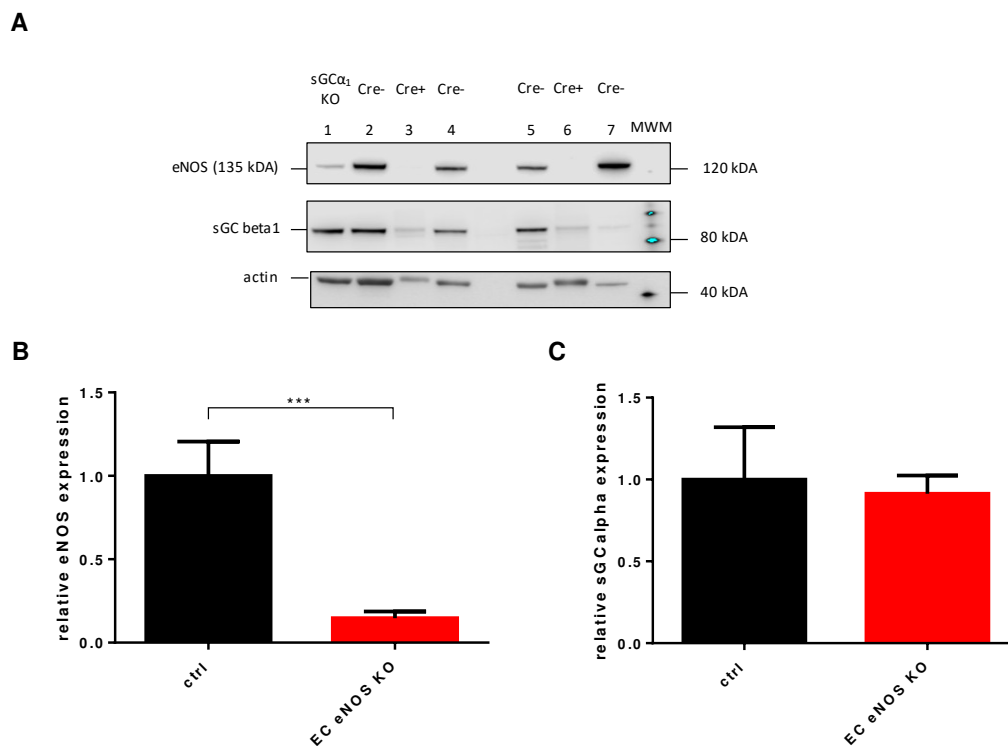
Figure 33 Levels of eNOS in EC eNOS KO and control mice in aorta

Effect of deletion of exon 2 of the eNOS gene was analyzed by Western blotting. A) A representative Western blot showing eNOS, sGC beta1-subunit and actin protein bands (after tamoxifen treatment) (molecular weight marker (MWM), lane 1: sGCα1 KO mouse, lanes 3,6: EC eNOS KO mice (Cre +) 2,4,5,7:ctrl (Cre -)). B) Relative changes of eNOS expression were normalized to the signal of actin (results from three different membranes) (Unpaired t test; ***: P < 0.001). C) Relative expression levels of sGC$_{α1}$ to signal of actin (results from two different membranes).
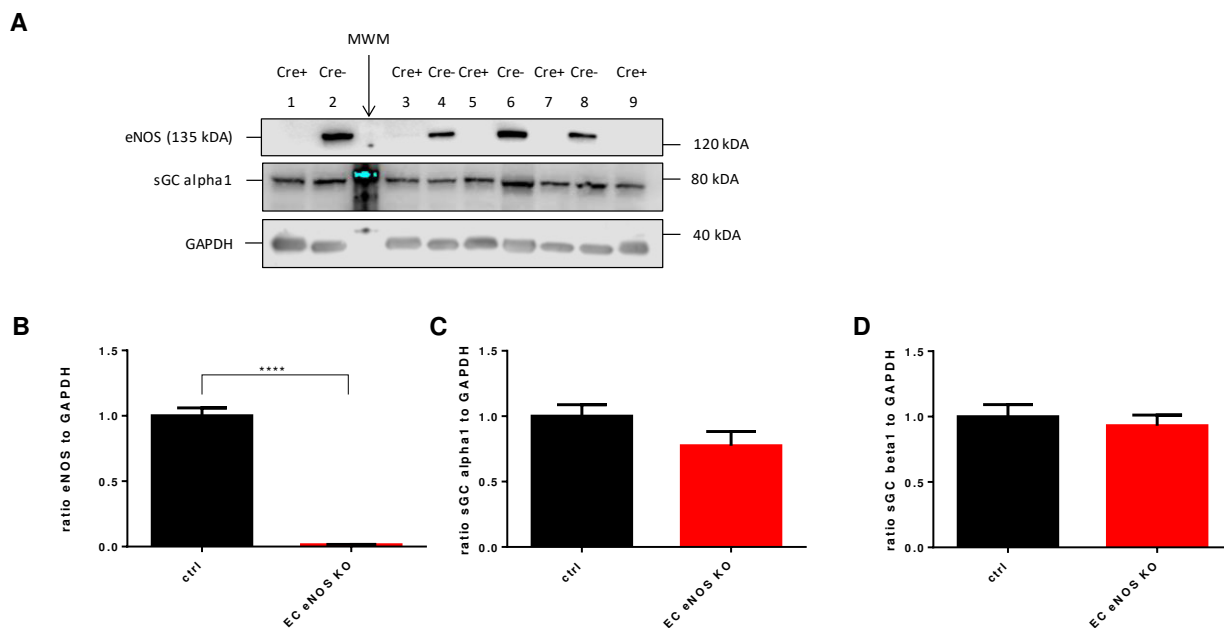
Figure 34 Myocardial levels of eNOS in EC eNOS KO and control mice in aorta

*Western blotting was conducted for semi-quantitative determination of eNOS protein levels. A) A representative Western blot showing eNOS, sGC alpha1 and GAPDH protein bands (molecular weight marker (MWM), lanes 1, 3, 5, 7, 9: EC eNOS KO mice, lanes 2, 4, 6, 8: control). B) Relative changes of eNOS expression were normalized to signal of GAPDH (results from eight different membranes) (Unpaired t test; ****: P < 0.0001.). C) Relative expression levels of sGCα1 to signal of GAPDH (results from three independent membranes). D) Relative expression levels of sGCα1 to signal of GAPDH (results from three independent membranes).*
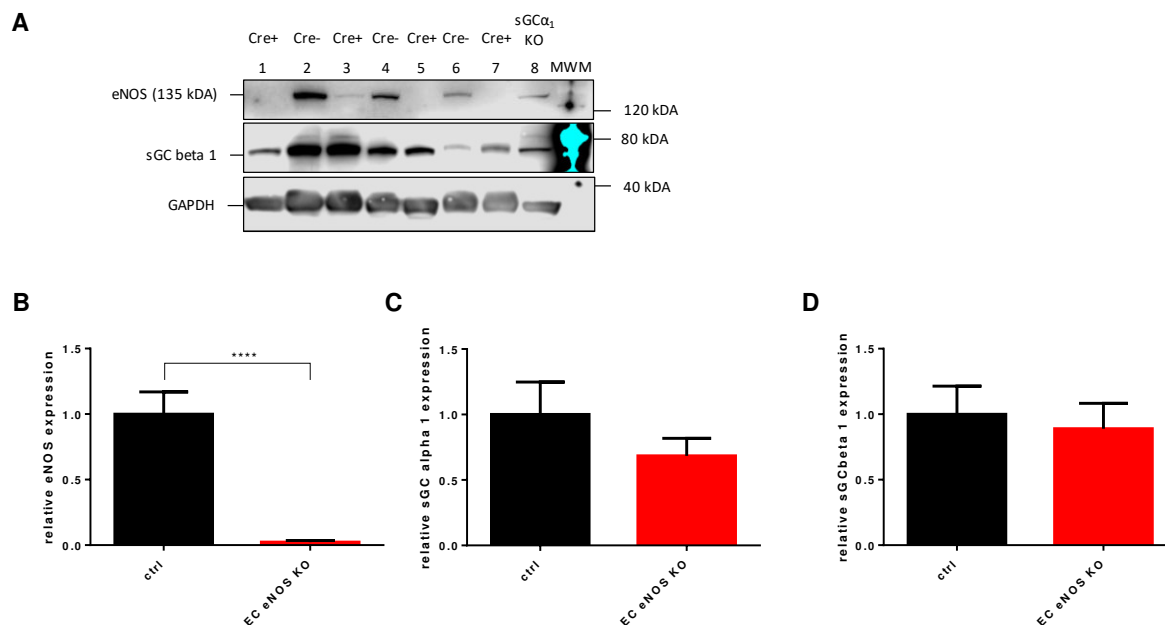
Figure 35 Levels of eNOS in skeletal muscle

*A) A representative Western blot showing eNOS, sGC beta1 and GAPDH protein bands (molecular weight marker (MWM), lanes 1, 3, 5, 7: EC eNOS KO mice, lanes 2, 4, 6: ctrl, lane 8: sGCα₁-KO. B) Relative changes of eNOS expression normalized to signal of GAPDH (results from seven different membranes) (Unpaired t test; ****: p < 0.0001). C) Relative expression levels of sGCα₁ to signal of GAPDH (results from 5 independent membranes). D) Relative expression levels of sGCβ₁ to signal of GAPDH (results from 2 independent membranes).*

4.3.5 Vascular endothelium function was reestablished in EC eNOS KI mice

In the next sections vascular endothelial function in EC eNOS KI mice (eNOS$^{inv/inv}$ / Cre pos.) versus control (eNOS$^{inv/inv}$) was investigated first without treatment and in the second set of experiments after treatment with tamoxifen. As an additional control the NOS inhibitor L-NAME was added in these experiments in order to prove that relaxation to acetylcholine was in fact NOS dependent relaxation. In the mice, which did not receive tamoxifen treatment acetylcholine dependent relaxation was blunted in both strains - control and EC eNOS KI – as expected when no functional eNOS is expressed (**Figure**

36 A). For all other measurements at baseline no marked differences were observable between control and EC eNOS KI before tamoxifen injection (**Figure 36 A – C**).
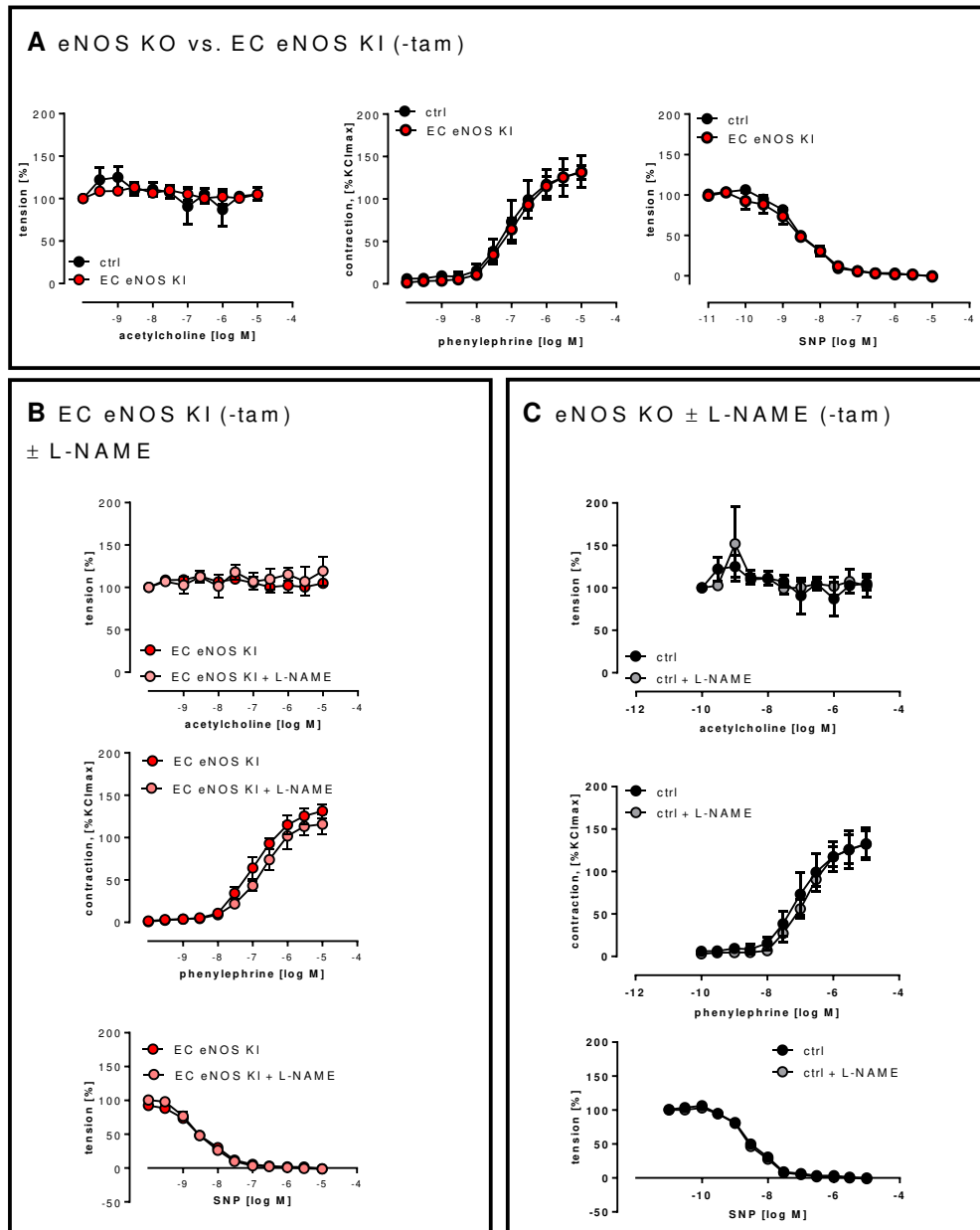
Figure 36 Aortic endothelial function of EC eNOS KI mice before tamoxifen treatment

Endothelium function was measured in aortic preparations in organ baths of three eNOS KO mice (eNOS$^{inv/inv}$ / Cre-ERT2 neg.) compared to three EC eNOS KI mice (eNOS$^{inv/inv}$ L-NAME / Cre-ERT2 pos.). A) Reactivity to acetylcholine was blunted in eNOS KO and

EC eNOS KI without tamoxifen treatment. No differences were visible in the reactivity to phenylephrine and SNP (2-way RM ANOVA; ctrl vs. endothelium eNOS KI; acetylcholine: P = 0.9484; phenylephrine: P = 0.7959; SNP: P = 0.5362; Sidak's multiple comparison test). B) Addition of the NOS inhibitor L-NAME resulted in no changes in reactivity to acetylcholine, phenylephrine and SNP (2-way RM ANOVA; ctrl vs. endothelium eNOS KI; acetylcholine: P = 0.7479; phenylephrine: P = 0.2660; SNP: P = 0.8085; Sidak's multiple comparison test). C) Addition of L-NAME to ctrl mice did not change aortic reactivity to acetylcholine, phenylephrine and SNP (2-way RM ANOVA; ctrl vs. endothelium eNOS KI; acetylcholine: P = 0.8108; phenylephrine: P = 0.7466; SNP: P = 0.4831; Sidak's multiple comparison test).

After tamoxifen injection, however, the KI of eNOS took place and clear changes became visible.

Observation of endothelium-dependent relaxation by application of a final dose of 1 mM acetylcholine resulted in a final dilation of 91.77 ± 11.75 % for the EC eNOS KI mice. In contrast to that after the same cumulative dose of acetylcholine a constriction of 8.72 ± 24.105 % was observed in the eNOS KO mice (**Figure 37 A**). This clearly demonstrated re-established endothelium function in EC eNOS KI mice. The already mentioned shifts in dose-response curves visible in eNOS KO mice vs. WT mice again become visible by an 86 % greater constriction in control mice than EC eNOS KI mice (**Figure 37**, middle panel). Next to that, eNOS KO mice were more responsive to SNP reflected by the EC_{50} values of $8.08 \cdot 10^{-9}$ M for eNOS KO mice and $17.40 \cdot 10^{-9}$ M for endothelium KI mice. Control experiments with the addition of L-NAME show that these observed effects are in fact due to NOS dependent signaling (**Figure 37 B – C**).
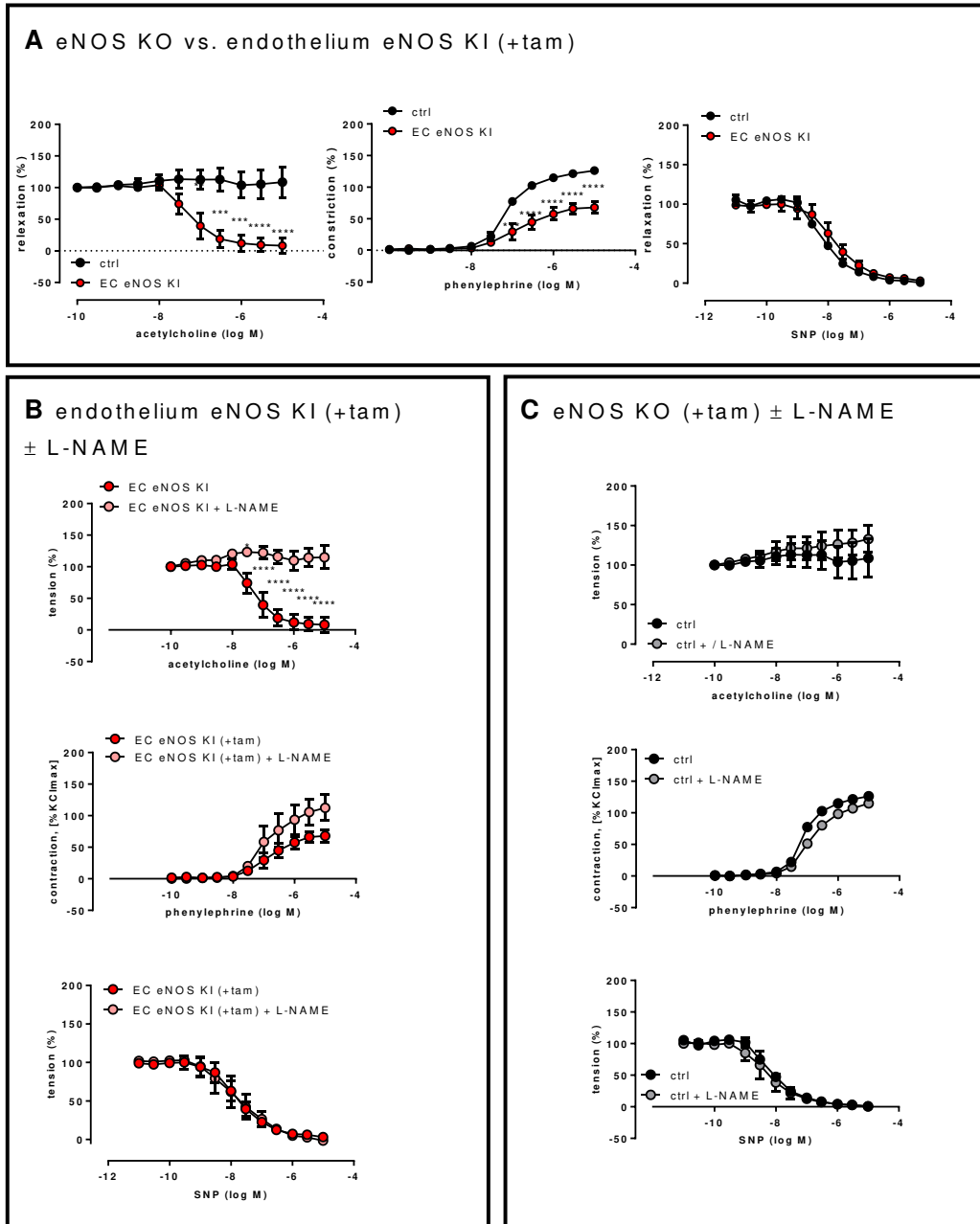
Figure 37 Aortic endothelial function of EC eNOS KI mice after tamoxifen treatment

Endothelium function was measured with aortic preparations in organ baths of two control (eNOS$^{inv/inv}$ / Cre-ERT2 neg.) and compared to three EC eNOS KI mice (eNOS$^{inv/inv}$ L-NAME / Cre-ERT2 pos.). A) Reactivity to acetylcholine was blunted in ctrl mice but re-established in EC eNOS KI with tamoxifen treatment. EC eNOS KI mice showed less maximal constriction to phenylephrine and were in tendency less responsive

80

to SNP (2-way RM ANOVA; ctrl vs. endothelium eNOS KI; acetylcholine: P = 0.0461; phenylephrine: P = 0.0242; SNP: P = 0.7005; Sidak's multiple comparison test; **: P ≤ 0.01, ***: P ≤ 0.001, ****: P ≤ 0.0001). B) Addition of the NOS inhibitor L-NAME completely blocked the reactivity to acetylcholine. (2-way RM ANOVA; ctrl vs. endothelium eNOS KI; acetylcholine: p = 0.0104; phenylephrine: p = 0.2257; SNP: p = 0.9852; Sidak's multiple comparison test; *: P < 0.05, **: P ≤ 0.01, ***: P ≤ 0.001, ****: P ≤ 0.0001). C) Addition of L-NAME to ctrl mice did not change vascular reactivity to acetylcholine, phenylephrine and SNP (2-way RM ANOVA; ctrl vs. endothelium eNOS KI; acetylcholine: P = 0.5885; phenylephrine: P = 0.0237; SNP: P = 0.4615; Sidak's multiple comparison test).

These results clearly demonstrated that tamoxifen treatment rescued endothelium function in EC eNOS KI mice compared to baseline and typical reactivity of a functional vessel to all stimuli was achieved.

4.3.6 RBC eNOS KO mice have increased blood pressure and unchanged vascular endothelial function

The mice deprived of eNOS specifically in RBCs (RBC eNOS KO mice) are of special interest since in previous studies a role of RBC eNOS for blood pressure regulation has been proposed (Wood, Cortese-Krott et al. 2013).

First hemodynamic investigations of RBC eNOS KO mice revealed indeed increased values of diastolic [59.33 ± 3.03 mmHg vs. 73.57 ± 2.58 mmHg; control vs. RBC eNOS KO; $P < 0.0039$] and systolic blood pressures [92.22 ± 2.58 mmHg vs. 108.40 ± 1.80 mmHg; control vs. RBC eNOS KO; $P < 0.0039$] (**Figure 38**). Also, heart rate was found to be significantly reduced [532.1 ± 19.3 bpm vs. 436.4 ± 30.5 bpm; control vs. RBC eNOS KO; $P < 0.0151$] (**Figure 38**).

An important participant in regulation of blood pressure is vascular endothelium function in conduit and resistive vasculature. The aim of the following section was to characterize the vascular endothelium function of arterial vessels representative for conduit arteries and resistive vasculature. If there were no changes in vascular endothelium function in

both types of vessels this would strongly imply that another mechanism was responsible for high blood pressure.
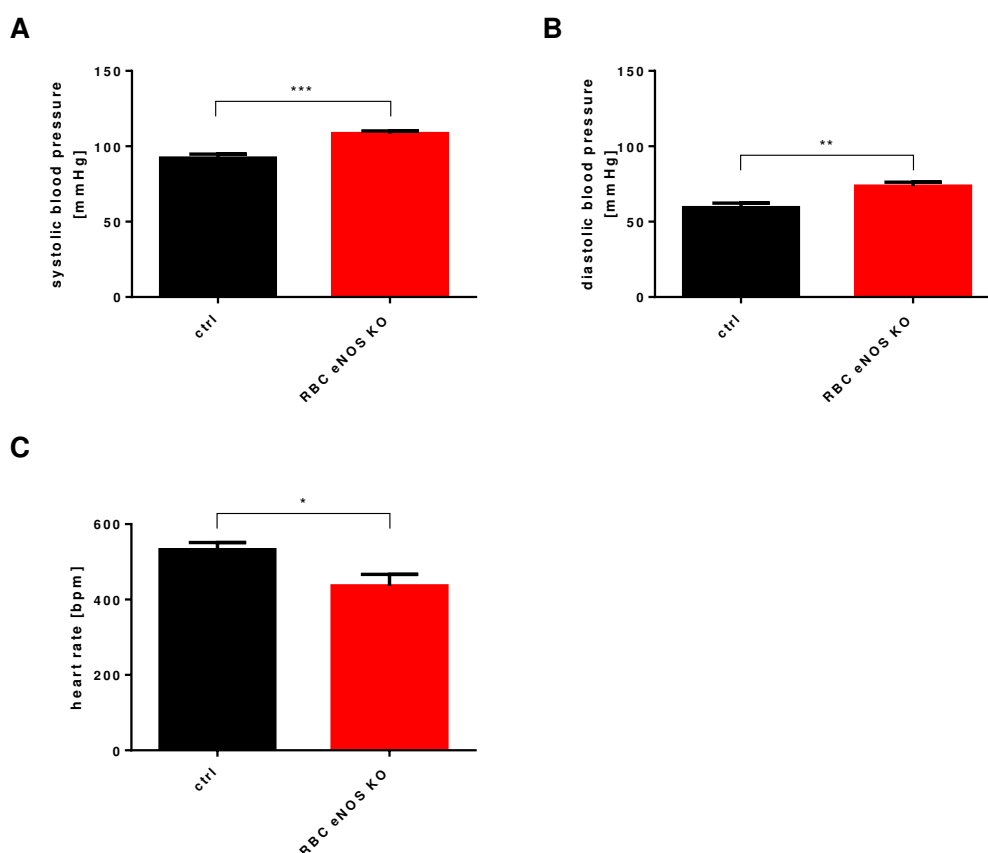
Figure 38 Systolic and diastolic blood pressure in RBC eNOS KO mice

Using invasive pressure catheter measurements, blood pressure parameters were measured in nine RBC eNOS KO mice vs. seven controls. A) Systolic blood pressure and B) diastolic blood pressure were significantly increased in RBC eNOS KO mice. (Unpaired t test; systolic blood pressure ***: P < 0.003; diastolic blood pressure P < 0.0039, heart rate P = 0.0151). Measurements conducted by S. Becher.

Functionality of aortas was fully preserved in the ex-vivo setting, which was reflected by superimposable dose-response curves for acetylcholine, phenylephrine and SNP of control and RBC eNOS KO mice (**Figure 39 A**). Additions of L-NAME to RBC eNOS KO and control vessels respectively resulted in completely blunted reactivity to acetylcholine confirming that the previous effect can be attributed to NOS dependent

signaling. Moreover, the typical increase response towards phenylephrine was evident after the application of L-NAME. Importantly the maximal constriction for RBC eNOS KO mice and control mice did not statistically differ [155.57 ± 22.73 % vs. 155.24 ± 8.44 %]. A tendency towards a, not statistically different, shift of vessels treated with L-NAME was measured (**Figure 39 B – C**).
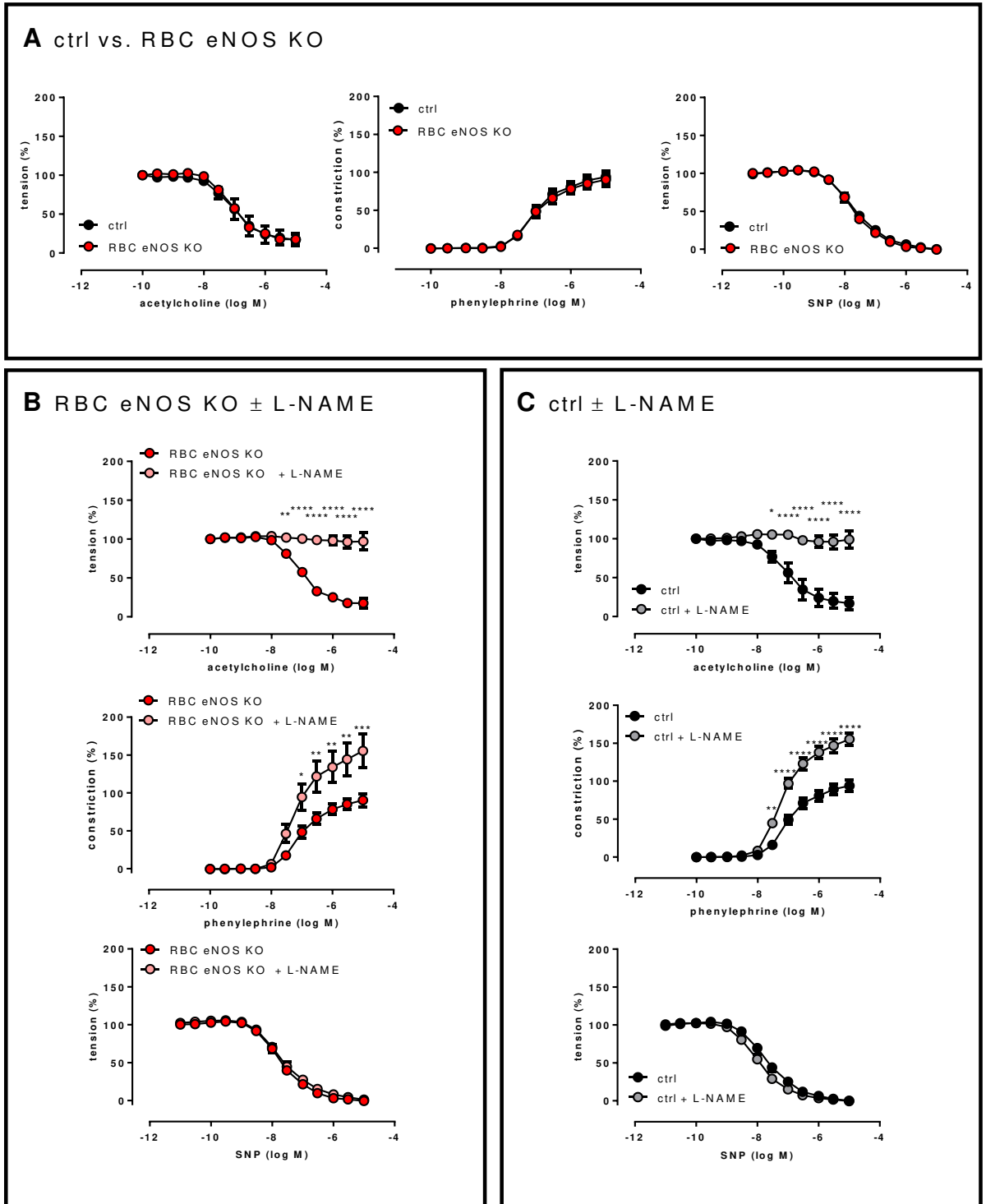
Figure 39 Aortic endothelial function of RBC eNOS KO mice

Endothelium function using aortic ring preparation in organ baths of five control (eNOS^{fl/fl}) and five RBC eNOS KO mice (eNOS^{fl/fl} x Hbb-Cre). A) Reactivity to acetylcholine was unchanged (2-way RM ANOVA; ctrl vs. RBC eNOS KO; acetylcholine:

P = 0.7636.; phenylephrine: P = 0.7625; SNP: P = 0.6956; Sidak's multiple comparison test). B) Addition of the NOS inhibitor L-NAME resulted in blunted reactivity to acetylcholine, higher sensitivity to exogenous NO and stronger reaction to phenylephrine (2-way RM ANOVA; ctrl vs. RBC eNOS KO; acetylcholine: P < 0.001; phenylephrine: P = 0.0373; SNP: P = 03430; Sidak's multiple comparison test; *: P < 0.05, **: P ≤ 0.01, ***: P ≤ 0.001, ****: P ≤ 0.0001). C) Addition of the NOS inhibitor L-NAME resulted in blunted reactivity to acetylcholine, higher sensitivity to exogenous NO and increased potency of phenylephrine (2-way RM ANOVA; ctrl vs. RBC eNOS KO; acetylcholine: P = 0.0011; phenylephrine: P = 0.0005; SNP: P = 0.0564; Sidak's multiple comparison test; *: P < 0.05, **: P ≤ 0.01, ***: P ≤ 0.001, ****: P ≤ 0.0001).

In mesenteric arteries testing RBC eNOS KO vs. control, no changes in response to cumulative doses of acetylcholine were observable [maximal dilation: EC_{50}: $1.56 \cdot 10^{-7}$ M vs. $1.61 \cdot 10^{-7}$ M] and reactivity to an initial dose of phenylephrine [constriction: 38.98 ± 9.54 % vs .44.63 ± 3.31 % in two and eleven mice, $P = 0.5263$].
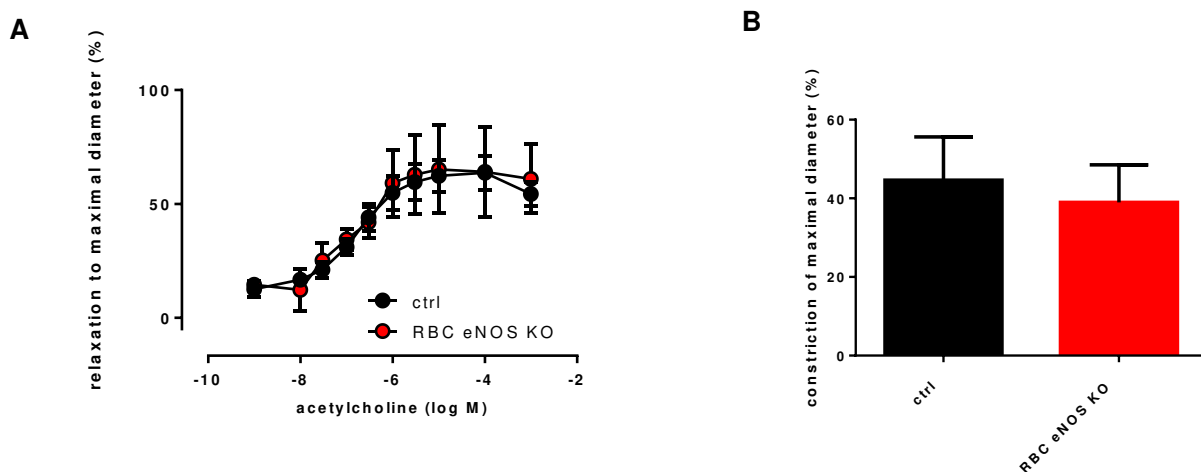
Figure 40 Endothelium function in mesenteric arteries of RBC eNOS KO

Endothelium function in mesenteric arteries was tested in two RBC eNOS KO mice ($eNOS^{fl/fl}$ x Hbb-Cre) and eleven control mice ($eNOS^{fl/fl}$)). A) Unchanged vascular inner diameters of mesenteric arteries after addition of cumulative doses of acetylcholine (2-way RM ANOVA; control vs. RBC eNOS KO; acetylcholine, P = 0.8778). B) Constriction

to maximal diameter to a single dose of phenylephrine was unchanged (Unpaired t-test; P = 0.5263).

To sum up, in both vascular beds no functional changes in mesenteric and aortic reactivity of RBC eNOS KO versus control mice were detectable. Thus, changes of blood pressure were not due to dysfunction of vessel physiology in aorta or mesenteric arterioles.

4.3.7 Summary

Taken together, EC and RBC eNOS transgenic, tissue specific mouse models were successfully generated and tested for their endothelium function. EC eNOS KO and KI mice demonstrated predicted endothelial phenotype, e.g. lack of aortic endothelial function in EC KO and restoration in EC KI mice. No changes were found in endothelium derived function in the aortic segments of RBC eNOS KO mice. Thus, changes in blood pressure of RBC eNOS KO mice cannot be attributed to endothelial dysfunction.

In hemodynamic measurements, a stepwise increase of blood pressure was found from RBC eNOS KO mice to EC eNOS KO mice. In EC eNOS KO mice no increased of heart rate were found, whereas RBC eNOS KO mice exhibited increased heart rates.

5   Discussion
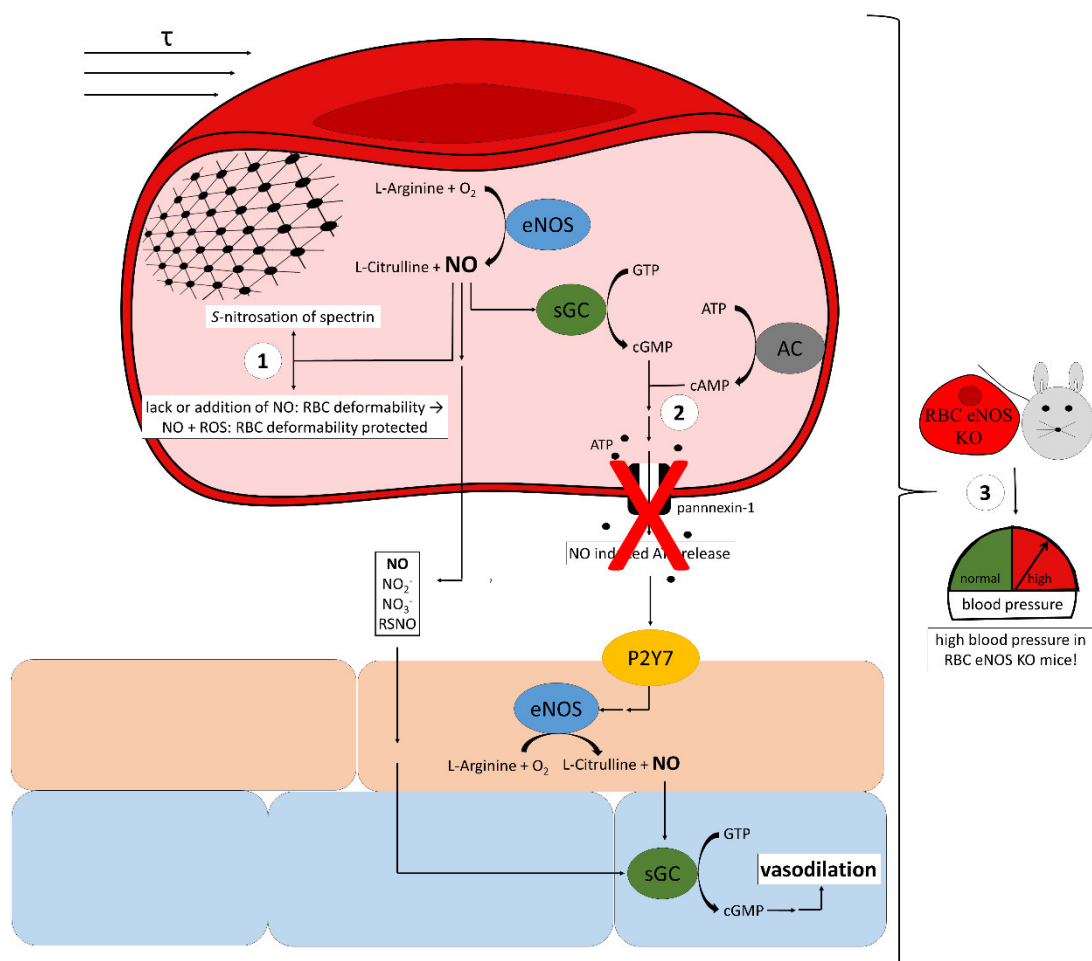
Figure 41 Main findings

1) NO per-se did not affect RBC deformability, however was able to protect from decreased RBC deformability induced by ROS. 2) NO did increase intracellular levels of cGMP, however no concomitant increases of extracellular ATP were found. 3) RBC specific KO mice of eNOS exhibited a hypertensive phenotype.

Aim of this study was to investigate the role of NO and its metabolites derived from RBCs on intrinsic properties and vascular tone. In particular, the aims were to investigate: 1) the effects of NO on RBC deformability in absence and presence of ROS ex-vivo. 2) the sGC and AC dependent controlled release of ATP from RBCs. 3) creation and first characterization (blood pressure, vascular endothelial function) of tissue specific eNOS transgene mouse models.

The following findings were presented here:

1. NO per-se did not affect RBC deformability, however was able to protect from reduced RBC deformability caused by oxidative stress.
2. NO did activate the sGC pathway in RBCs and increase intracellular levels of cGMP, but this did not lead to controlled release of ATP. Also, induction of cAMP did not lead to controlled release of ATP.
3. Transgenic RBC specific eNOS KO mice exhibited increased blood pressure and preserved vascular endothelial function ex-vivo.

5.1 NO did not improve RBC deformability; however, can be protective against decreases of deformability induced by oxidation

The effects of NO on the intrinsic properties of RBCs, determining the deformability, have been intensively discussed and no mutual consent about the role of NO dependent signaling in the regulation of RBC deformability exists.

Reports postulating a role of NO in regulation of RBC deformability demonstrated improved deformability after activation of the eNOS–sGC pathway. It was shown that incubation of RBCs with the substrate of eNOS (L-arginine) and with NO donors (DEA/NO, DETA NONOate, SNP) were capable to improve RBC deformability (Bor-Kucukatay, Wenby et al. 2003, Grau, Pauly et al. 2013). In support of this findings, administration of NOS inhibitor L-NAME or sGC inhibitor 1H-[1,2,4]oxadiazolo-[4-3-a]quinoxylin-1one (ODQ) decreased RBC deformability (Bor-Kucukatay, Wenby et al. 2003, Grau, Pauly et al. 2013).

However, investigations of others were unable to reproduce these findings (Barodka, Mohanty et al. 2014, Belanger, Keggi et al. 2015, Cortese-Krott, Evathia et al. 2018). Neither RBCs of healthy patients treated using the eNOS substrate L-arginine, NO donors DEA/NO or SNP, nor NOS inhibitor L-NAME caused any changes of maximal RBC deformability to untreated controls (Belanger, Keggi et al. 2015). In addition to that another study did not find any changes in RBC deformability after incubation of RBCs with ODQ or the product of sGC cGMP (Cortese-Krott, Mergia et al. 2018).

These contradictory findings clearly ask for careful investigation of the effects of NO on RBC deformability.

5.1.1 Higher ROS levels and unchanged NO bioavailability in RBCs of hypertensive patients

To address the role of NO in regulation of RBC deformability an observational study of hypertensive patients was conducted. In particular, hypertensive patients were of interest, since RBCs in these patients already have been shown to demonstrate decreased deformability (Vaya, Martinez et al. 1992, Cicco and Pirrelli 1999, Cicco, Vicenti et al. 1999). This finding was confirmed in this study as RBC deformability was found to be

decreased for a shear stress of 2.68 Pa, however not for higher shear stresses. Moreover, as demonstrated in animal models of hypertension (Koller and Huang 1994, Matrougui, Maclouf et al. 1997) and confirmed in humans with hypertensive disease (Panza, Quyyumi et al. 1990, Gokce, Holbrook et al. 2001) hypertensive patients are typically characterized by a significant decrease of FMD (**Table 2**), which was shown to be caused by lower bioavailability of NO in the endothelium (Doshi, Naka et al. 2001, Green, Dawson et al. 2014). In agreement with these findings of published data, also in this study decreased response in FMD response was evident in the patient cohort studied here.

This led to the assumption that RBCs of hypertensive patients might demonstrate decreased NO bioavailability, as observed in the endothelium. It is tempting to speculate that decreased NO bioavailability might in turn be the cause for the observed impaired deformability due to a lack of NO.

Measurement of intracellular levels of NO using the DAF-FM probe, indicative of intracellular NO levels, were unchanged in RBCs of hypertensive patients compared to the healthy control group. Also, relative eNOS expression in RBCs of hypertensive patients compared to the control group was not significant different, in contrast to the finding of decreased eNOS expression in patients with coronary artery disease (Cortese-Krott, Rodriguez-Mateos et al. 2012).

These findings taken together clearly indicate that decreased RBC deformability of hypertensive patients is not correlated with lower NO bioavailability.

During further characterization of RBCs higher levels of DCF, a probe indicative for ROS, were found in the hypertensive group. ROS have been shown to affect RBC deformability in multiple studies (Corry, Meiselman et al. 1980, Pfafferott, Meiselman et al. 1982, Snyder, Fortier et al. 1988, Kuypers, Scott et al. 1990, Becatti, Marcucci et al. 2016) and thus seem to be the more likely cause for the decrease of RBC deformability in RBCs of hypertensive patients.

In the following chapters, the effects of changes in intracellular redox status in RBCs were further investigated. In total, the role of NO regulation of RBC deformability needs to be further investigated.

5.1.2 Changes in intracellular redox status impact RBC deformability

After the discovery of decreased RBC deformability, concomitant with increased levels of ROS in the study of hypertensive patients, a further characterization of RBC redox state and deformability after exposure to ROS was conducted.

To change intracellular redox state, RBCs – isolated from human volunteers - were treated with the organic peroxide t-BuOOH. It is a widely used pro-oxidant, membrane-permeable agent and has been used to inflict oxidative damage on RBCs before (Corry, Meiselman et al. 1980, Caprari, Bozzi et al. 1995). Oxidants were shown to be able to induce morphological changes of the cytoskeleton and at the same time change parameters of RBC deformability, e.g. membrane shear modulus (Sinha, Chu et al. 2015) or membrane rigidity (Rice-Evans, Baysal et al. 1985).

Damages caused by oxidation of RBCs can cause disturbance of membrane potential and symmetry (Jain 1985, Duranton, Huber et al. 2002), hemoglobin degradation connected to formation of aggregates (Rifkind and Nagababu 2013) and peroxidation of membrane components (Stocks and Dormandy 1971). Oxidation thus may have severe effect on RBC functionality.

To characterize the effects of t-BuOOH on intracellular redox status the ratio of the redox couple GSH and GSSG was measured as an indicator for intracellular redox status (Griendling, Touyz et al. 2016). In agreement with previous reports, also here impressively high concentrations of t-BuOOH were necessary to induce intracellular changes of redox state (**Figure 6 A-B**) (Corry, Meiselman et al. 1980, Trotta, Sullivan et al. 1983, Freikman, Ringel et al. 2011). This finding demonstrated the high redox burden RBCs are able to cope with. In their approximately 120 days life time - without being able to replace proteins that become damaged – a high antioxidant capacity is necessary to resist to oxidative challenges that commonly exist in RBCs (Kuhn, Diederich et al. 2017).

Characterization of morphological changes of RBCs, after treatment using t-BuOOH demonstrated that the effects of t-BuOOH are comparable to in-vivo changes of RBCs exposed to high levels of ROS. For example t-BuOOH treatment was shown to induce binding of hemoglobin to the RBC membrane (Rice-Evans, Baysal et al. 1985), which was also found in-vivo under conditions of high oxidative stress, as extreme exercise

(Welbourn, Wilson et al. 2017) or the hereditary, anemic disease sickle cell anemia (Kannan, Labotka et al. 1988). In addition to that, after treatment using t-BuOOH, RBCs also demonstrate characteristics of RBCs isolated from thalassemia patients (Rice-Evans, Baysal et al. 1985), a hereditary anemic disease connected to increased oxidative burden of RBCs (Cappellini, Tavazzi et al. 1999).

In a next step, functional aspects of RBCs were investigated after t-BuOOH incubation. When challenged with millimolar concentrations of oxidant, exceeding the threshold of RBC redox capacity, sudden functional changes of RBC deformability and whole blood viscosity became visible. Decrease of intracellular redox capacity, represented by GSH to GSSG ratio, was ongoing with decreases of RBC deformability and increases in whole blood viscosity (**Figure 6 C-E**).

Whole blood viscosity is determined by its cellular components, which are in majority RBCs and by its liquid component plasma (Stuart and Nash 1990, Baskurt and Meiselman 1997). Dependent on the shear rate applied, the contribution of the two components to whole blood viscosity changes. At low shear rates changes of RBC deformability have high impact on whole blood viscosity. At high shear rates, on the other hand, the properties of plasma outweigh the contribution of the cellular components to the overall viscosity (Baskurt and Meiselman 1997). The same relation could be confirmed in this work, since changes of RBC deformability increased viscosity especially at low shear rates. With higher shear rates the observed increase in whole blood viscosity was lost (**Figure 6 D**).

The experiments discussed until now were conducted in RBCs obtained from human volunteers and treated ex-vivo with the oxidant t-BuOOH. To get an impression of the effects of changes in antioxidant capacity on deformability of RBCs in vivo a mice line deficient in the transcription factor Nrf2 was chosen.

Nrf2 KO mice are characterized by low levels of antioxidants and anti-oxidant enzymes (Itoh, Wakabayashi et al. 1999, Suzuki and Yamamoto 2015). In specific Nrf2 is responsible for transcriptional regulation of antioxidant defense mechanisms. The lack of Nrf2 causes decreased expression levels of detoxifying phase II enzymes (glutathione S-transferase; NADPH oxidoreductase 1) and impaired synthesis of antioxidant molecules due to lower levels of cystine/glutamate exchange transporter, which is essential for the

uphold of intracellular L-cysteine levels, a substrate for GSH synthesis (Itoh, Chiba et al. 1997, Itoh, Wakabayashi et al. 1999, McMahon, Itoh et al. 2001).

In Nrf2 KO mice, the lack of critical, antioxidant enzymes leads to lower efficiency in degradation of oxidants and a higher sensitivity to xenobiotic oxidants, as for example acetaminophen or other known carcinogens (Chan, Han et al. 2001, Ramos-Gomez, Kwak et al. 2001). This decrease of capacity to tackle oxidants also affects the cardiovascular system. Nrf2 KO mice present with cardiac hypertrophy and left ventricular diastolic dysfunction (Erkens, Kramer et al. 2015). Moreover, after myocardial infarction a KO of Nrf2 leads to rapid development of heart failure and higher mortality rates compared to WT mice (Strom and Chen 2017).

In particular RBCs are exposed to a high and steady oxidative challenge due to transport of oxygen, which causes low levels of constant intracellular oxidation mainly of hemoglobin (**Equation 2**) (Zhang, Levy et al. 1991). In the center of the prosthetic heme subunit of hemoglobin, the central iron ion can serve as starting point for further oxidative reactions, which is the case in hereditary anemic diseases, as for example sickle cell disease or β-thalassemia (Hebbel, Morgan et al. 1988, Shinar and Rachmilewitz 1990).

Ultimately intracellular oxidative reactions have been shown to be able to cause decreases of RBC deformability (Chien, Usami et al. 1970). Bringing the phenotype of high susceptibility to oxidants of Nrf2 KO mice together, with previous findings of RBCs being a steady source of oxidants suggest that deformability of RBCs in Nrf2 KO mice could be impaired due to constant oxidative damage and a lack of antioxidant defense.

In contrast to what was expected, RBC deformability in Nrf2 KO mice did not differ to the deformability of RBCs in WT mice (**Figure 8 A**). Next, it was assumed that the lack of antioxidant enzymes in theory should weaken the response of RBCs to oxidative stresses. Indeed, with increasing concentrations of *t*-BuOOH the RBC deformability decreased more pronounced in RBCs isolated from Nrf2 KO mice than in the WT controls (**Figure 8 B-C**). Thus, RBCs in Nrf2 KO mice seem to be able to compensate for a loss of parts of their defense against oxidants at low levels of oxidants, demonstrating again how well equipped these cells are to tackle oxidants. If challenged by external stimuli however, RBCs of Nrf2 KO mice are not able to compensate for loss of their antioxidant defense.

To sum up, the previously acquired data impressively demonstrates that RBCs possess high capacity to challenge internal and external oxidants. Moreover, RBC redox state is of major importance to sustain RBC deformability and whole blood viscosity.

5.1.3 NO per-se does not improve RBC deformability

The next step was to investigate the effects of NO on RBC deformability in-vitro.

5.1.3.1 Cytoskeletal spectrin is a possible target for posttranslational modification by *S*-nitrosation

As possible mechanisms, responsible for beneficial effects of NO on RBC deformability, data suggested activation of the eNOS–sGC pathway and *S*-nitrosation of RBC cytoskeletal spectrin (Bor-Kucukatay, Wenby et al. 2003, Grau, Pauly et al. 2013).

Spectrin is the main protein of the cytoskeleton of RBCs and has been shown to be highly flexible and elastic and can be imagined to behave like a mechanical spring. Beneath the RBC membrane, spectrin is part of a hexagonal network that is connected to the membrane by junctional complexes (Lux 2016). Due to its dominant role in the cytoskeleton and previous reports of possible modifications of spectrin, it seemed to be a likely target for posttranslational modifications (Smith and Palek 1983, Ogasawara, Komiyama et al. 2010, Krieger, An et al. 2011)

Indeed, in §4.1.3, *S*-nitrosation of the cytoskeletal protein spectrin was demonstrated in purified preparations of spectrin, in RBC ghosts and in RBCs after application of exogenous stimuli for nitrosation (**Figure 14**-**Figure 16**). Using the biotin switch assay and CLD, two different approaches were applied to measure *S*-nitrosation of spectrin. In concordance with literature *S*-nitrosation of spectrin in samples of purified spectrin, going to RBC ghosts and then naïve RBCs after application of extracellular stimuli agrees with findings in other studies (Grau, Pauly et al. 2013, Riccio, Zhu et al. 2015).

Since application of high exogenous concentrations of NO donors cannot be considered as physiological significant for in-vivo *S*-nitrosation, RBCs were incubated with increasing concentrations of nitrite under hypoxic conditions. Interestingly EPR measurements demonstrated a signal for hemoglobin-NO (**Figure 17**) and an steady increase of Hb(III) under hypoxic conditions after application of nitrate, which might

result from the reduction of nitrate to NO as shown by Liu et al. (**Equation 7**) (Liu, Wajih et al. 2015).

Equation 7 Reduction of nitrite by hemoglobin under hypoxic conditions

$$Hb(II) + NO_2^- + H^+ \rightarrow Hb(III) + OH^- + NO$$
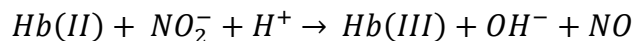
In the same samples, a biotin switch assay was executed and *S*-nitrosation of spectrin was demonstrated, supporting the assumption of nitrite reduction to NO followed by *S*-nitrosation of freely accessible thiols (**Figure 18**). *S*-nitrosation of spectrin is a surprising finding, since the under hypoxia synthesized NO was believed to be directly scavenged by surrounding deoxygenated hemoglobin to form nitrosylated hemoglobin (**Equation 4**) or oxygenated hemoglobin to form nitrate due to the high reaction rates of 3-7 10^7 $M^{-1}s^{-1}$ (**Equation 5**)(Doyle and Hoekstra 1981, Eich, Li et al. 1996, Herold, Exner et al. 2001).

Taking these findings together, *S*-nitrosation of spectrin could be a possible mechanism for improvement of RBC deformability and moreover demonstrates that spectrin can be a possible target for posttranslational modifications in general.

5.1.3.2 NO per-se does not change RBC deformability

To assess the functional influence of NO on RBC deformability, RBCs were incubated with the NO donor DEA/NO and the NO^+ donor CysNO. In contrast to other studies (Bor-Kucukatay, Wenby et al. 2003, Grau, Pauly et al. 2013), no beneficial effects on RBC deformability were detected, putting into doubt that the eNOS–sGC pathway or *S*-nitrosation play a role in regulation of RBC deformability.

For very high concentrations of DEA/NO or CysNO decreased deformability of RBCs was found, which might be explained by a previous work, where the authors have shown that *S*-nitrosation leads to disulfide formation and protein crosslinking (Wolhuter, Whitwell et al. 2018).

Further, the effects of lack of eNOS in RBCs on deformability were investigated. Of note, the lack of eNOS synthesized NO in eNOS KO mice did not result in changes of RBC deformability (**Figure 19 C**). Underlining the previous findings of no effects of intrinsic or extrinsic NO on RBC deformability.

The conclusion of the experiments was that spectrin can be a target for *S*-nitrosation, but a clear link between nitrosation and the mechanism changing RBC deformability is to my knowledge until today not presented.

The scientific work proposing a role of *S*-nitrosation for deformability of RBCs was able to demonstrate *S*-nitrosation and was able to show a correlation of increased signal of R-SNO in spectrin to RBC deformability (Grau, Pauly et al. 2013). Disregarding the fact that in this work, no improvement of NO on RBC deformability was found, the correlation shown by Grau et al. does only imply that nitrosative state of RBCs might have contributed to changes in RBC deformability. There are plenty of other possible target proteins that should have been considered given that *S*-nitrosation can occur in parallel in multiple proteins. One RBC protein shown to be a possible target of *S*-nitrosation is for example glyceradehyde-3-phosphate, which plays an essential role in the glycolytic breakdown in RBCs (Galli, Rovidati et al. 1998)

To exclude that the different results of the effect of NO on RBC deformability were caused by different incubation conditions of RBCs with NO donors or the measurement conditions to measure RBC deformability, all parameters were critically analyzed. However, no differences were found that could explain the discrepancy (**Table 6**).

Table 6 Comparison of protocol parameters for RBC deformability

Protocol	(Bor-Kucukatay, Wenby et al. 2003)	(Grau, Pauly et al. 2013)	This work
sample	whole blood washed using phosphate buffered saline (pH = 7.4)	whole blood centrifuged and cell pellet re-suspended	whole blood centrifuged and cell pellet re-suspended
treatment buffer	plasma	autologous buffer	HBSS
timeframe	4-6 hours after collection	n / a	immediate
treatment hematocrit	40%	40%	25%
treatment	10^{-6}-10^{-2} M L-Name and SMT, 10^{-4}-10^{-7} M SNP and DETA-NONOate	3 mM L-arginine, 10 µM L-NIO, 10 µM wortmannin, 200 pM insulin, 300 µM cPTIO, 100 µM SNP	1 – 200 µM DEA/NO, 0.001 µM - 50,000 µM CysNO, eNOS KO (without processing)

treatment duration	60 minutes at room temperature	60 minutes at 37°C	10 minutes 37 °C
rheometer medium	70 kDA dextran	isotonic polyvinylpyrrolidone	isotonic polyvinylpyrrolidone
final hematocrite	low hct solution	0.4%	0.125 %
shear rate (1/s)	0.5 - 15 Pa*	10 - 1666.67	10 - 1666.67
finding	NO is a regulator of RBC deformability	EImax increased with L-arginine, insulin, SNP EImax decreased with L-NIO, wortmannin, cPTIO	no improved RBC deformability for any treatment under basal conditions

* no viscosity of measuring medium available

Main factors of RBC deformability measurement protocols to determine the influence of NO (modified from (Diederich, Suvorava et al. 2018))

Yet, the authors of these publications present their data in a particular fashion. In one publication the authors are showing changes of the EI only for a shear stress of 1.58 Pa (Bor-Kucukatay, Wenby et al. 2003). Calculated back to shear rate, this value corresponds to a shear rate of 52.67 1/s, which lies below the range of physiological important shear rates. Physiological shear rates in vivo range from 130 1/s in aorta, 1000 1/s in capillary and 8000 1/s in arterioles (Vennemann, Kiger et al. 2006). In another publication data is transformed by the Lineweaver-Burk transformation and values for $SS_{1/2}$ and the theoretical value of EImax are calculated (Grau, Pauly et al. 2013). This method is not applicable under every condition, due to bad fit of the data to the Lineweaver-Burk transformation (**Table 3**).

In this study, the application of NO did not improve RBC deformability, excluding a role of the eNOS–sGC pathway and *S*-nitrosation for regulation of RBC deformability. Moreover, these findings together demonstrate the need for standardized presentation of data regarding RBC deformability to avoid misinterpretations.

5.1.3.3 NO protects RBCs from oxidative stress induced decreased deformability

In a next step, it was investigated if *S*-nitrosation might have protective effects on oxidation induced damages to RBCs. It was shown that oxidants are capable to crosslink RBC proteins (Fischer, Haest et al. 1978, Haest, Fischer et al. 1980), being the basis for

the assumption that NO might bind to critical thiol groups and by this form protection groups against oxidative crosslinking.

Surprisingly, in this study pre- and post-incubation of RBCs with CysNO were able to reduce the effects caused by oxidation. Since not only pre-treatment had protective effects, the results did not fully support the theory of NO binding to critical thiol groups and formation of protection groups.

The finding of NO being able to limit ROS induced decreases of RBC deformability is in line with findings of several reports that have shown decreased RBC deformability and increased oxidative stress in for transfusion stored RBCs (Frank, Abazyan et al. 2013, Collard, White et al. 2014, Nagababu, Scott et al. 2016). Application of NO has been demonstrated to improve the deformability of RBCs stored for transfusion (Muenster, Beloiartsev et al. 2016). However, this study did not provide a possible mechanism for these findings.

Possible explanation might be that nitrosylation of hemoglobin protects hemoglobin from oxidatively induced degradation. In an interesting study, erythroid cells were incubated with the oxidant *t*-BuOOH and the generation of free radical species was reduced in the presence of NO measured by EPR (Gorbunov, Yalowich et al. 1997). Another suggestion made in the past was that formation of methemoglobin might protect versus oxidative damage (Trotta, Sullivan et al. 1983). However, the exact mechanisms behind these observations require further investigation.

NO per-se did not improve RBC deformability, but nitrosative conditions were capable to rescue RBCs from oxidative damage induced decrease of RBC deformability.

5.1.4 Conclusion

This study demonstrated that decreased RBC deformability in hypertensive patients is not caused by a lower NO bioavailability. Yet, RBCs of hypertensive patients demonstrated increased levels of ROS leading to the assumption that these might be the cause for decreased RBC deformability.

Further investigations of changes of intracellular redox status ex-vivo demonstrated that exhaustion of intracellular redox capacity is tightly connected to functional impairment and decreased RBC deformability resulting in increased whole blood viscosity.

Further investigations of NO on RBC deformability demonstrated that neither the eNOS–sGC pathway nor *S*-nitrosation improved RBC deformability. However, NO was capable to rescue by ROS induced decreased RBC deformability by an unknown mechanism.

5.2 The cGMP and cAMP – pannexin-1 dependent pathway is not involved in regulated ATP release from RBCs

The mechanisms behind NO dependent signaling in controlled release of ATP from RBCs are not completely understood until today.

ATP was identified early on as an important signaling molecular in the cardiovascular system (Berne 1963). It exerts multiple effects on vasculature, for example vasodilation under hypoxia (Bergfeld and Forrester 1992, Bodin and Burnstock 1995) and under conditions of high shear stress (Bodin, Bailey et al. 1991, Bodin and Burnstock 1995) and was shown to play a role in the adaption of vascular tone in skeletal muscles during exercise training (Dietrich, Ellsworth et al. 2000, Ellsworth 2004).

The mechanism proposed to induce release of ATP under hypoxic conditions is by hypoxia induced activation of Gi coupled G protein receptor (Sprague, Bowles et al. 2002, Olearczyk, Stephenson et al. 2004), activation of AC (Sprague, Ellsworth et al. 2001, Sprague, Bowles et al. 2008), which increases levels of intracellular cAMP and activates PKA (Sprague, Ellsworth et al. 2001) and leads to release of ATP by an unknown intermediate step via the pannexin-1 channel (Sridharan, Adderley et al. 2010). cGMP was shown to have a regulatory function in this system by inhibition of phosphodiesterase 3, an enzyme responsible for degradation of cAMP (Richards, Bowles et al. 2015).

5.2.1 RBCs do not release ATP after in-vitro stimulation of sGC and AC

Application of pharmacological stimuli of the eNOS–sGC pathway (DEA/NO, Bay 41) in combination with phosphodiesterase 5 inhibitor sildenafil did increase cGMP levels, confirming the activity of this pathway in RBCs (**Figure 22**) (Cortese-Krott, Evathia et al. 2018). In the same samples, no increase of extracellular ATP levels was detectable, putting into doubt the findings of a role for the eNOS–sGC pathway in regulation of controlled ATP release (Richards, Bowles et al. 2015).

In the same set of experiments pharmacological activators of the AC pathway (forskolin, isoproterenol), as well, confirmed the activity of the AC pathway, as reported in data of other research groups before (Rodan, Rodan et al. 1976). Measurement of extracellular ATP levels in the supernatants of the same preparations did not show any increases of

extracellular ATP, contradictory to the results found by others (Sprague, Ellsworth et al. 2001, Sridharan, Adderley et al. 2010).

No treatment induced increases of extracellular hemoglobin levels, which excluded confounding results due to hemolysis (rupture of RBCs and release of intracellular components). However, low levels of hemoglobin were measured in the supernatant of all samples. In every supernatant there was a low level of hemolysis, due to experimental procedure that cannot be circumvented (blood withdrawal, centrifugation).

This major finding of lack of ATP release, in contrast to reports of others (Sprague, Ellsworth et al. 2001, Sridharan, Adderley et al. 2010), could be attributed to the fact that most of these scientific investigations did not take hemolysis into account. Several stimuli are known to induce hemolysis, as for example hypoxia, xenophobic chemicals (dimethyl sulfoxide (DMSO)) or mechanical stress (Sikora, Orlov et al. 2014). These stimuli might have occurred during experimental procedures as centrifugation, pipetting or addition of - in solvents, as for example DMSO - solved pharmacological drugs (Sikora, Orlov et al. 2014) and interpreted as controlled release of ATP. To avoid misinterpretation of data, it is thus of major importance to exclude major hemolysis.

These findings taken together led to the conclusion that rise of intracellular levels of cGMP and cAMP do not regulate the controlled release of ATP from RBCs.

5.2.2 Pannexin-1 is unlikely to play an important role in RBC dependent regulation of vascular tone

The aim of the following investigations was to put the hypothesis of pannexin-1 mediated release of ATP to a final test.

As part of this work the presence of pannexin-1 on RBCs was confirmed (Keller, Diederich et al. 2017). Pannexin-1 was suggested to be the ATP releasing channel in RBCs as proposed by several working groups (Locovei, Bao et al. 2006, Sridharan, Adderley et al. 2010, Qiu, Wang et al. 2011, Cinar, Zhou et al. 2015). If cGMP / cAMP mediated release of ATP by pannexin-1 is of that great importance for vasodilation in conditions of hypoxia as proposed by others, pannexin-1 global KO mice should be incapable to adapt to hypoxic conditions, i.e. exhaustive exercise.

However, pannexin-1 global KO mice did not demonstrate any impairment of adaption to forced exercise. To confirm that baseline physiological conditions were comparable, age matched mice were used and no differences in body weight or maximal exhaustion level (post-exercise lactate) were detectable (**Figure 26**). Furthermore, in course of the same studies, it was found that direct stimulation of RBCs isolated from WT mice and pannexin-1 KO mice using cAMP analogs did not induce release of ATP (Keller, Diederich et al. 2017).

Taking all this information together, a cGMP / cAMP mediated release of ATP via pannexin-1 can be excluded as a mechanism for ATP release from RBCs.

This however does not exclude that other mechanisms of RBCs' ATP release might exist. Experiments in fluidic micro-channels suggested a role for the mechanosensing protein Piezo 1 in mechanotransduction (Cinar, Zhou et al. 2015). However, in the methodical setup unspecific pharmacological inhibitors were used that do not allow the definite conclusions made by the authors.

The notion that there might be RBC regulated ATP release, rose after discovery of ATP release directly within the vasculature (Ellsworth, Forrester et al. 1995, Mortensen, Thaning et al. 2011). In the context of high intensity exercise and increased shear stress, some proposed that vascular dilation by RBCs is caused by hemolysis of a small fraction of cells. These cells release intracellular components, as for example ATP (Thomas 2014). This theory contains one major concern. Release of intracellular proteins would also imply release of hemoglobin, a very potent scavenger of the vasodilator NO, which might cause vasoconstriction (Gibson and Roughton 1957).

This section demonstrates that pannexin-1 is not essential for adaption to exercise training and pannexin-1 is unlikely to be involved in the controlled release of ATP via RBCs.

5.2.3   Conclusion

To conclude, cGMP / cAMP mediated release of ATP can be excluded as possible pathways. Also, pannexin-1 in RBCs does not seem to be involved in major regulation of vascular tone by the release of ATP, since pannexin-1 KO mice did not demonstrate impairment of maximal endurance capacity.

5.3   eNOS in RBCs contributes to blood pressure regulation

The importance of eNOS for regulation of hemodynamics is well known and long established, yet was attributed for a long time to eNOS localized in ECs only. Here the role of RBC eNOS in regulation of hemodynamics will be discussed.

Global eNOS KO mice exhibit an increased mean arterial blood pressure of 117 mmHg compared to 97 mmHg, as first shown by Huang et al. (Huang, Huang et al. 1995). Further studies were able to confirm the finding of high blood pressure in eNOS KO mice (Shesely, Maeda et al. 1996, Godecke, Decking et al. 1998). In addition to that a 70 % decrease of circulating nitrite levels in plasma was found in eNOS KO mice (Kleinbongard, Dejam et al. 2003).

With the discovery of eNOS protein in cells of the blood stream, as for example platelet rich plasma (Radomski, Palmer et al. 1990, Sase and Michel 1995, Chen and Mehta 1996), leukocytes (Chen and Mehta 1996, de, Sanchez de Miguel et al. 2001, Muhl and Pfeilschifter 2003, Saluja, Jyoti et al. 2011) and RBCs (Kleinbongard, Schulz et al. 2006, Cortese-Krott, Rodriguez-Mateos et al. 2012), the question arose, if eNOS in the cell lines of the blood stream could contribute to blood pressure regulation and the nitrite pool in plasma (Wood, Cortese-Krott et al. 2013). In particular RBCs were focused due to their abundance in blood stream, compared to other cellular components in whole blood (Wood, Cortese-Krott et al. 2013).

In a model of chimeric KO mice Wood et al. demonstrated by transfer of bone marrow from eNOS KO mice to irradiated WT mice and vice versa effects of blood stream eNOS on blood pressure regulation (Wood, Cortese-Krott et al. 2013). The model of chimeric mice however has limitations as for example the chimeras are not specific for the KO of eNOS in RBCs, irradiation might have multiple consequences, as for example inflammatory response, accompanied by upregulation of another source of NO the iNOS and residual circulating blood cells of the host animal (Cortese-Krott and Kelm 2014).

These disadvantages can be circumvented by transgenic KO and KI models of eNOS in ECs and RBCs generated using the loxP-Cre system (creation scheme § 3.21.)

5.3.1 Tamoxifen injections can have influence on cardiovascular parameters

As described in §3.21, tamoxifen was used as activator of the Cre-ERT2 fusion protein. Only with application of tamoxifen, the Cre-ERT2 is able to translocate to the nucleus, recognize and cut loxP sequences. Tamoxifen, as a selective estrogen receptor modulator, is mainly used in estrogen dependent breast cancer therapy (Fisher, Bryant et al. 2002) and could have undesired effects on the model. Different publications in humans and animal studies described effects of tamoxifen on cardiovascular functions.

In humans, effects described were improvement of endothelium derived FMD in a cohort of men diagnosed with coronary artery disease (Clarke, Schofield et al. 2001) and slowdown of atherosclerosis progression accompanied by decreases in LDL cholesterol and improvement in FMD in postmenopausal women (Stamatelopoulos, Lekakis et al. 2004). Similar findings were confirmed in a postmenopausal model of rats, in which improvement of endothelial dysfunction was found after application of selective estrogen receptor modulators (Lamas, Caliman et al. 2015)

Besides influence on cardiovascular functions, further observations found that women under a tamoxifen treatment regime had significant higher weight gain than women without tamoxifen (Hoskin, Ashley et al. 1992, Heideman, Russell et al. 2009). As obesity has been identified as one cause for endothelial dysfunction (Steinberg, Chaker et al. 1996, Arcaro, Zamboni et al. 1999), changes in weight gain could affect vascular endothelial function.

To answer, if tamoxifen might interfere with the cardiovascular characterization in our models the influence on aortic endothelial function and weight gain was investigated. In this experiment, a set of eNOS$^{fl/fl}$ mice was treated with tamoxifen solved in peanut oil and a set only with peanut oil, as a control group. No changes in weight gain were observable (**Figure 27**). This finding in contrast to previous findings might be explainable by the short period of the tamoxifen administration. In the beforehand mentioned studies, showing weight gain due to tamoxifen, tamoxifen was administered over several months (Hoskin, Ashley et al. 1992, Heideman, Russell et al. 2009). Thus, the five-day injection of 7.5 mg of tamoxifen did not seem sufficient to have impact on weight gain.

Regular, intra-peritoneal injections of tamoxifen might induce inflammation and acute inflammatory responses have been demonstrated to affect vascular function in conductive

and resistive vessels (Hingorani, Cross et al. 2000, Clapp, Hirschfield et al. 2005). To exclude upregulation of leukocytes, blood counts were measured at the beginning of tamoxifen treatment (baseline) and at the end. No changes of cell number of inflammatory cells were detectable excluding major inflammation due to injections of tamoxifen (**Table 5**).

Furthermore, the results of the blood counts, were compared to data published in other works. In contrast, no changes in mean platelet volume (MPV) were found under a tamoxifen treatment regime, as shown in administration of tamoxifen to breast cancer patients (Karagoz, Bilgi et al. 2010). This discrepancy might be due to the long treatment period of one-year treatment, which was not the case in our method. Moreover, no changes due to tamoxifen administration were found except for an increase in RBC distribution width (RDW) and RBC counts. RDW indicates the size distribution of RBCs and changes to higher values if younger, bigger RBCs are in circulation, or shifts to smaller values, if smaller, older (or quicker "aged") RBCs are in circulation. In several studies RDW is associated to disease aggravation as for example coronary artery disease (Bujak, Wasilewski et al. 2015), fatty liver disease (Yang, Huang et al. 2014), carotid atherosclerosis (Nam, Ahn et al. 2018) and hepatitis B virus induced liver disease (Fan, Deng et al. 2018).

Future investigations should clarify if changes of RDW and RBC counts due to treatment of tamoxifen affect other cardiovascular functions in the here established loxP-Cre models.

A state-of-the-art method to judge vascular endothelium function in aorta is the organ bath setting. In this setting vessel characteristics can be investigated under exclusion of humoral or neuronal factors. By application of this method, it was found that vascular endothelium function was unchanged in the control treated group vs. tamoxifen treated group. The studies previously mentioned (Clarke, Schofield et al. 2001, Stamatelopoulos, Lekakis et al. 2004, Lamas, Caliman et al. 2015) showed in-vivo changes of vascular endothelium function in patients and animals after long-term tamoxifen administration. However, these findings were not confirmed in this setting. Unchanged aortic endothelial function might be again explainable by the different time frames of treatment regimens. In the human studies tamoxifen was applied for several months (Clarke, Schofield et al. 2001, Stamatelopoulos, Lekakis et al. 2004) and the animal experiments using rats were

done under constant tamoxifen treatment for 14 days (Lamas, Caliman et al. 2015). In this case however, mice are treated for five consecutive days and, after a washout period of 21 days, experiments were conducted. This time frame was chosen to achieve maximal efficacy of tamoxifen regarding the activity of Cre and complete eNOS KO or KI (Metzger and Chambon 2001). And in addition to that a washout phase of tamoxifen is of major importance, because of its long half-life of 48 hours and many pharmacologic active metabolites (Fromson, Pearson et al. 1973).

The results thus reflect that tamoxifen has no influence on vascular endothelium function in this administration scheme and thus observed changes in other models are not due to the treatment necessary to activate the fusion protein Cre-ERT2. Yet changes in blood cell count and RDW need further investigations. To exclude confounding effects by tamoxifen treatment, tamoxifen will be administrated to control and intervention group.

5.3.2   EC KO and KI models work

To investigate the role of endothelium specific eNOS KO and KI, eNOS$^{fl/fl}$ mice were crossed with Cre-ERT2 mice (resulting in EC eNOS KO) and eNOS$^{inv/inv}$ mice with Cre-ERT2 mice (resulting in EC eNOS KI). As a test of the loxP-Cre construct eNOS$^{inv/inv}$ mice were crossed with ubiquitous expressing Cre mice (

Figure 4).

5.3.2.1 Global eNOS KI mice exhibit recovered aortic endothelial function

As a general test for the functionality of the loxP-Cre machinery, the KI construct was created. Therefore eNOS$^{inv/inv}$ mice were breed with mice expressing the Cre protein ubiquitously (

Figure **4**).

At baseline the eNOS$^{inv/inv}$ (eNOS KO) mice present with typical signs of vascular endothelium dysfunction. After crossing, all three measured parameters (acetylcholine dependent relaxation, SNP dependent relaxation, phenylephrine dependent constriction) were without visible differences compared to WT mice (**Figure 30**).

This finding indicated that the Cre-recombinase was capable to invert the inversed sequence of interest and a functional eNOS enzyme was expressed. In this model

however, one cannot distinguish in which tissue eNOS expression is of major importance for vascular endothelium function explaining the creation of the further mouse lines.

5.3.2.2 EC eNOS KO mice exhibit increased blood pressure and abolished aortic endothelial function

The major role of the endothelium and in specific EC eNOS in regulation of vascular dilation was found in the 80s and 90s of the last century (Furchgott and Zawadzki 1980, Palmer, Ferrige et al. 1987, Mitchell, Forstermann et al. 1991, Huang, Huang et al. 1995).

Thus it was not surprising, to find in accordance with these well-established findings and investigations of aortic endothelial function of eNOS KO mice, a blunted reactivity towards acetylcholine in EC eNOS KO mice (Huang, Huang et al. 1995).

The shift in dose response curves towards higher sensitivity after administration of NO donors of endothelium eNOS KO mice compared to controls – in this case SNP – was also evident in this model (Brandes, Kim et al. 2000, Suvorava, Stegbauer et al. 2015). The mechanism behind the increased sensitivity is not completely understood yet.

One possible mechanism proposed was decreased sensitivity of sGC after exposure to NO, since the group of Brandes et al. did not find any changes in sGC subunits expression levels (Brandes, Kim et al. 2000). A further study proposed that the loss in sGC sensitivity might be caused by *S*-nitrosation of critical cysteines in sGC and by this inhibition of enzyme activity itself, serving as a negative feedback mechanism of NO signaling. Mutation of the identified two critical cysteine amino acids significantly reduced desensitizing of sGC after administration of CysNO (Sayed, Baskaran et al. 2007). These findings applied to the model of EC eNOS KO mice, it would allow the conclusion that without any level of baseline *S*-nitrosation of sGC, higher sensitivity to exogenous applied NO might cause the observed shift in dose response curves.

Another proposed mechanism was the compensatory up-regulation of sGC expression levels (Hussain, Hobbs et al. 1999), a finding that was not supported by the findings of Brandes et al. (Brandes, Kim et al. 2000). Also in the model of EC eNOS KO mice created here, no increased expression levels of the sGC subunits in aorta, heart or skeletal muscle were found, confirming the finding of stable levels of sGC on a protein level (**Figure 33**-**Figure 35**).

Reactivity towards the α1-adrenergic receptor agonist phenylephrine was in tendency increased in EC eNOS KO. This is in concordance with the concept of myoendothelial feedback response. It was found that administration of vasoconstrictors led to an signaling cascade resulting in an increase of intracellular calcium(II) levels in ECs and eNOS dependent release of NO (Angus, Cocks et al. 1986, Martin, Furchgott et al. 1986, Gebska, Stevenson et al. 2011). Lack of eNOS would impair the functionality of this pathway and explain the tendency to stronger responses towards application of agents causing vasoconstriction.

Fitting to the finding of impaired endothelial function, EC eNOS KO mice exhibited increased levels of systolic and diastolic blood pressure. This is in line with findings of hypertension in chimeric mice expressing eNOS only in the blood cell compartment (Wood, Cortese-Krott et al. 2013). Although blood pressure was increased, measurement of the heart rate did not show any differences compared to control. In contrast, eNOS KO mice heart rates were found to be significantly decreased, although the mechanisms behind this observation are unknown (Shesely, Maeda et al. 1996, Godecke, Decking et al. 1998). One suggestion was that decreases of heart rate are a compensatory response to increased blood pressure (Shesely, Maeda et al. 1996). Since in the model of induced EC eNOS KO the lack of eNOS is induced only several weeks before measurements were undertaken, the adaptive mechanism might not become evident yet.

Altogether, the results demonstrate that the EC eNOS KO construct works and EC eNOS KO mice demonstrate vascular endothelial dysfunction, high blood pressure and unchanged heart rate, confirming the important role of eNOS in ECs for hemodynamic regulation.

5.3.2.3 EC eNOS KI mice exhibit reestablished aortic endothelial function

eNOS KI mice are a highly interesting model since the unbiased effects of only in endothelium expressed eNOS become visible.

At baseline, aortas of these mice should behave as aortas isolated from global eNOS KO mouse, since inversion of the gene sequence of interest should only occur after induction of KI using tamoxifen. Indeed, no differences were visible at baseline in control (eNOS KO) and endothelium eNOS KI mice before tamoxifen treatment.

After treatment with tamoxifen, Cre-protein negative mice (eNOS KO) still demonstrated blunted endothelium-dependent vasodilation as seen before under baseline conditions without tamoxifen injection (**Figure 37**).

Strikingly, the Cre-protein positive mice (EC eNOS KI) demonstrated properties comparable to WT mice after injection of tamoxifen (**Figure 29**). Endothelium-dependent vasorelaxation was reestablished, the eNOS dependent feedback mechanism by the endothelium was reestablished as well, seen by a blunted reactivity to phenylephrine and a not statistically significant decrease in reactivity towards exogenously applied NO. Comparison of Cre negative (eNOS KO) to Cre positive mice (EC eNOS KI) resulted in dose response curves comparable to findings in comparison of eNOS KO mice and WT mice.

All together these results demonstrate that KI of eNOS in the endothelium was able to fully reestablish aortic endothelial function in an organ bath setting. As a future perspective this model might be of great value to investigate further, which tissue is important for effects attributed to eNOS. One interesting topic would be to narrow down in which tissue eNOS expression exerts the protection of eNOS after myocardial ischemia reperfusion injury (Jones, Girod et al. 1999, Pong, Scherrer-Crosbie et al. 2014). However, eNOS expression was demonstrated in ECs, RBCs and cardiomyocytes (Feron, Belhassen et al. 1996) and it is still unclear which cell type is accountable for the protective effects or if all cell types act in a synergistic fashion.

5.3.3 RBC specific eNOS KO mice exhibit high blood pressure and unchanged vascular endothelium function

RBC specific eNOS KO mice exhibited a significant increase in systolic and diastolic blood pressure. High blood pressure in RBC eNOS KO mice agrees with the previous study of chimeric mice, demonstrating increased blood pressure in mice lacking eNOS in blood stream cells (Wood, Cortese-Krott et al. 2013). As found in chimeric mice, also in the loxP-Cre models stepwise increases of blood pressure were found dependent on the tissue eNOS was knocked-out from. KO of eNOS in RBCs led to an increase of systolic blood pressure to 108.4 ± 1.8 mmHg and diastolic blood pressure of 73.6 ± 1.8 mmHg compared to a higher increase of blood pressure in EC eNOS KO mice with a systolic blood pressure of 118.8 ± 4.2 mmHg and diastolic blood pressure of 84.9 ± 3.9 mmHg.

This observation leads to the conclusion that eNOS in both tissues is important for the regulation of blood pressure, however that eNOS in ECs has a greater effect on blood pressure levels.

Table 7 Blood pressure parameters of transgenic eNOS KO models

Transgenic mouse line	Systolic blood pressure (mmHg)	Diastolic blood pressure (mmHg)	Heart rate (bpm)
Control	92.2 ± 2.6	59.33 ± 3.0	532.1 ± 19.3
RBC eNOS KO	108.4 ± 1.8	73.6 ± 2.6	436.4 ± 30.5
EC eNOS KO	118.8 ± 4.2	84.9 ± 3.9	540.0 ± 22.9

Summary of systolic blood pressure, diastolic blood pressure and heart rate for control mice, RBC eNOS KO and EC eNOS KO mice.

Of note RBC eNOS KO mice were characterized by a decrease of heart rate that was not evident in EC eNOS KO mice, even though they exhibited higher blood pressure. This might be due to the fact that RBC eNOS KO mice are born with the lack of eNOS in RBCs and develop high blood pressure early on, whereas in EC eNOS KO mice lack of eNOS and high blood pressure persist for a relatively short time of three weeks. This would be in support of the theory that lower heart rates in eNOS KO mice are an adaptive mechanism to high blood pressure (Shesely, Maeda et al. 1996)

To exclude effects of the loxP-Cre system on vascular endothelial function of conductive and resistive vessels, endothelium function was measured ex-vivo to exclude that changes in blood pressure were caused by changes in vascular functionality.

In concordance to the study of the chimeric mice, no difference was detectable in the comparison of RBC eNOS KO mice and control animals (**Figure 39**). Moreover, representative for resistive vessels, mesenteric arteries were investigated and no changes of RBC eNOS KO on vascular endothelium function were found, compared to control mice (**Figure 40**). Taken together, these findings show that the discovered hypertension of RBC eNOS KO mice was not due to vascular endothelium dysfunction.

The mechanism by which RBCs exert influence on blood pressure, is not clear yet and the designed models might be a valuable tool in identification of these. There are different theories, how RBC eNOS might exert its effect on blood pressure regulation, despite the 10 mM concentration of the potent NO scavenger hemoglobin in RBCs. A direct effect of RBC eNOS derived NO on the vascular wall seems unlikely, since this would need NO to diffuse from RBC to plasma, through ECs to its receptor sGC in smooth muscle cells.

One theory is that NO might reversibly *S*-nitrosate cysteine-93 in the hemoglobin beta chain and release NO in conditions of low oxygen by conformational changes of hemoglobin from the oxygenated R-state to the deoxygenated T-state and released by *S*-nitrosoglutathione (Jia, Bonaventura et al. 1996). This theory was heavily challenged by a battery of independent research groups presenting findings contradictory to the report by Jia et al. Findings challenging the "hemoglobin-SNO"-theory are: comparable binding rates for NO to hemoglobin in the R-state and T-state (Huang, Ucer et al. 2002), degradation of NO by hemoglobin rather than preservation (Joshi, Ferguson et al. 2002), same levels of pulmonary vasoconstriction of lungs perfused with hemoglobin-SNO or oxyhemoglobin (Deem, Gladwin et al. 2001), intracellular instability of hemoglobin-SNO in RBCs (Gladwin, Wang et al. 2002) and unchanged hemodynamics in a mouse expressing human hemoglobin with cysteine-93 substituted with an alanine amino acid (Isbell, Sun et al. 2008). Taken all these considerations together, make the formation of *S*-nitrosated hemoglobin as a mediator of RBC eNOS signaling unlikely.

Another theory postulates that RBC eNOS contributes to the overall pool of circulating nitrite. As demonstrated in the investigation of deficiency of eNOS in blood cells of chimeric mice, plasma pool of nitrite decreases when blood cells are deprived of eNOS (Wood, Cortese-Krott et al. 2013). Nitrite has been shown to actively take part in regulation of vascular tone by different mechanisms in different tissues (Lundberg and Weitzberg 2005, Lundberg, Weitzberg et al. 2008, Gilchrist, Shore et al. 2011). RBCs as well have been shown to take part in the reduction of nitrite to NO by the reaction with deoxyhemoglobin and induction of vascular dilation (Cosby, Partovi et al. 2003). In support of the notion of RBCs being important for nitrite bio-activation is that RBCs contain the highest portion of nitrite in the vessels (300 nM nitrite in RBCs to 200 nM

nitrite in whole blood) (Dejam, Hunter et al. 2005). The exact mechanism of RBC eNOS dependent signaling in the vascular tone remains unknown.

To conclude, eNOS in RBCs contributes to blood pressure regulation, by a mechanism that has to be identified in future studies. The RBC eNOS KO mice might be a valuable tool in these investigations.

5.3.4   Conclusion

To sum up, the developed loxP-Cre models of tissue specific KO and KI work and will be a valuable tool to investigate the tissue specific effects of eNOS. The major conclusion that can be drawn is that eNOS in RBCs contributes to blood pressure regulation.

6   Summary & Outlook

From the findings presented in this study it can be concluded that NO in RBCs is able to modulate intrinsic properties and NO derived from RBCs is potentially an indirect regulator of vascular tone.

It was shown that NO does not increase RBC deformability, however is able to protect from decreased RBC deformability induced by ROS. As a future perspective, it would be of great interest if the found decreased changes of RBC deformability after application of NO and oxidants are also evident in in-vivo models of oxidative stress. For this purpose, mouse models of hereditary, anemic diseases or pharmacologically induced anemias could be a useful tool. The effects of stimulation of in-vivo NO synthesis or exogenously applied NO on RBC deformability could be investigated. Moreover, the mechanism behind the observed effects should be addressed in further investigations. An approach might be the further characterization of the cellular changes that take place due to oxidative treatment with and without NO present and narrow down which of three determinants of RBC deformability was rescued. The results of these investigations might be applicable in a translational approach to help patients that suffer from the aftermath of impaired RBC deformability due to increased intracellular stress and might be a base for NO therapies.

It was demonstrated as well, that NO did increase intracellular levels of cGMP without concomitant release of extracellular ATP. With the finding of neither NO and the eNOS-sGC pathway being involved in release of ATP, nor intracellular increases of cAMP, the question still remains, how controlled release from RBCs is mediated. Understanding the mechanism is an essential prerequisite, before investigation of dysfunction in different disease states can be undertaken and a possible treatment strategy established. These investigations should be conducted with extreme care, in order to avoid misinterpretation of hemolysis of RBCs as a controlled release of ATP.

Lastly, RBC specific KO of eNOS exhibited a hypertensive phenotype. The developed tissue specific, transgenic mouse lines give many opportunities for further research. The different mouse lines will be valuable tools, to dissect the effect of eNOS in different

tissues in the cardiovascular system. In specific further cardiovascular characterization of all mice lines needs to be finished to assure a completely functional model.

The discovery of elevated blood pressure in RBC eNOS KO mice leads to the open question by what mechanism this effect is mediated. Possibly, full characterization of NO metabolites in the different compartments of whole blood will shed light into the open question, which metabolite might be responsible for the observed hemodynamic change and help identify the role of eNOS signaling in RBCs in regulation of vascular tone and splenic sequestration.

7 References

Aamand, R., T. Dalsgaard, F. B. Jensen, U. Simonsen, A. Roepstorff and A. Fago (2009). "Generation of nitric oxide from nitrite by carbonic anhydrase: a possible link between metabolic activity and vasodilation." Am J Physiol Heart Circ Physiol **297**(6): H2068-2074.

Agre, P., J. F. Casella, W. H. Zinkham, C. McMillan and V. Bennett (1985). "Partial deficiency of erythrocyte spectrin in hereditary spherocytosis." Nature **314**(6009): 380-383.

Angus, J. A., T. M. Cocks and K. Satoh (1986). "The alpha adrenoceptors on endothelial cells." Fed Proc **45**(9): 2355-2359.

Arcaro, G., M. Zamboni, L. Rossi, E. Turcato, G. Covi, F. Armellini, O. Bosello and A. Lechi (1999). "Body fat distribution predicts the degree of endothelial dysfunction in uncomplicated obesity." Int J Obes Relat Metab Disord **23**(9): 936-942.

Arnold, W. P., C. K. Mittal, S. Katsuki and F. Murad (1977). "Nitric oxide activates guanylate cyclase and increases guanosine 3':5'-cyclic monophosphate levels in various tissue preparations." Proc Natl Acad Sci U S A **74**(8): 3203-3207.

Barodka, V., J. G. Mohanty, A. K. Mustafa, L. Santhanam, A. Nyhan, A. K. Bhunia, G. Sikka, D. Nyhan, D. E. Berkowitz and J. M. Rifkind (2014). "Nitroprusside inhibits calcium-induced impairment of red blood cell deformability." Transfusion **54**(2): 434-444.

Barodka, V. M., E. Nagababu, J. G. Mohanty, D. Nyhan, D. E. Berkowitz, J. M. Rifkind and J. J. Strouse (2014). "New insights provided by a comparison of impaired deformability with erythrocyte oxidative stress for sickle cell disease." Blood Cells Mol Dis **52**(4): 230-235.

Baskurt, O. K. and H. J. Meiselman (1997). "Cellular determinants of low-shear blood viscosity." Biorheology **34**(3): 235-247.

Baskurt, O. K. and H. J. Meiselman (2013). "Data reduction methods for ektacytometry in clinical hemorheology." Clin Hemorheol Microcirc **54**(1): 99-107.

Becatti, M., R. Marcucci, A. M. Gori, L. Mannini, E. Grifoni, A. Alessandrello Liotta, A. Sodi, R. Tartaro, N. Taddei, S. Rizzo, D. Prisco, R. Abbate and C. Fiorillo (2016). "Erythrocyte oxidative stress is associated with cell deformability in patients with retinal vein occlusion." J Thromb Haemost **14**(11): 2287-2297.

Belanger, A. M., C. Keggi, T. Kanias, M. T. Gladwin and D. B. Kim-Shapiro (2015). "Effects of nitric oxide and its congeners on sickle red blood cell deformability." Transfusion **55**(10): 2464-2472.

Bergfeld, G. R. and T. Forrester (1992). "Release of ATP from human erythrocytes in response to a brief period of hypoxia and hypercapnia." Cardiovasc Res **26**(1): 40-47.

Bernatova, I. (2014). "Endothelial dysfunction in experimental models of arterial hypertension: cause or consequence?" Biomed Res Int **2014**: 598271.

Berne, R. M. (1963). "Cardiac nucleotides in hypoxia: possible role in regulation of coronary blood flow." Am J Physiol **204**: 317-322.

Bjerrum, P. J. (1979). "Hemoglobin-depleted human erythrocyte ghosts: characterization of morphology and transport functions." J Membr Biol **48**(1): 43-67.

Bodin, P., D. Bailey and G. Burnstock (1991). "Increased flow-induced ATP release from isolated vascular endothelial cells but not smooth muscle cells." Br J Pharmacol **103**(1): 1203-1205.

Bodin, P. and G. Burnstock (1995). "Synergistic effect of acute hypoxia on flow-induced release of ATP from cultured endothelial cells." Experientia **51**(3): 256-259.

Bor-Kucukatay, M., R. B. Wenby, H. J. Meiselman and O. K. Baskurt (2003). "Effects of nitric oxide on red blood cell deformability." Am J Physiol Heart Circ Physiol **284**(5): H1577-1584.

Born, G. V. and M. A. Kratzer (1984). "Source and concentration of extracellular adenosine triphosphate during haemostasis in rats, rabbits and man." J Physiol **354**: 419-429.

Brandes, R. P., D. Kim, F. H. Schmitz-Winnenthal, M. Amidi, A. Godecke, A. Mulsch and R. Busse (2000). "Increased nitrovasodilator sensitivity in endothelial nitric oxide synthase knockout mice: role of soluble guanylyl cyclase." Hypertension **35**(1 Pt 2): 231-236.

Braunwald, E. (1997). "Shattuck lecture--cardiovascular medicine at the turn of the millennium: triumphs, concerns, and opportunities." N Engl J Med **337**(19): 1360-1369.

Buckley, B. J., Z. Mirza and A. R. Whorton (1995). "Regulation of Ca(2+)-dependent nitric oxide synthase in bovine aortic endothelial cells." Am J Physiol **269**(3 Pt 1): C757-765.

Bujak, K., J. Wasilewski, T. Osadnik, S. Jonczyk, A. Kolodziejska, M. Gierlotka and M. Gasior (2015). "The Prognostic Role of Red Blood Cell Distribution Width in Coronary Artery Disease: A Review of the Pathophysiology." Dis Markers **2015**: 824624.

Butler, A. R., I. L. Megson and P. G. Wright (1998). "Diffusion of nitric oxide and scavenging by blood in the vasculature." Biochim Biophys Acta **1425**(1): 168-176.

Buvinic, S., R. Briones and J. P. Huidobro-Toro (2002). "P2Y(1) and P2Y(2) receptors are coupled to the NO/cGMP pathway to vasodilate the rat arterial mesenteric bed." Br J Pharmacol **136**(6): 847-856.

Canham, P. B. and A. C. Burton (1968). "Distribution of size and shape in populations of normal human red cells." Circ Res **22**(3): 405-422.

Cantow, K., B. Flemming, M. Ladwig-Wiegard, P. B. Persson and E. Seeliger (2017). "Low dose nitrite improves reoxygenation following renal ischemia in rats." Sci Rep **7**(1): 14597.

Cao, Z., J. B. Bell, J. G. Mohanty, E. Nagababu and J. M. Rifkind (2009). "Nitrite enhances RBC hypoxic ATP synthesis and the release of ATP into the vasculature: a new mechanism for nitrite-induced vasodilation." Am J Physiol Heart Circ Physiol **297**(4): H1494-1503.

Cappellini, M. D., D. Tavazzi, L. Duca, G. Graziadei, F. Mannu, F. Turrini, P. Arese and G. Fiorelli (1999). "Metabolic indicators of oxidative stress correlate with haemichrome attachment to membrane, band 3 aggregation and erythrophagocytosis in beta-thalassaemia intermedia." Br J Haematol **104**(3): 504-512.

Caprari, P., A. Bozzi, W. Malorni, A. Bottini, F. Iosi, M. T. Santini and A. M. Salvati (1995). "Junctional sites of erythrocyte skeletal proteins are specific targets of tert-butylhydroperoxide oxidative damage." Chem Biol Interact **94**(3): 243-258.

Cassoly, R. and Q. Gibson (1975). "Conformation, co-operativity and ligand binding in human hemoglobin." J Mol Biol **91**(3): 301-313.

Celermajer, D. S., K. E. Sorensen, V. M. Gooch, D. J. Spiegelhalter, O. I. Miller, I. D. Sullivan, J. K. Lloyd and J. E. Deanfield (1992). "Non-invasive detection of endothelial dysfunction in children and adults at risk of atherosclerosis." Lancet **340**(8828): 1111-1115.

Chan, K., X. D. Han and Y. W. Kan (2001). "An important function of Nrf2 in combating oxidative stress: detoxification of acetaminophen." Proc Natl Acad Sci U S A **98**(8): 4611-4616.

Chasis, J. A. and N. Mohandas (1986). "Erythrocyte membrane deformability and stability: two distinct membrane properties that are independently regulated by skeletal protein associations." J Cell Biol **103**(2): 343-350.

Chen, L. Y. and J. L. Mehta (1996). "Variable effects of L-arginine analogs on L-arginine-nitric oxide pathway in human neutrophils and platelets may relate to different nitric oxide synthase isoforms." J Pharmacol Exp Ther **276**(1): 253-257.

Chen, L. Y. and J. L. Mehta (1998). "Evidence for the presence of L-arginine-nitric oxide pathway in human red blood cells: relevance in the effects of red blood cells on platelet function." J Cardiovasc Pharmacol **32**(1): 57-61.

Chen, P. F., A. L. Tsai and K. K. Wu (1994). "Cysteine 184 of endothelial nitric oxide synthase is involved in heme coordination and catalytic activity." J Biol Chem **269**(40): 25062-25066.

Chiang, B. N., L. V. Perlman and F. H. Epstein (1969). "Overweight and hypertension. A review." Circulation **39**(3): 403-421.

Chien, S., S. Usami, R. J. Dellenback and M. I. Gregersen (1970). "Shear-dependent deformation of erythrocytes in rheology of human blood." Am J Physiol **219**(1): 136-142.

Cicco, G., M. C. Carbonara, G. D. Stingi and A. Pirrelli (2001). "Cytosolic calcium and hemorheological patterns during arterial hypertension." Clin Hemorheol Microcirc **24**(1): 25-31.

Cicco, G. and A. Pirrelli (1999). "Red blood cell (RBC) deformability, RBC aggregability and tissue oxygenation in hypertension." Clin Hemorheol Microcirc **21**(3-4): 169-177.

Cicco, G., P. Vicenti, G. D. Stingi, Tarallo and A. Pirrelli (1999). "Hemorheology in complicated hypertension." Clin Hemorheol Microcirc **21**(3-4): 315-319.

Cinar, E., S. Zhou, J. DeCourcey, Y. Wang, R. E. Waugh and J. Wan (2015). "Piezo1 regulates mechanotransductive release of ATP from human RBCs." Proc Natl Acad Sci U S A **112**(38): 11783-11788.

Clapp, B. R., G. M. Hirschfield, C. Storry, J. R. Gallimore, R. P. Stidwill, M. Singer, J. E. Deanfield, R. J. MacAllister, M. B. Pepys, P. Vallance and A. D. Hingorani (2005). "Inflammation and endothelial function: direct vascular effects of human C-reactive protein on nitric oxide bioavailability." Circulation **111**(12): 1530-1536.

Clarke, S. C., P. M. Schofield, A. A. Grace, J. C. Metcalfe and H. L. Kirschenlohr (2001). "Tamoxifen effects on endothelial function and cardiovascular risk factors in men with advanced atherosclerosis." Circulation **103**(11): 1497-1502.

Cokelet, G. R. and H. J. Meiselman (1968). "Rheological comparison of hemoglobin solutions and erythrocyte suspensions." Science **162**(3850): 275-277.

Collard, K., D. White and A. Copplestone (2014). "The influence of storage age on iron status, oxidative stress and antioxidant protection in paediatric packed cell units." Blood Transfus **12**(2): 210-219.

Cooper, C. E. (1999). "Nitric oxide and iron proteins." Biochim Biophys Acta **1411**(2-3): 290-309.

Corry, W. D., H. J. Meiselman and P. Hochstein (1980). "t-Butyl hydroperoxide-induced changes in the physicochemical properties of human erythrocytes." Biochim Biophys Acta **597**(2): 224-234.

Cortese-Krott, M. M., M. Evathia, C. M. Kamer, W. Lückstädt, J. Yang, G. Wolff, C. Panknin, T. Bracht, B. Sitek, J. Pernow, J.-P. Stasch, M. Feelisch, D. Koesling and M. Kelm (2018). "Identification of a soluble guanylate cyclase in red blood cells: preserved activity in patients with coronary artery disease." Redox Biol **14**: 328-337.

Cortese-Krott, M. M. and M. Kelm (2014). "Endothelial nitric oxide synthase in red blood cells: key to a new erythrocrine function?" Redox Biol **2**: 251-258.

Cortese-Krott, M. M., E. Mergia, C. M. Kramer, W. Luckstadt, J. Yang, G. Wolff, C. Panknin, T. Bracht, B. Sitek, J. Pernow, J. P. Stasch, M. Feelisch, D. Koesling and M. Kelm (2018). "Identification of a soluble guanylate cyclase in RBCs: preserved activity in patients with coronary artery disease." Redox Biol **14**: 328-337.

Cortese-Krott, M. M., A. Rodriguez-Mateos, G. G. Kuhnle, G. Brown, M. Feelisch and M. Kelm (2012). "A multilevel analytical approach for detection and visualization of intracellular NO production and nitrosation events using diaminofluoresceins." Free Radic Biol Med **53**(11): 2146-2158.

Cortese-Krott, M. M., A. Rodriguez-Mateos, R. Sansone, G. G. Kuhnle, S. Thasian-Sivarajah, T. Krenz, P. Horn, C. Krisp, D. Wolters, C. Heiss, K. D. Kroncke, N. Hogg, M. Feelisch and M. Kelm (2012). "Human red blood cells at work: identification and visualization of erythrocytic eNOS activity in health and disease." Blood **120**(20): 4229-4237.

Cosby, K., K. S. Partovi, J. H. Crawford, R. P. Patel, C. D. Reiter, S. Martyr, B. K. Yang, M. A. Waclawiw, G. Zalos, X. Xu, K. T. Huang, H. Shields, D. B. Kim-Shapiro, A. N. Schechter, R. O. Cannon, 3rd and M. T. Gladwin (2003). "Nitrite reduction to nitric oxide by deoxyhemoglobin vasodilates the human circulation." Nat Med **9**(12): 1498-1505.

Crane, B. R., A. S. Arvai, D. K. Ghosh, C. Wu, E. D. Getzoff, D. J. Stuehr and J. A. Tainer (1998). "Structure of nitric oxide synthase oxygenase dimer with pterin and substrate." Science **279**(5359): 2121-2126.

Crawford, J. H., T. S. Isbell, Z. Huang, S. Shiva, B. K. Chacko, A. N. Schechter, V. M. Darley-Usmar, J. D. Kerby, J. D. Lang, Jr., D. Kraus, C. Ho, M. T. Gladwin and R. P. Patel (2006). "Hypoxia, red blood cells, and nitrite regulate NO-dependent hypoxic vasodilation." Blood **107**(2): 566-574.

Crosby, W. H. (1972). "Splenectomy in hematologic disorders." N Engl J Med **286**(23): 1252-1254.

de, F., L. Sanchez de Miguel, J. Farre, J. Gomez, J. Romero, P. Marcos-Alberca, A. Nunez, L. Rico and A. Lopez-Farre (2001). "Expression of an endothelial-type nitric oxide synthase isoform in human neutrophils: modification by tumor necrosis factor-alpha and during acute myocardial infarction." J Am Coll Cardiol **37**(3): 800-807.

Deem, S., M. T. Gladwin, J. T. Berg, M. E. Kerr and E. R. Swenson (2001). "Effects of S-nitrosation of hemoglobin on hypoxic pulmonary vasoconstriction and nitric oxide flux." Am J Respir Crit Care Med **163**(5): 1164-1170.

Dejam, A., C. J. Hunter, M. M. Pelletier, L. L. Hsu, R. F. Machado, S. Shiva, G. G. Power, M. Kelm, M. T. Gladwin and A. N. Schechter (2005). "Erythrocytes are the major intravascular storage sites of nitrite in human blood." Blood **106**(2): 734-739.

Deplaine, G., I. Safeukui, F. Jeddi, F. Lacoste, V. Brousse, S. Perrot, S. Biligui, M. Guillotte, C. Guitton, S. Dokmak, B. Aussilhou, A. Sauvanet, D. Cazals Hatem, F. Paye, M. Thellier, D. Mazier, G. Milon, N. Mohandas, O. Mercereau-Puijalon, P. H. David and P. A. Buffet (2011). "The sensing of poorly deformable red blood cells by the human spleen can be mimicked in vitro." Blood **117**(8): e88-95.

Diederich, L., T. Suvorava, R. Sansone, T. C. S. t. Keller, F. Barbarino, T. R. Sutton, C. M. Kramer, W. Luckstadt, B. E. Isakson, H. Gohlke, M. Feelisch, M. Kelm and M. M. Cortese-Krott (2018). "On the Effects of Reactive Oxygen Species and Nitric Oxide on Red Blood Cell Deformability." Front Physiol **9**: 332.

Dietrich, H. H., M. L. Ellsworth, R. S. Sprague and R. G. Dacey, Jr. (2000). "Red blood cell regulation of microvascular tone through adenosine triphosphate." Am J Physiol Heart Circ Physiol **278**(4): H1294-1298.

Doshi, S. N., K. K. Naka, N. Payne, C. J. Jones, M. Ashton, M. J. Lewis and J. Goodfellow (2001). "Flow-mediated dilatation following wrist and upper arm occlusion in humans: the contribution of nitric oxide." Clin Sci (Lond) **101**(6): 629-635.

Doyle, M. P. and J. W. Hoekstra (1981). "Oxidation of nitrogen oxides by bound dioxygen in hemoproteins." J Inorg Biochem **14**(4): 351-358.

Duranton, C., S. M. Huber and F. Lang (2002). "Oxidation induces a Cl(-)-dependent cation conductance in human red blood cells." J Physiol **539**(Pt 3): 847-855.

Dzierzak, E. and S. Philipsen (2013). "Erythropoiesis: development and differentiation." Cold Spring Harb Perspect Med **3**(4): a011601.

Eber, S. W., J. M. Gonzalez, M. L. Lux, A. L. Scarpa, W. T. Tse, M. Dornwell, J. Herbers, W. Kugler, R. Ozcan, A. Pekrun, P. G. Gallagher, W. Schroter, B. G. Forget and S. E. Lux (1996). "Ankyrin-1 mutations are a major cause of dominant and recessive hereditary spherocytosis." Nat Genet **13**(2): 214-218.

Eich, R. F., T. Li, D. D. Lemon, D. H. Doherty, S. R. Curry, J. F. Aitken, A. J. Mathews, K. A. Johnson, R. D. Smith, G. N. Phillips, Jr. and J. S. Olson (1996). "Mechanism of NO-induced oxidation of myoglobin and hemoglobin." Biochemistry **35**(22): 6976-6983.

Ellsworth, M. L. (2004). "Red blood cell-derived ATP as a regulator of skeletal muscle perfusion." Med Sci Sports Exerc **36**(1): 35-41.

Ellsworth, M. L., T. Forrester, C. G. Ellis and H. H. Dietrich (1995). "The erythrocyte as a regulator of vascular tone." Am J Physiol **269**(6 Pt 2): H2155-2161.

Ellsworth, M. L. and R. S. Sprague (2012). "Regulation of blood flow distribution in skeletal muscle: role of erythrocyte-released ATP." J Physiol **590**(20): 4985-4991.

Erkens, R., C. M. Kramer, W. Luckstadt, C. Panknin, L. Krause, M. Weidenbach, J. Dirzka, T. Krenz, E. Mergia, T. Suvorava, M. Kelm and M. M. Cortese-Krott (2015). "Left ventricular diastolic dysfunction in Nrf2 knock out mice is associated with cardiac hypertrophy, decreased expression of SERCA2a, and preserved endothelial function." Free Radic Biol Med **89**: 906-917.

Fago, A., A. L. Crumbliss, M. P. Hendrich, L. L. Pearce, J. Peterson, R. Henkens and C. Bonaventura (2013). "Oxygen binding to partially nitrosylated hemoglobin." Biochim Biophys Acta **1834**(9): 1894-1900.

Fan, X., H. Deng, X. Wang, S. Fu, Z. Liu, J. Sang, X. Zhang, N. Li, Q. Han and Z. Liu (2018). "Association of red blood cell distribution width with severity of hepatitis B virus-related liver diseases." Clin Chim Acta **482**: 155-160.

Feron, O., L. Belhassen, L. Kobzik, T. W. Smith, R. A. Kelly and T. Michel (1996). "Endothelial nitric oxide synthase targeting to caveolae. Specific interactions with caveolin isoforms in cardiac myocytes and endothelial cells." J Biol Chem **271**(37): 22810-22814.

Fischer, T. M., C. W. Haest, M. Stohr, D. Kamp and B. Deuticke (1978). "Selective alteration of erythrocyte deformabiliby by SH-reagents: evidence for an involvement of spectrin in membrane shear elasticity." Biochim Biophys Acta **510**(2): 270-282.

Fisher, B., J. Bryant, J. J. Dignam, D. L. Wickerham, E. P. Mamounas, E. R. Fisher, R. G. Margolese, L. Nesbitt, S. Paik, T. M. Pisansky, N. Wolmark, B. National Surgical Adjuvant and P. Bowel (2002). "Tamoxifen, radiation therapy, or both for prevention of ipsilateral breast tumor recurrence after lumpectomy in women with invasive breast cancers of one centimeter or less." J Clin Oncol **20**(20): 4141-4149.

Fisslthaler, B., A. E. Loot, A. Mohamed, R. Busse and I. Fleming (2008). "Inhibition of endothelial nitric oxide synthase activity by proline-rich tyrosine kinase 2 in response to fluid shear stress and insulin." Circ Res **102**(12): 1520-1528.

Forrester, T. and A. R. Lind (1969). "Identification of adenosine triphosphate in human plasma and the concentration in the venous effluent of forearm muscles before, during and after sustained contractions." J Physiol **204**(2): 347-364.

Forstermann, U., J. S. Pollock, H. H. Schmidt, M. Heller and F. Murad (1991). "Calmodulin-dependent endothelium-derived relaxing factor/nitric oxide synthase activity is present in the particulate and cytosolic fractions of bovine aortic endothelial cells." Proc Natl Acad Sci U S A **88**(5): 1788-1792.

Forsyth, A. M., J. Wan, P. D. Owrutsky, M. Abkarian and H. A. Stone (2011). "Multiscale approach to link red blood cell dynamics, shear viscosity, and ATP release." Proc Natl Acad Sci U S A **108**(27): 10986-10991.

Frank, S. M., B. Abazyan, M. Ono, C. W. Hogue, D. B. Cohen, D. E. Berkowitz, P. M. Ness and V. M. Barodka (2013). "Decreased erythrocyte deformability after transfusion and the effects of erythrocyte storage duration." Anesth Analg **116**(5): 975-981.

Freikman, I., I. Ringel and E. Fibach (2011). "Oxidative stress-induced membrane shedding from RBCs is Ca flux-mediated and affects membrane lipid composition." J Membr Biol **240**(2): 73-82.

Fromson, J. M., S. Pearson and S. Bramah (1973). "The metabolism of tamoxifen (I.C.I. 46,474). I. In laboratory animals." Xenobiotica **3**(11): 693-709.

Fulton, D., J. E. Church, L. Ruan, C. Li, S. G. Sood, B. E. Kemp, I. G. Jennings and R. C. Venema (2005). "Src kinase activates endothelial nitric-oxide synthase by phosphorylating Tyr-83." J Biol Chem **280**(43): 35943-35952.

Furchgott, R. F. and J. V. Zawadzki (1980). "The obligatory role of endothelial cells in the relaxation of arterial smooth muscle by acetylcholine." Nature **288**(5789): 373-376.

Galli, F., S. Rovidati, L. Ghibelli and F. Canestrari (1998). "S-nitrosylation of glyceraldehyde-3-phosphate dehydrogenase decreases the enzyme affinity to the erythrocyte membrane." Nitric Oxide **2**(1): 17-27.

Garcin, E. D., C. M. Bruns, S. J. Lloyd, D. J. Hosfield, M. Tiso, R. Gachhui, D. J. Stuehr, J. A. Tainer and E. D. Getzoff (2004). "Structural basis for isozyme-specific regulation of electron transfer in nitric-oxide synthase." J Biol Chem **279**(36): 37918-37927.

Gebska, M. A., B. K. Stevenson, A. R. Hemnes, T. J. Bivalacqua, A. Haile, G. G. Hesketh, C. I. Murray, A. L. Zaiman, M. K. Halushka, N. Krongkaew, T. D. Strong, C. A. Cooke, H. El-Haddad, R. M. Tuder, D. E. Berkowitz and H. C. Champion (2011). "Phosphodiesterase-5A (PDE5A) is localized to the endothelial caveolae and modulates NOS3 activity." Cardiovasc Res **90**(2): 353-363.

Ghosh, S. M., V. Kapil, I. Fuentes-Calvo, K. J. Bubb, V. Pearl, A. B. Milsom, R. Khambata, S. Maleki-Toyserkani, M. Yousuf, N. Benjamin, A. J. Webb, M. J. Caulfield, A. J. Hobbs and A. Ahluwalia (2013). "Enhanced vasodilator activity of nitrite in hypertension: critical role for erythrocytic xanthine oxidoreductase and translational potential." Hypertension **61**(5): 1091-1102.

Gibson, Q. H. and F. J. Roughton (1957). "The kinetics and equilibria of the reactions of nitric oxide with sheep haemoglobin." J Physiol **136**(3): 507-524.

Gilchrist, M., A. C. Shore and N. Benjamin (2011). "Inorganic nitrate and nitrite and control of blood pressure." Cardiovasc Res **89**(3): 492-498.

Gladwin, M. T., A. N. Schechter, D. B. Kim-Shapiro, R. P. Patel, N. Hogg, S. Shiva, R. O. Cannon, 3rd, M. Kelm, D. A. Wink, M. G. Espey, E. H. Oldfield, R. M. Pluta, B. A. Freeman, J. R. Lancaster, Jr., M. Feelisch and J. O. Lundberg (2005). "The emerging biology of the nitrite anion." Nat Chem Biol **1**(6): 308-314.

Gladwin, M. T., J. H. Shelhamer, A. N. Schechter, M. E. Pease-Fye, M. A. Waclawiw, J. A. Panza, F. P. Ognibene and R. O. Cannon, 3rd (2000). "Role of circulating nitrite and

S-nitrosohemoglobin in the regulation of regional blood flow in humans." Proc Natl Acad Sci U S A **97**(21): 11482-11487.

Gladwin, M. T., X. Wang, C. D. Reiter, B. K. Yang, E. X. Vivas, C. Bonaventura and A. N. Schechter (2002). "S-Nitrosohemoglobin is unstable in the reductive erythrocyte environment and lacks O2/NO-linked allosteric function." J Biol Chem **277**(31): 27818-27828.

Godecke, A., U. K. Decking, Z. Ding, J. Hirchenhain, H. J. Bidmon, S. Godecke and J. Schrader (1998). "Coronary hemodynamics in endothelial NO synthase knockout mice." Circ Res **82**(2): 186-194.

Gokce, N., M. Holbrook, S. J. Duffy, S. Demissie, L. A. Cupples, E. Biegelsen, J. F. Keaney, Jr., J. Loscalzo and J. A. Vita (2001). "Effects of race and hypertension on flow-mediated and nitroglycerin-mediated dilation of the brachial artery." Hypertension **38**(6): 1349-1354.

Goldman, D., G. M. Fraser, C. G. Ellis, R. S. Sprague, M. L. Ellsworth and A. H. Stephenson (2012). "Toward a multiscale description of microvascular flow regulation: o(2)-dependent release of ATP from human erythrocytes and the distribution of ATP in capillary networks." Front Physiol **3**: 246.

Gorbunov, N. V., J. C. Yalowich, A. Gaddam, P. Thampatty, V. B. Ritov, E. R. Kisin, N. M. Elsayed and V. E. Kagan (1997). "Nitric oxide prevents oxidative damage produced by tert-butyl hydroperoxide in erythroleukemia cells via nitrosylation of heme and non-heme iron. Electron paramagnetic resonance evidence." J Biol Chem **272**(19): 12328-12341.

Grau, M., S. Pauly, J. Ali, K. Walpurgis, M. Thevis, W. Bloch and F. Suhr (2013). "RBC-NOS-dependent S-nitrosylation of cytoskeletal proteins improves RBC deformability." PLoS One **8**(2): e56759.

Green, D. J., E. A. Dawson, H. M. Groenewoud, H. Jones and D. H. Thijssen (2014). "Is flow-mediated dilation nitric oxide mediated?: A meta-analysis." Hypertension **63**(2): 376-382.

Griendling, K. K., R. M. Touyz, J. L. Zweier, S. Dikalov, W. Chilian, Y. R. Chen, D. G. Harrison, A. Bhatnagar and S. American Heart Association Council on Basic Cardiovascular (2016). "Measurement of Reactive Oxygen Species, Reactive Nitrogen Species, and Redox-Dependent Signaling in the Cardiovascular System: A Scientific Statement From the American Heart Association." Circ Res **119**(5): e39-75.

Haest, C. W., T. M. Fischer, G. Plasa and B. Deuticke (1980). "Stabilization of erythrocyte shape by a chemical increase in membrane shear stiffness." Blood Cells **6**(3): 539-553.

Hebbel, R. P., W. T. Morgan, J. W. Eaton and B. E. Hedlund (1988). "Accelerated autoxidation and heme loss due to instability of sickle hemoglobin." Proc Natl Acad Sci U S A **85**(1): 237-241.

Heideman, W. H., N. S. Russell, C. Gundy, M. A. Rookus and D. W. Voskuil (2009). "The frequency, magnitude and timing of post-diagnosis body weight gain in Dutch breast cancer survivors." Eur J Cancer **45**(1): 119-126.

Helms, C. and D. B. Kim-Shapiro (2013). "Hemoglobin-mediated nitric oxide signaling." Free Radic Biol Med **61**: 464-472.

Herold, S. (2004). "The outer-sphere oxidation of nitrosyliron(II)hemoglobin by peroxynitrite leads to the release of nitrogen monoxide." Inorg Chem **43**(13): 3783-3785.

Herold, S., M. Exner and T. Nauser (2001). "Kinetic and mechanistic studies of the NO*-mediated oxidation of oxymyoglobin and oxyhemoglobin." Biochemistry **40**(11): 3385-3395.

Hingorani, A. D., J. Cross, R. K. Kharbanda, M. J. Mullen, K. Bhagat, M. Taylor, A. E. Donald, M. Palacios, G. E. Griffin, J. E. Deanfield, R. J. MacAllister and P. Vallance (2000). "Acute systemic inflammation impairs endothelium-dependent dilatation in humans." Circulation **102**(9): 994-999.

Hoskin, P. J., S. Ashley and J. R. Yarnold (1992). "Weight gain after primary surgery for breast cancer--effect of tamoxifen." Breast Cancer Res Treat **22**(2): 129-132.

Huang, P. L., Z. Huang, H. Mashimo, K. D. Bloch, M. A. Moskowitz, J. A. Bevan and M. C. Fishman (1995). "Hypertension in mice lacking the gene for endothelial nitric oxide synthase." Nature **377**(6546): 239-242.

Huang, Z., K. B. Ucer, T. Murphy, R. T. Williams, S. B. King and D. B. Kim-Shapiro (2002). "Kinetics of nitric oxide binding to R-state hemoglobin." Biochem Biophys Res Commun **292**(4): 812-818.

Hussain, M. B., A. J. Hobbs and R. J. MacAllister (1999). "Autoregulation of nitric oxide-soluble guanylate cyclase-cyclic GMP signalling in mouse thoracic aorta." Br J Pharmacol **128**(5): 1082-1088.

Ignarro, L. J., H. Lippton, J. C. Edwards, W. H. Baricos, A. L. Hyman, P. J. Kadowitz and C. A. Gruetter (1981). "Mechanism of vascular smooth muscle relaxation by organic nitrates, nitrites, nitroprusside and nitric oxide: evidence for the involvement of S-nitrosothiols as active intermediates." J Pharmacol Exp Ther **218**(3): 739-749.

Isbell, T. S., C. W. Sun, L. C. Wu, X. Teng, D. A. Vitturi, B. G. Branch, C. G. Kevil, N. Peng, J. M. Wyss, N. Ambalavanan, L. Schwiebert, J. Ren, K. M. Pawlik, M. B. Renfrow, R. P. Patel and T. M. Townes (2008). "SNO-hemoglobin is not essential for red blood cell-dependent hypoxic vasodilation." Nat Med **14**(7): 773-777.

Itoh, K., T. Chiba, S. Takahashi, T. Ishii, K. Igarashi, Y. Katoh, T. Oyake, N. Hayashi, K. Satoh, I. Hatayama, M. Yamamoto and Y. Nabeshima (1997). "An Nrf2/small Maf heterodimer mediates the induction of phase II detoxifying enzyme genes through antioxidant response elements." Biochem Biophys Res Commun **236**(2): 313-322.

Itoh, K., N. Wakabayashi, Y. Katoh, T. Ishii, K. Igarashi, J. D. Engel and M. Yamamoto (1999). "Keap1 represses nuclear activation of antioxidant responsive elements by Nrf2 through binding to the amino-terminal Neh2 domain." Genes Dev **13**(1): 76-86.

Jackson, E. K., J. Ren and Z. Mi (2009). "Extracellular 2',3'-cAMP is a source of adenosine." J Biol Chem **284**(48): 33097-33106.

Jain, S. K. (1985). "In vivo externalization of phosphatidylserine and phosphatidylethanolamine in the membrane bilayer and hypercoagulability by the lipid peroxidation of erythrocytes in rats." J Clin Invest **76**(1): 281-286.

Jarolim, P., J. L. Murray, H. L. Rubin, W. M. Taylor, J. T. Prchal, S. K. Ballas, L. M. Snyder, L. Chrobak, W. D. Melrose, V. Brabec and J. Palek (1996). "Characterization of

13 novel band 3 gene defects in hereditary spherocytosis with band 3 deficiency." <u>Blood</u> **88**(11): 4366-4374.

Jia, L., C. Bonaventura, J. Bonaventura and J. S. Stamler (1996). "S-nitrosohaemoglobin: a dynamic activity of blood involved in vascular control." <u>Nature</u> **380**(6571): 221-226.

Jones, S. P., W. G. Girod, A. J. Palazzo, D. N. Granger, M. B. Grisham, D. Jourd'Heuil, P. L. Huang and D. J. Lefer (1999). "Myocardial ischemia-reperfusion injury is exacerbated in absence of endothelial cell nitric oxide synthase." <u>Am J Physiol</u> **276**(5 Pt 2): H1567-1573.

Joshi, M. S., T. B. Ferguson, Jr., T. H. Han, D. R. Hyduke, J. C. Liao, T. Rassaf, N. Bryan, M. Feelisch and J. R. Lancaster, Jr. (2002). "Nitric oxide is consumed, rather than conserved, by reaction with oxyhemoglobin under physiological conditions." <u>Proc Natl Acad Sci U S A</u> **99**(16): 10341-10346.

Ju, H., R. Zou, V. J. Venema and R. C. Venema (1997). "Direct interaction of endothelial nitric-oxide synthase and caveolin-1 inhibits synthase activity." <u>J Biol Chem</u> **272**(30): 18522-18525.

Kamga Pride, C., L. Mo, K. Quesnelle, R. K. Dagda, D. Murillo, L. Geary, C. Corey, R. Portella, S. Zharikov, C. St Croix, S. Maniar, C. T. Chu, N. K. Khoo and S. Shiva (2014). "Nitrite activates protein kinase A in normoxia to mediate mitochondrial fusion and tolerance to ischaemia/reperfusion." <u>Cardiovasc Res</u> **101**(1): 57-68.

Kannan, R., R. Labotka and P. S. Low (1988). "Isolation and characterization of the hemichrome-stabilized membrane protein aggregates from sickle erythrocytes. Major site of autologous antibody binding." <u>J Biol Chem</u> **263**(27): 13766-13773.

Karagoz, B., O. Bilgi, A. Alacacioglu, A. Ozgun, O. Sayan, A. A. Erikci and E. G. Kandemir (2010). "Mean platelet volume increase after tamoxifen, but not after anastrazole in adjuvant therapy of breast cancer." <u>Med Oncol</u> **27**(2): 199-202.

Keller, A. S., L. Diederich, C. Panknin, L. J. DeLalio, J. C. Drake, R. Sherman, E. K. Jackson, Z. Yan, M. Kelm, M. M. Cortese-Krott and B. E. Isakson (2017). "Possible roles for ATP release from RBCs exclude the cAMP-mediated Panx1 pathway." <u>Am J Physiol Cell Physiol</u> **313**(6): C593-C603.

Kennedy, C. and G. Burnstock (1985). "ATP produces vasodilation via P1 purinoceptors and vasoconstriction via P2 purinoceptors in the isolated rabbit central ear artery." <u>Blood Vessels</u> **22**(3): 145-155.

Kleinbongard, P., A. Dejam, T. Lauer, T. Rassaf, A. Schindler, O. Picker, T. Scheeren, A. Godecke, J. Schrader, R. Schulz, G. Heusch, G. A. Schaub, N. S. Bryan, M. Feelisch and M. Kelm (2003). "Plasma nitrite reflects constitutive nitric oxide synthase activity in mammals." <u>Free Radic Biol Med</u> **35**(7): 790-796.

Kleinbongard, P., R. Schulz, T. Rassaf, T. Lauer, A. Dejam, T. Jax, I. Kumara, P. Gharini, S. Kabanova, B. Ozuyaman, H. G. Schnurch, A. Godecke, A. A. Weber, M. Robenek, H. Robenek, W. Bloch, P. Rosen and M. Kelm (2006). "Red blood cells express a functional endothelial nitric oxide synthase." <u>Blood</u> **107**(7): 2943-2951.

Koller, A. and A. Huang (1994). "Impaired nitric oxide-mediated flow-induced dilation in arterioles of spontaneously hypertensive rats." <u>Circ Res</u> **74**(3): 416-421.

Krieger, C. C., X. An, H. Y. Tang, N. Mohandas, D. W. Speicher and D. E. Discher (2011). "Cysteine shotgun-mass spectrometry (CS-MS) reveals dynamic sequence of protein structure changes within mutant and stressed cells." Proc Natl Acad Sci U S A **108**(20): 8269-8274.

Kuhn, V., L. Diederich, T. C. S. t. Keller, C. M. Kramer, W. Luckstadt, C. Panknin, T. Suvorava, B. E. Isakson, M. Kelm and M. M. Cortese-Krott (2017). "Red Blood Cell Function and Dysfunction: Redox Regulation, Nitric Oxide Metabolism, Anemia." Antioxid Redox Signal **26**(13): 718-742.

Kuypers, F. A., M. D. Scott, M. A. Schott, B. Lubin and D. T. Chiu (1990). "Use of ektacytometry to determine red cell susceptibility to oxidative stress." J Lab Clin Med **116**(4): 535-545.

Laker, R. C., J. C. Drake, R. J. Wilson, V. A. Lira, B. M. Lewellen, K. A. Ryall, C. C. Fisher, M. Zhang, J. J. Saucerman, L. J. Goodyear, M. Kundu and Z. Yan (2017). "Ampk phosphorylation of Ulk1 is required for targeting of mitochondria to lysosomes in exercise-induced mitophagy." Nat Commun **8**(1): 548.

Lamas, A. Z., I. F. Caliman, P. L. Dalpiaz, A. F. de Melo, Jr., G. R. Abreu, E. M. Lemos, S. A. Gouvea and N. S. Bissoli (2015). "Comparative effects of estrogen, raloxifene and tamoxifen on endothelial dysfunction, inflammatory markers and oxidative stress in ovariectomized rats." Life Sci **124**: 101-109.

Lekakis, J., P. Abraham, A. Balbarini, A. Blann, C. M. Boulanger, J. Cockcroft, F. Cosentino, J. Deanfield, A. Gallino, I. Ikonomidis, D. Kremastinos, U. Landmesser, A. Protogerou, C. Stefanadis, D. Tousoulis, G. Vassalli, H. Vink, N. Werner, I. Wilkinson and C. Vlachopoulos (2011). "Methods for evaluating endothelial function: a position statement from the European Society of Cardiology Working Group on Peripheral Circulation." Eur J Cardiovasc Prev Rehabil **18**(6): 775-789.

Lewington, S., R. Clarke, N. Qizilbash, R. Peto, R. Collins and C. Prospective Studies (2002). "Age-specific relevance of usual blood pressure to vascular mortality: a meta-analysis of individual data for one million adults in 61 prospective studies." Lancet **360**(9349): 1903-1913.

Liu, C., N. Wajih, X. Liu, S. Basu, J. Janes, M. Marvel, C. Keggi, C. C. Helms, A. N. Lee, A. M. Belanger, D. I. Diz, P. J. Laurienti, D. L. Caudell, J. Wang, M. T. Gladwin and D. B. Kim-Shapiro (2015). "Mechanisms of human erythrocytic bioactivation of nitrite." J Biol Chem **290**(2): 1281-1294.

Liu, S. C. and J. Palek (1980). "Spectrin tetramer-dimer equilibrium and the stability of erythrocyte membrane skeletons." Nature **285**(5766): 586-588.

Liu, X., M. J. Miller, M. S. Joshi, H. Sadowska-Krowicka, D. A. Clark and J. R. Lancaster, Jr. (1998). "Diffusion-limited reaction of free nitric oxide with erythrocytes." J Biol Chem **273**(30): 18709-18713.

Locovei, S., L. Bao and G. Dahl (2006). "Pannexin 1 in erythrocytes: function without a gap." Proc Natl Acad Sci U S A **103**(20): 7655-7659.

Lollar, P. and W. G. Owen (1981). "Active-site-dependent, thrombin-induced release of adenine nucleotides from cultured human endothelial cells." Ann N Y Acad Sci **370**: 51-56.

Lowry, O. H., N. J. Rosebrough, A. L. Farr and R. J. Randall (1951). "Protein measurement with the Folin phenol reagent." J Biol Chem **193**(1): 265-275.

Lundberg, J. O., M. T. Gladwin and E. Weitzberg (2015). "Strategies to increase nitric oxide signalling in cardiovascular disease." Nat Rev Drug Discov **14**(9): 623-641.

Lundberg, J. O. and E. Weitzberg (2005). "NO generation from nitrite and its role in vascular control." Arterioscler Thromb Vasc Biol **25**(5): 915-922.

Lundberg, J. O., E. Weitzberg and M. T. Gladwin (2008). "The nitrate-nitrite-nitric oxide pathway in physiology and therapeutics." Nat Rev Drug Discov **7**(2): 156-167.

Luthje, J. (1989). "Origin, metabolism and function of extracellular adenine nucleotides in the blood." Klin Wochenschr **67**(6): 317-327.

Lux, S. E. t. (2016). "Anatomy of the red cell membrane skeleton: unanswered questions." Blood **127**(2): 187-199.

Maher, A. R., A. B. Milsom, P. Gunaruwan, K. Abozguia, I. Ahmed, R. A. Weaver, P. Thomas, H. Ashrafian, G. V. Born, P. E. James and M. P. Frenneaux (2008). "Hypoxic modulation of exogenous nitrite-induced vasodilation in humans." Circulation **117**(5): 670-677.

Mannick, J. B., A. Hausladen, L. Liu, D. T. Hess, M. Zeng, Q. X. Miao, L. S. Kane, A. J. Gow and J. S. Stamler (1999). "Fas-induced caspase denitrosylation." Science **284**(5414): 651-654.

Martin, W., R. F. Furchgott, G. M. Villani and D. Jothianandan (1986). "Depression of contractile responses in rat aorta by spontaneously released endothelium-derived relaxing factor." J Pharmacol Exp Ther **237**(2): 529-538.

Matrougui, K., J. Maclouf, B. I. Levy and D. Henrion (1997). "Impaired nitric oxide- and prostaglandin-mediated responses to flow in resistance arteries of hypertensive rats." Hypertension **30**(4): 942-947.

McMahon, M., K. Itoh, M. Yamamoto, S. A. Chanas, C. J. Henderson, L. I. McLellan, C. R. Wolf, C. Cavin and J. D. Hayes (2001). "The Cap'n'Collar basic leucine zipper transcription factor Nrf2 (NF-E2 p45-related factor 2) controls both constitutive and inducible expression of intestinal detoxification and glutathione biosynthetic enzymes." Cancer Res **61**(8): 3299-3307.

Mesquita, R., B. Picarra, C. Saldanha and J. Martins e Silva (2002). "Nitric oxide effects on human erythrocytes structural and functional properties--an in vitro study." Clin Hemorheol Microcirc **27**(2): 137-147.

Metzger, D. and P. Chambon (2001). "Site- and time-specific gene targeting in the mouse." Methods **24**(1): 71-80.

Michell, B. J., M. B. Harris, Z. P. Chen, H. Ju, V. J. Venema, M. A. Blackstone, W. Huang, R. C. Venema and B. E. Kemp (2002). "Identification of regulatory sites of phosphorylation of the bovine endothelial nitric-oxide synthase at serine 617 and serine 635." J Biol Chem **277**(44): 42344-42351.

Mitchell, J. A., U. Forstermann, T. D. Warner, J. S. Pollock, H. H. Schmidt, M. Heller and F. Murad (1991). "Endothelial cells have a particulate enzyme system responsible for EDRF formation: measurement by vascular relaxation." Biochem Biophys Res Commun **176**(3): 1417-1423.

Mohandas, N. and P. G. Gallagher (2008). "Red cell membrane: past, present, and future." Blood **112**(10): 3939-3948.

Moller, M., H. Botti, C. Batthyany, H. Rubbo, R. Radi and A. Denicola (2005). "Direct measurement of nitric oxide and oxygen partitioning into liposomes and low density lipoprotein." J Biol Chem **280**(10): 8850-8854.

Mortensen, S. P., P. Thaning, M. Nyberg, B. Saltin and Y. Hellsten (2011). "Local release of ATP into the arterial inflow and venous drainage of human skeletal muscle: insight from ATP determination with the intravascular microdialysis technique." J Physiol **589**(Pt 7): 1847-1857.

Muenster, S., A. Beloiartsev, B. Yu, E. Du, S. Abidi, M. Dao, G. Fabry, J. A. Graw, M. Wepler, R. Malhotra, B. O. Fernandez, M. Feelisch, K. D. Bloch, D. B. Bloch and W. M. Zapol (2016). "Exposure of Stored Packed Erythrocytes to Nitric Oxide Prevents Transfusion-associated Pulmonary Hypertension." Anesthesiology **125**(5): 952-963.

Muhl, H. and J. Pfeilschifter (2003). "Endothelial nitric oxide synthase: a determinant of TNFalpha production by human monocytes/macrophages." Biochem Biophys Res Commun **310**(3): 677-680.

Nagababu, E., A. V. Scott, D. J. Johnson, I. M. Dwyer, J. A. Lipsitz, V. M. Barodka, D. E. Berkowitz and S. M. Frank (2016). "Oxidative stress and rheologic properties of stored red blood cells before and after transfusion to surgical patients." Transfusion **56**(5): 1101-1111.

Nam, J. S., C. W. Ahn, S. Kang, K. R. Kim and J. S. Park (2018). "Red Blood Cell Distribution Width Is Associated with Carotid Atherosclerosis in People with Type 2 Diabetes." J Diabetes Res **2018**: 1792760.

Ogasawara, Y., M. Komiyama, M. Funakoshi and K. Ishii (2010). "Disruption of glutathione homeostasis causes accumulation of S-glutathionyl proteins in response to exposure to reactive oxygen species in human erythrocytes." Biol Pharm Bull **33**(12): 1925-1931.

Olearczyk, J. J., A. H. Stephenson, A. J. Lonigro and R. S. Sprague (2004). "Heterotrimeric G protein Gi is involved in a signal transduction pathway for ATP release from erythrocytes." Am J Physiol Heart Circ Physiol **286**(3): H940-945.

Paddle, B. M. and G. Burnstock (1974). "Release of ATP from perfused heart during coronary vasodilatation." Blood Vessels **11**(3): 110-119.

Palmer, R. M., D. S. Ashton and S. Moncada (1988). "Vascular endothelial cells synthesize nitric oxide from L-arginine." Nature **333**(6174): 664-666.

Palmer, R. M., A. G. Ferrige and S. Moncada (1987). "Nitric oxide release accounts for the biological activity of endothelium-derived relaxing factor." Nature **327**(6122): 524-526.

Panza, J. A., P. R. Casino, D. M. Badar and A. A. Quyyumi (1993). "Effect of increased availability of endothelium-derived nitric oxide precursor on endothelium-dependent vascular relaxation in normal subjects and in patients with essential hypertension." Circulation **87**(5): 1475-1481.

Panza, J. A., P. R. Casino, C. M. Kilcoyne and A. A. Quyyumi (1993). "Role of endothelium-derived nitric oxide in the abnormal endothelium-dependent vascular relaxation of patients with essential hypertension." Circulation **87**(5): 1468-1474.

Panza, J. A., A. A. Quyyumi, J. E. Brush, Jr. and S. E. Epstein (1990). "Abnormal endothelium-dependent vascular relaxation in patients with essential hypertension." N Engl J Med **323**(1): 22-27.

Parthasarathi, K. and H. H. Lipowsky (1999). "Capillary recruitment in response to tissue hypoxia and its dependence on red blood cell deformability." Am J Physiol **277**(6 Pt 2): H2145-2157.

Pearson, J. D. and J. L. Gordon (1979). "Vascular endothelial and smooth muscle cells in culture selectively release adenine nucleotides." Nature **281**(5730): 384-386.

Peterson, K. R., H. Fedosyuk, L. Zelenchuk, B. Nakamoto, E. Yannaki, G. Stamatoyannopoulos, S. Ciciotte, L. L. Peters, L. M. Scott and T. Papayannopoulou (2004). "Transgenic Cre expression mice for generation of erythroid-specific gene alterations." Genesis **39**(1): 1-9.

Pfafferott, C., H. J. Meiselman and P. Hochstein (1982). "The effect of malonyldialdehyde on erythrocyte deformability." Blood **59**(1): 12-15.

Pong, T., M. Scherrer-Crosbie, D. N. Atochin, K. D. Bloch and P. L. Huang (2014). "Phosphomimetic modulation of eNOS improves myocardial reperfusion and mimics cardiac postconditioning in mice." PLoS One **9**(1): e85946.

Qiu, F., J. Wang, D. C. Spray, E. Scemes and G. Dahl (2011). "Two non-vesicular ATP release pathways in the mouse erythrocyte membrane." FEBS Lett **585**(21): 3430-3435.

Radomski, M. W., R. M. Palmer and S. Moncada (1990). "An L-arginine/nitric oxide pathway present in human platelets regulates aggregation." Proc Natl Acad Sci U S A **87**(13): 5193-5197.

Ramos-Gomez, M., M. K. Kwak, P. M. Dolan, K. Itoh, M. Yamamoto, P. Talalay and T. W. Kensler (2001). "Sensitivity to carcinogenesis is increased and chemoprotective efficacy of enzyme inducers is lost in nrf2 transcription factor-deficient mice." Proc Natl Acad Sci U S A **98**(6): 3410-3415.

Riccio, D. A., H. Zhu, M. W. Foster, B. Huang, C. L. Hofmann, G. M. Palmer and T. J. McMahon (2015). "Renitrosylation of banked human red blood cells improves deformability and reduces adhesivity." Transfusion **55**(10): 2452-2463.

Rice-Evans, C., E. Baysal, D. P. Pashby and P. Hochstein (1985). "t-butyl hydroperoxide-induced perturbations of human erythrocytes as a model for oxidant stress." Biochim Biophys Acta **815**(3): 426-432.

Richards, J. P., E. A. Bowles, W. R. Gordon, M. L. Ellsworth, A. H. Stephenson and R. S. Sprague (2015). "Mechanisms of C-peptide-mediated rescue of low O2-induced ATP release from erythrocytes of humans with type 2 diabetes." Am J Physiol Regul Integr Comp Physiol **308**(5): R411-418.

Rifkind, J. M. and E. Nagababu (2013). "Hemoglobin redox reactions and red blood cell aging." Antioxid Redox Signal **18**(17): 2274-2283.

Rifkind, J. M., L. Zhang, A. Levy and P. T. Manoharan (1991). "The hypoxic stress on erythrocytes associated with superoxide formation." Free Radic Res Commun **12-13 Pt 2**: 645-652.

Rodan, S. B., G. A. Rodan and R. I. Sha'afi (1976). "Demonstration of adenylate cyclase activity in human red blood cell ghosts." Biochim Biophys Acta **428**(2): 509-515.

Roth, G. A., M. H. Forouzanfar, A. E. Moran, R. Barber, G. Nguyen, V. L. Feigin, M. Naghavi, G. A. Mensah and C. J. Murray (2015). "Demographic and epidemiologic drivers of global cardiovascular mortality." N Engl J Med **372**(14): 1333-1341.

Saluja, R., A. Jyoti, M. Chatterjee, S. Habib, A. Verma, K. Mitra, M. K. Barthwal, V. K. Bajpai and M. Dikshit (2011). "Molecular and biochemical characterization of nitric oxide synthase isoforms and their intracellular distribution in human peripheral blood mononuclear cells." Biochim Biophys Acta **1813**(10): 1700-1707.

Sandhagen, B., G. Frithz, U. Waern and G. Ronquist (1990). "Increased whole blood viscosity combined with decreased erythrocyte fluidity in untreated patients with essential hypertension." J Intern Med **228**(6): 623-626.

Sase, K. and T. Michel (1995). "Expression of constitutive endothelial nitric oxide synthase in human blood platelets." Life Sci **57**(22): 2049-2055.

Sauer, B. and N. Henderson (1989). "Cre-stimulated recombination at loxP-containing DNA sequences placed into the mammalian genome." Nucleic Acids Res **17**(1): 147-161.

Sayed, N., P. Baskaran, X. Ma, F. van den Akker and A. Beuve (2007). "Desensitization of soluble guanylyl cyclase, the NO receptor, by S-nitrosylation." Proc Natl Acad Sci U S A **104**(30): 12312-12317.

Schaue, D., E. D. Micewicz, J. A. Ratikan, M. W. Xie, G. Cheng and W. H. McBride (2015). "Radiation and inflammation." Semin Radiat Oncol **25**(1): 4-10.

Shesely, E. G., N. Maeda, H. S. Kim, K. M. Desai, J. H. Krege, V. E. Laubach, P. A. Sherman, W. C. Sessa and O. Smithies (1996). "Elevated blood pressures in mice lacking endothelial nitric oxide synthase." Proc Natl Acad Sci U S A **93**(23): 13176-13181.

Shinar, E. and E. A. Rachmilewitz (1990). "Oxidative denaturation of red blood cells in thalassemia." Semin Hematol **27**(1): 70-82.

Sies, H. (1999). "Glutathione and its role in cellular functions." Free Radic Biol Med **27**(9-10): 916-921.

Sikora, J., S. N. Orlov, K. Furuya and R. Grygorczyk (2014). "Hemolysis is a primary ATP-release mechanism in human erythrocytes." Blood **124**(13): 2150-2157.

Sinha, A., T. T. Chu, M. Dao and R. Chandramohanadas (2015). "Single-cell evaluation of red blood cell bio-mechanical and nano-structural alterations upon chemically induced oxidative stress." Sci Rep **5**: 9768.

Smith, D. K. and J. Palek (1983). "Sulfhydryl reagents induce altered spectrin self-association, skeletal instability, and increased thermal sensitivity of red cells." Blood **62**(6): 1190-1196.

Snyder, L. M., N. L. Fortier, L. Leb, J. McKenney, J. Trainor, H. Sheerin and N. Mohandas (1988). "The role of membrane protein sulfhydryl groups in hydrogen

peroxide-mediated membrane damage in human erythrocytes." Biochim Biophys Acta **937**(2): 229-240.

Sprague, R. S., E. A. Bowles, M. S. Hanson, E. A. DuFaux, M. Sridharan, S. Adderley, M. L. Ellsworth and A. H. Stephenson (2008). "Prostacyclin analogs stimulate receptor-mediated cAMP synthesis and ATP release from rabbit and human erythrocytes." Microcirculation **15**(5): 461-471.

Sprague, R. S., E. A. Bowles, J. J. Olearczyk, A. H. Stephenson and A. J. Lonigro (2002). "The role of G protein beta subunits in the release of ATP from human erythrocytes." J Physiol Pharmacol **53**(4 Pt 1): 667-674.

Sprague, R. S. and M. L. Ellsworth (2012). "Erythrocyte-derived ATP and perfusion distribution: role of intracellular and intercellular communication." Microcirculation **19**(5): 430-439.

Sprague, R. S., M. L. Ellsworth, A. H. Stephenson and A. J. Lonigro (1996). "ATP: the red blood cell link to NO and local control of the pulmonary circulation." Am J Physiol **271**(6 Pt 2): H2717-2722.

Sprague, R. S., M. L. Ellsworth, A. H. Stephenson and A. J. Lonigro (2001). "Participation of cAMP in a signal-transduction pathway relating erythrocyte deformation to ATP release." Am J Physiol Cell Physiol **281**(4): C1158-1164.

Sridharan, M., S. P. Adderley, E. A. Bowles, T. M. Egan, A. H. Stephenson, M. L. Ellsworth and R. S. Sprague (2010). "Pannexin 1 is the conduit for low oxygen tension-induced ATP release from human erythrocytes." Am J Physiol Heart Circ Physiol **299**(4): H1146-1152.

Srihirun, S., T. Sriwantana, S. Unchern, D. Kittikool, E. Noulsri, K. Pattanapanyasat, S. Fucharoen, B. Piknova, A. N. Schechter and N. Sibmooh (2012). "Platelet inhibition by nitrite is dependent on erythrocytes and deoxygenation." PLoS One **7**(1): e30380.

Stamatelopoulos, K. S., J. P. Lekakis, N. A. Poulakaki, C. M. Papamichael, K. Venetsanou, K. Aznaouridis, A. D. Protogerou, T. G. Papaioannou, S. Kumar and S. F. Stamatelopoulos (2004). "Tamoxifen improves endothelial function and reduces carotid intima-media thickness in postmenopausal women." Am Heart J **147**(6): 1093-1099.

Starzyk, D., R. Korbut and R. J. Gryglewski (1997). "The role of nitric oxide in regulation of deformability of red blood cells in acute phase of endotoxaemia in rats." J Physiol Pharmacol **48**(4): 731-735.

Stauss, H. M., A. Godecke, R. Mrowka, J. Schrader and P. B. Persson (1999). "Enhanced blood pressure variability in eNOS knockout mice." Hypertension **33**(6): 1359-1363.

Steinberg, H. O., H. Chaker, R. Leaming, A. Johnson, G. Brechtel and A. D. Baron (1996). "Obesity/insulin resistance is associated with endothelial dysfunction. Implications for the syndrome of insulin resistance." J Clin Invest **97**(11): 2601-2610.

Sternberg, N. and D. Hamilton (1981). "Bacteriophage P1 site-specific recombination. I. Recombination between loxP sites." J Mol Biol **150**(4): 467-486.

Stocks, J. and T. L. Dormandy (1971). "The autoxidation of human red cell lipids induced by hydrogen peroxide." Br J Haematol **20**(1): 95-111.

Strom, J. and Q. M. Chen (2017). "Loss of Nrf2 promotes rapid progression to heart failure following myocardial infarction." Toxicol Appl Pharmacol **327**: 52-58.

Stuart, J. and G. B. Nash (1990). "Red cell deformability and haematological disorders." Blood Rev **4**(3): 141-147.

Suvorava, T., J. Stegbauer, M. Thieme, S. Pick, S. Friedrich, L. C. Rump, T. Hohlfeld and G. Kojda (2015). "Sustained hypertension despite endothelial-specific eNOS rescue in eNOS-deficient mice." Biochem Biophys Res Commun **458**(3): 576-583.

Suzuki, T. and M. Yamamoto (2015). "Molecular basis of the Keap1-Nrf2 system." Free Radic Biol Med **88**(Pt B): 93-100.

Taddei, S., A. Virdis, P. Mattei, L. Ghiadoni, C. B. Fasolo, I. Sudano and A. Salvetti (1997). "Hypertension causes premature aging of endothelial function in humans." Hypertension **29**(3): 736-743.

Tarride, J. E., M. Lim, M. DesMeules, W. Luo, N. Burke, D. O'Reilly, J. Bowen and R. Goeree (2009). "A review of the cost of cardiovascular disease." Can J Cardiol **25**(6): e195-202.

Thomas, S. L. (2014). "Intravascular hemolysis: the sacrifice of few." Blood **124**(13): 2011-2012.

Tomaiuolo, G. (2014). "Biomechanical properties of red blood cells in health and disease towards microfluidics." Biomicrofluidics **8**(5): 051501.

Trotta, R. J., S. G. Sullivan and A. Stern (1983). "Lipid peroxidation and haemoglobin degradation in red blood cells exposed to t-butyl hydroperoxide. The relative roles of haem- and glutathione-dependent decomposition of t-butyl hydroperoxide and membrane lipid hydroperoxides in lipid peroxidation and haemolysis." Biochem J **212**(3): 759-772.

Vaya, A., M. Martinez, J. Garcia, M. Labios and J. Aznar (1992). "Hemorheological alterations in mild essential hypertension." Thromb Res **66**(2-3): 223-229.

Vennemann, P., K. T. Kiger, R. Lindken, B. C. Groenendijk, S. Stekelenburg-de Vos, T. L. ten Hagen, N. T. Ursem, R. E. Poelmann, J. Westerweel and B. P. Hierck (2006). "In vivo micro particle image velocimetry measurements of blood-plasma in the embryonic avian heart." J Biomech **39**(7): 1191-1200.

Vilsen, B. and H. Nielsen (1984). "Reaction of phenylhydrazine with erythrocytes. Cross-linking of spectrin by disulfide exchange with oxidized hemoglobin." Biochem Pharmacol **33**(17): 2739-2748.

Wan, J., W. D. Ristenpart and H. A. Stone (2008). "Dynamics of shear-induced ATP release from red blood cells." Proc Natl Acad Sci U S A **105**(43): 16432-16437.

Wang, Y., M. Nakayama, M. E. Pitulescu, T. S. Schmidt, M. L. Bochenek, A. Sakakibara, S. Adams, A. Davy, U. Deutsch, U. Luthi, A. Barberis, L. E. Benjamin, T. Makinen, C. D. Nobes and R. H. Adams (2010). "Ephrin-B2 controls VEGF-induced angiogenesis and lymphangiogenesis." Nature **465**(7297): 483-486.

Webb, A. J., A. B. Milsom, K. S. Rathod, W. L. Chu, S. Qureshi, M. J. Lovell, F. M. Lecomte, D. Perrett, C. Raimondo, E. Khoshbin, Z. Ahmed, R. Uppal, N. Benjamin, A. J. Hobbs and A. Ahluwalia (2008). "Mechanisms underlying erythrocyte and endothelial nitrite reduction to nitric oxide in hypoxia: role for xanthine oxidoreductase and endothelial nitric oxide synthase." Circ Res **103**(9): 957-964.

Webb, A. J., N. Patel, S. Loukogeorgakis, M. Okorie, Z. Aboud, S. Misra, R. Rashid, P. Miall, J. Deanfield, N. Benjamin, R. MacAllister, A. J. Hobbs and A. Ahluwalia (2008).

"Acute blood pressure lowering, vasoprotective, and antiplatelet properties of dietary nitrate via bioconversion to nitrite." Hypertension **51**(3): 784-790.

Welbourn, E. M., M. T. Wilson, A. Yusof, M. V. Metodiev and C. E. Cooper (2017). "The mechanism of formation, structure and physiological relevance of covalent hemoglobin attachment to the erythrocyte membrane." Free Radic Biol Med **103**: 95-106.

WHO. (2017). "Key facts Cardiovascular diseases (CVDs)." Retrieved (2018, July 30) 2018, from http://www.who.int/en/news-room/fact-sheets/detail/cardiovascular-diseases-(cvds).

Wolf, M. M. and R. M. Berne (1956). "Coronary vasodilator properties of purine and pyrimidine derivatives." Circ Res **4**(3): 343-348.

Wolhuter, K., H. J. Whitwell, C. H. Switzer, J. R. Burgoyne, J. F. Timms and P. Eaton (2018). "Evidence against Stable Protein S-Nitrosylation as a Widespread Mechanism of Post-translational Regulation." Mol Cell **69**(3): 438-450 e435.

Wood, K. C., M. M. Cortese-Krott, J. C. Kovacic, A. Noguchi, V. B. Liu, X. Wang, N. Raghavachari, M. Boehm, G. J. Kato, M. Kelm and M. T. Gladwin (2013). "Circulating blood endothelial nitric oxide synthase contributes to the regulation of systemic blood pressure and nitrite homeostasis." Arterioscler Thromb Vasc Biol **33**(8): 1861-1871.

Xu, L., J. P. Eu, G. Meissner and J. S. Stamler (1998). "Activation of the cardiac calcium release channel (ryanodine receptor) by poly-S-nitrosylation." Science **279**(5348): 234-237.

Yang, W., H. Huang, Y. Wang, X. Yu and Z. Yang (2014). "High red blood cell distribution width is closely associated with nonalcoholic fatty liver disease." Eur J Gastroenterol Hepatol **26**(2): 174-178.

Zhang, L., A. Levy and J. M. Rifkind (1991). "Autoxidation of hemoglobin enhanced by dissociation into dimers." J Biol Chem **266**(36): 24698-24701.

Zhao, Y., P. M. Vanhoutte and S. W. Leung (2015). "Vascular nitric oxide: Beyond eNOS." J Pharmacol Sci **129**(2): 83-94.

8   Acknowledgments

9   Curriculum Vitae

Name:	Lukas Dominik Vornholz geb. Diederich
Beruf:	Apotheker
Adresse:	Wissmannstr. 19
	40219 Düsseldorf
Geburtstag/-ort:	19.04.1988 / Mainz
Familienstand:	ledig

BERUFLICHER WERDEGANG

09/2015 – heute	Universitätsklinikum Düsseldorf, Klinik für Kardiologie, Pneumologie und Angiologie
10 – 2014 / 08 – 2015	Farma-Plus Apotheke in Worms
11/2013 – 04/2014	University of Florida in Gainesville (USA)
05/2013 – 10/2013	Struwwelpeter Apotheken in Frankfurt am Main

AUSBILDUNG

09/2014	Approbation zum Apotheker
04/2009 – 04/2013	Studium der Pharmazie an der Johann Wolfgang von Goethe Universität in Frankfurt am Main
08/1999 – 03/2008	Eleonoren Gymnasium in Worms

ZIVILDIENST

04/2008 – 03/2009	Freiwilliges Soziales Jahr im Sport im Wormser Ruderclub Blau-Weiß 1883 e.V.

PRAKTIKA

09/2010 – 10/2010	Abbott GmbH & Co. KG, Abteilung GMP-Services, Ludwigshafen
08/2009 – 09/2009	Seebach Apotheke in Westhofen